University of Kentucky
UKnowledge

Theses and Dissertations--Plant Pathology | Plant Pathology

2022

THE ROLE OF NITRIC OXIDE IN INTER- AND INTRA- CELLULAR SIGNALING IN PLANT DEFENSE

Fan Xia
University of Kentucky, xiafan2016@gmail.com
Author ORCID Identifier:
https://orcid.org/0000-0002-8091-2426
Digital Object Identifier: https://doi.org/10.13023/etd.2022.77

Right click to open a feedback form in a new tab to let us know how this document benefits you.

Recommended Citation

Xia, Fan, "THE ROLE OF NITRIC OXIDE IN INTER- AND INTRA- CELLULAR SIGNALING IN PLANT DEFENSE" (2022). *Theses and Dissertations--Plant Pathology*. 36.
https://uknowledge.uky.edu/plantpath_etds/36

This Doctoral Dissertation is brought to you for free and open access by the Plant Pathology at UKnowledge. It has been accepted for inclusion in Theses and Dissertations--Plant Pathology by an authorized administrator of UKnowledge. For more information, please contact UKnowledge@lsv.uky.edu.

STUDENT AGREEMENT:

I represent that my thesis or dissertation and abstract are my original work. Proper attribution has been given to all outside sources. I understand that I am solely responsible for obtaining any needed copyright permissions. I have obtained needed written permission statement(s) from the owner(s) of each third-party copyrighted matter to be included in my work, allowing electronic distribution (if such use is not permitted by the fair use doctrine) which will be submitted to UKnowledge as Additional File.

I hereby grant to The University of Kentucky and its agents the irrevocable, non-exclusive, and royalty-free license to archive and make accessible my work in whole or in part in all forms of media, now or hereafter known. I agree that the document mentioned above may be made available immediately for worldwide access unless an embargo applies.

I retain all other ownership rights to the copyright of my work. I also retain the right to use in future works (such as articles or books) all or part of my work. I understand that I am free to register the copyright to my work.

REVIEW, APPROVAL AND ACCEPTANCE

The document mentioned above has been reviewed and accepted by the student's advisor, on behalf of the advisory committee, and by the Director of Graduate Studies (DGS), on behalf of the program; we verify that this is the final, approved version of the student's thesis including all changes required by the advisory committee. The undersigned agree to abide by the statements above.

Fan Xia, Student

Dr. Pradeep Kachroo, Major Professor

Dr. Rick Bennett, Director of Graduate Studies

THE ROLE OF NITRIC OXIDE IN INTER- AND INTRA- CELLULAR SIGNALING IN PLANT DEFENSE

DISSERTATION

A dissertation submitted in partial fulfillment of the
requirements for the degree of Doctor of Philosophy in the
College of Agriculture, Food and Environment
at the University of Kentucky

By

Fan Xia

Lexington, Kentucky

Director: Dr. Pradeep Kachroo, Professor of Plant Pathology

Lexington, Kentucky

2022

Copyright © Fan Xia 2022
https://orcid.org/0000-0002-8091-2426

ABSTRACT OF DISSERTATION

THE ROLE OF NITRIC OXIDE IN INTER- AND INTRA- CELLULAR SIGNALING IN PLANT DEFENSE

Plants have evolved a sophisticated immune system to defend themselves against pathogens. This immune response can be triggered in response to pathogen-associated molecular patterns (PAMP) or specialized effectors that are recognized by the plant resistance (R) proteins. The latter, commonly referred to as effector-triggered immunity (ETI), is well known to induce broad-spectrum resistance throughout the plants. This phenomenon known as systemic acquired resistance (SAR) is regulated by several chemical signals including salicylic acid (SA), and free radical nitric oxide (NO) and reactive oxygen species (ROS). These signals operate in two parallel branches with NO/ROS functioning downstream of pipecolic acid (Pip) and upstream of azelaic acid (AzA) and glycerol-3-phosphate (G3P). Earlier work has shown that optimum levels of NO/ROS are required for the induction of SAR with high concentrations inhibiting SAR. To characterize the role of NO in SAR, I evaluated SAR associated signaling in an *Arabidopsis thaliana* GSNOR1 (S-NITROSOGLUTATHIONE REDUCTASE 1) mutant that accumulates elevated levels of NO and shows compromised SAR. The pathogen inoculated *gsnor1* plants accumulated wild type (WT) like levels of AzA and G3P, suggesting that increased NO levels were not associated with hyperactivation of the NO-AzA-G3P branch of the SAR pathway. Consistent with these results, the *gsnor1* plants showed WT like levels of lipid transfer proteins DIR1 (DEFECTIVE IN INDUCED RESISTANCE 1) and AZI1 (AZELAIC ACID INDUCED 1), which operate in a feedback loop with G3P. Interestingly, the *gsnor1* plants accumulated reduced levels of Pip, which in turn was associated with reduced expression of the gene encoding SARD1 (SYSTEMIC ACQUIRED RESISTANCE DEFICIENT 1) transcription factor. Since SARD1 regulates both SA and Pip biosynthetic genes, the *gsnor1* plants also accumulated reduced levels of SA in infected leaves. Mutations in CAMTA (CALMODULIN BINDING TRANSCRIPTION ACTIVATOR) transcription factors, that negatively regulate *SARD1* expression were able to partially elevate *SARD1* expression and SA and Pip levels in *gsnor1* plants but were unable to normalize the SAR phenotype. Petiole exudate transport assays showed normal transport of G3P, but defective transport of SA, in pathogen inoculated *gsnor1* plants. Likewise, the *gsnor1* plants showed reduced transport of exogenously applied cold or ^{14}C labeled SA. Consequently, localized application of exogenous SA was unable to confer SAR on *gsnor1* plants. Notably, SA delivered via root drench was able to confer SAR on *gsnor1* plants, suggesting that these plants were specifically affected in SA transport. Reduced transport of SA in the presence of NO donor suggested that increased levels of NO affected SAR by impairing transport of SA. These results further reinforce the importance of SA transport in SAR.

To characterize NO-mediated signaling in relation to chloroplast-nucleus retrograde signaling, I next characterized the *ssi2* mutant that accumulates elevated levels

of NO in the chloroplast and shows constitutive defense phenotypes. *SSI2* (*SUPPRESSOR OF SA INSENSISTIVE 2*) encodes stearoyl-ACP (acyl-carrier-protein) desaturase that catalyzes the conversion of 18:0 to 18:1 fatty acid. The *ssi2*-mediated activation of defense is associated with 18:1 levels and normalization of 18:1 levels restores their NO levels and defense phenotypes to wild-type like levels. Interestingly, a mutation in *NO OVERPRODUCER 1 (NOX1)*, which encodes a plastid membrane localized phosphoenolpyruvate (PEP) phosphate translocator, normalizes wild-type-like defense phenotypes in *ssi2* even though these plants accumulate elevated levels of NO in plastids. NOX1 facilitates import of PEP into the stroma, which in turn serves as a precursor to aromatic amino acid biosynthesis. Indeed, treatment with phenylalanine, but not tyrosine or tryptophane, was able to restore defense phenotypes in *ssi2 nox1* plants. Together, these results suggest NO-mediated retrograde defense signaling in *ssi2* is mediated via phenylalanine.

KEYWORDS: S-nitrosoglutathione reductase, SAR, SA transport, nitric oxide, chloroplast-nucleus retrograde signaling, phenylalanine

Fan Xia

(Name of Student)

04/26/2022

Date

THE ROLE OF NITRIC OXIDE IN INTER- AND INTRA- CELLULAR SIGNALING IN PLANT DEFENSE

By
Fan Xia

Pradeep Kachroo
Director of Thesis

Rick Bennett
Director of Graduate Studies

04-27-2022
Date

ACKNOWLEDGMENTS

After many years of study, I have finally reached this important milestone. First, I would like to thank my advisor Dr. Pradeep Kachroo for providing me this precious opportunity to explore science. His passion for research and his pursuit of excellence is a huge inspiration to me. I especially thank him for the enormous amount of time he spent on helping me with my research. I also want to thank Dr. Aardra Kachroo for her insights on my work and her encouragements throughout the past five and a half years, which have helped keep me on track.

I am very grateful to all my committee members, Dr. Sharyn Perry, Dr. Bruce Downie, Dr. Nicholas McLetchie and Dr. Emily Pfeufer, for their helpful comments and advice on my research and study. I would like to express special thanks to Dr. Bruce Downie for writing recommendation letters for me and helping me in many other ways. I also appreciate Dr. Zhu Hongyan for being my outside examiner.

I'd like to thank Dr. Rick Bennet and Dr. Lisa Vaillancourt for updating me fellowship opportunities and reminding me academic requirements and important deadlines. I thank all the other faculty and staff members of the Plant Pathology department for providing me support and convenience. I'd like to pay special thanks to Shirley Harris and Cheryl Kaiser for always being kind and helpful.

I express my deep gratitude to Wendy Havens and Dr. Ludmila Lapchyk for maintaining the lab and providing me the best assistance whenever I need anything for my experiments. I thank John Johnson for helping me with GC-MS quantifications and Amy Crume for taking care of our plant growth facility and the greenhouse. I thank Dr. Keshun Yu for his help with ^{14}C-SA transport assay and fatty acid analysis and his assistance in many other experiments. I thank Dr. Stephen Ryu and Dr. Andrea Pitzschke for 35S-DIR1-GFP, 35S-AZI1-MYC seeds, respectively. I thank Huazhen Liu for contributing to GC protocol development. I thank past and present members of the Kachroo lab, many of you have helped me in my research and life.

My deepest gratitude goes to my wife Xinyu Yuan and my parents, I could not have completed this journey without the love and support from them.

TABLE OF CONTENTS

ACKNOWLEDGMENTS iii
LIST OF TABLES vii
LIST OF FIGURES viii
CHAPTER 1. INTRODUCTION 1
1.1 Plants and plant diseases 1
1.2 PAMP-triggered immunity (PTI) and effector-triggered immunity (ETI) 2
1.3 Systemic acquired resistance (SAR) 3
1.4 SAR signals 3
1.4.1 Salicylic acid (SA) 4
1.4.2 Methyl salicylate (MeSA) 5
1.4.3 Pipecolic acid (Pip) and N-hydroxy-pipecolic acid (NHP) 5
1.4.4 Nitric oxide (NO)- reactive oxygen species (ROS)- azelaic acid (AzA)- glycerol-3-phosphate (G3P) cascade 6
CHAPTER 2. METHODS 10
2.1 Plant growth conditions and plant materials used 10
2.2 DNA extraction and genotyping analysis 10
2.3 Pathogen infection 10
2.4 Petiole exudate and apoplastic fluid collection 11
2.5 G3P, AzA, SA, Pip and NHP quantifications 12
2.6 Amino acids extraction and quantifications 13
2.7 Fatty acid analysis 13
2.8 Galactolipid analysis 13
2.9 Chemical treatments 14
2.10 RNA extraction, reverse transcription and quantitative real-time PCR 15
2.11 Protein extraction and immunoblot analysis 15
2.12 Trypan blue staining 15
2.13 Hydrogen peroxide staining (DAB staining) 16
2.14 Conductivity (Ion leakage) assays 16
2.15 GSNOR1-pGWB5 vector construction and generation of transgenic plants 16
2.16 Confocal microscopy 16
2.17 NO staining 17
2.18 Protoplast ^{14}C-SA transport assays 17
2.19 D7-FAM transport assays 17
2.20 Statistics and reproducibility 18
CHAPTER 3. CHARACTERIZATION THE ROLE OF S-NITROSOGLUTATHIONE REDUCTASE 1 (GSNOR1) IN SYSTEMIC ACQUIRED RESISTANCE 22
3.1 Introduction 22
3.2 Results 24
3.2.1 The *gsnor1* mutant plants are compromised in SAR 24

3.2.2 AzA/G3P pathway is not affected in the *gsnor1* plants 24
3.2.3 The *gsnor1* plants are defective in SA transport..... 25
3.2.4 The *gsnor1* plants are competent in generation of SAR signal 27
3.2.5 Increased NO levels attenuate transport of SA to distal leaves 27
3.2.6 GSNOR1 is epistatic to CAMTA and WRKY70 29
3.3 Discussion 30
CHAPTER 4. DISSERCTING GSNOR1-REGULATED HYPERSENSITIVE RESPONSE AND LOCAL RESISTANCE IN *ARABIDOPSIS* 50
4.1 Introduction 50
4.2 Results and discussion 52
4.2.1 The *gsnor1* mutant shows different HR phenotypes in different *R*-Avr interactions..... 52
4.2.2 The HR phenotypes in *gsnor1* mutant are independent of SID2, NPR1, ALD1 and RBOHD 53
4.2.3 SA induction pattern can be altered by different *R*-Avr interactions 53
4.2.4 SA is not the only factor that affects local resistance in gsnor1 plant..... 54
CHAPTER 5. NOX1 REGULATES SSI2-MEDIATED DEFENSE SIGNALING IN *ARABIDOPSIS* 59
5.1 Introduction 59
5.2 Results 62
5.2.1 The *ssi2* plants show activated Pip biosynthesis and this activation is dependent on ALD1 62
5.2.2 The morphology and cell death phenotypes of *ssi2* are not associated with increased levels of Pip..... 63
5.2.3 A mutation in the *NOX1* gene reverses *ssi2* morphological phenotypes..... 64
5.2.4 The *nox1* mutation does not alter 18:1 levels in the *ssi2* background..... 64
5.2.5 The *nox1* mutation reverses *ssi2* triggered defense phenotypes..... 65
5.2.6 Exogenous Phe treatments reconstitute *ssi2* like phenotypes in *ssi2 nox1* plants 66
5.2.7 The *ssi2* mutant contains high levels of Phe whereas *nox1* is deficient in Phe biosynthesis and Phe is involved in plant defense..... 67
5.2.8 The *nox1* plants are less sensitive to glycerol induced reduction of 18:1 levels 68
5.2.9 The *nox1* plants are not severely impaired in SA and Pip pathways..... 69
5.2.10 NO levels in the *ssi2 nox1* plants remain high..... 70
5.2.11 The relationships between NO overproducers mutant *nox1*, *gsnor1* and autoimmunity mutant *ssi2*, *camta1/2/3*..... 70
5.3 Discussion 71
SUMMARY.....89
APPENDIX 91

REFERENCES 95
VITA 102

LIST OF TABLES

Table 2.1 Seed materials used in this study 19
Table 2.2 List of primers used in this study 20

LIST OF FIGURES

Figure 1.1 PTI and ETI signaling in plant immune system 8
Figure 1.2 A simplified diagram showing SAR signals and their interactions..... 9
Figure 3.1 The *gsnor1* mutants are compromised in SAR 33
Figure 3.2 AzA/G3P pathway is not affected in the *gsnor1* plants..... 34
Figure 3.3 The *gsnor1* plants are defective in SA transport 36
Figure 3.4 The *gsnor1* plants are competent in generation of the SAR signal 40
Figure 3.5 Increased NO levels attenuate transport of SA to distal leaves..... 41
Figure 3.6 GSNOR1 is epistatic to CAMTA and WRKY70 45
Figure 4.1 The *gsnor1* mutant shows different HR phenotypes in different *R*-Avr interactions..... 55
Figure 4.2 GSNOR1 regulates HR phenotype independent of SID2, ALD1, RBOHD or NPR1 56
Figure 4.3 SA induction pattern in *gnsor1* plants can be altered by different *R*-Avr interactions..... 57
Figure 4.4 SA is not the only factor that affects local resistance in *gsnor1* plants 58
Figure 5.1 The *ssi2* plants constitutively accumulate Pip and Pip derivative NHP and Pip accumulation is dependent on ALD1 76
Figure 5.2 A mutation in *ALD1* or *FMO1* slightly increases the morphology of *ssi2* plants but does not significantly alter cell death phenotype in the *ssi2* background 77
Figure 5.3 A mutation in *NOX1* rescues *ssi2* morphology 77
Figure 5.4 The *nox1* mutation does not alter 18:1 levels in *ssi2* plants 78
Figure 5.5 The *nox1* mutation alters *ssi2* defense phenotypes 79
Figure 5.6 Phenylalanine (Phe) reconstitutes *ssi2* like phenotypes in *ssi2 nox1* plants.... 81
Figure 5.7 Phe levels in *ssi2* and *nox1* plants and Phe plays a role in defense..... 82
Figure 5.8 The 18:1-triggered defense signaling is inhibited in *nox1* plants..... 83
Figure 5.9 The *nox1* plants are not severely impaired in SA and Pip pathways..... 85
Figure 5.10 The *ssi2 nox1* plants continue to accumulate NO 86
Figure 5.11 The relationship between *nox1* and *gsnor1*, *ssi2* and *camta1/2/3* plants..... 87

CHAPTER 1. INTRODUCTION

1.1 Plants and plant diseases

In plants, photosynthesis transforms water and carbon dioxide into sugar and oxygen in sun light. Photosynthesis provides human and animals food to eat and oxygen to breath. Plants also have the ability to produce amino acids from inorganic nitrogen and organic-carbon compounds and synthesize vitamins that are indispensable for human health (Robbins, 1944).

Plants are constantly challenged by various of pathogens in nature and over 10% of crop yield loss are caused by plant diseases every year (Strange and Scott, 2005). Fungi, bacteria, viruses and oomycete are the most common pathogens that cause plant diseases (Chisholm et al., 2006). Potato (*Solanum tuberosum* L.) blight, a disease caused by the oomycete pathogen *Phytophthora infestans* led to potato plant failure and devastated the Irish population during 1840-1850s, it's estimated that up to one million Irish people died of famine caused by potato blight (Grunwald, 2005). American chestnut tree (*Castanea dentata*) historically had important biological and economical importance in North America. In early twenty century, the Japanese chestnut trees (*C. crenata*) were introduced into the United States for commercial purposes, bringing in chestnut blight (caused by *Cryphonectria parasitica*) disease that almost wiped out all mature American chestnut trees in the following few decades (Rigling and Prospero, 2018).

Understanding how plants response to pathogen attack and activate defense signaling could help scientists and crop breeders to better utilize plant disease resistance and overcome disease susceptibility in the field and ultimately will be beneficial to sustainable agriculture (Sanchez-Martin and Keller, 2019).

Unlike vertebrate animals and humans, plants do not have specific immune cells (Rast et al., 2006). Plants share some similarities with animals in terms of immune response but also have some unique features. Same as human skin, a cuticle covers plant surfaces and it forms a barrier for pathogen invasion (Ziv et al., 2018). Bacteria and certain fungal pathogens enter plants through natural openings such as wounds and stomatal pores (Melotto et al., 2008). Some filamentous pathogens use specialized structures (such as

appressoria) or secrete cell wall-degrading enzymes to penetrate into plants directly (Asai and Shirasu, 2015). Once pathogen entered, depending on the specificity of the plant-pathogen interaction, plants can activate several different but inter-connected immune responses.

1.2 PAMP-triggered immunity (PTI) and effector-triggered immunity (ETI)

Pathogen-associated molecular patterns (PAMPs) are conserved molecules among pathogens. Well studied PAMPs include flagellin and elongation factor Tu (EF-Tu) in bacteria, chitin and xylanase in fungi (Bittel and Robatzek, 2007; Zipfel and Robatzek, 2010). PAMP triggered immunity (PTI) is initiated when plasma membrane localized pattern-recognition receptors (PRRs) detect PAMPs from pathogens (Nicaise et al., 2009). For instance, during a pathogen attack, PAMP flg22 (a 22 amino acid stretch in the N terminus of bacterial flagellin) is recognized by the receptor-like kinase (RLK) FLS2 (FLAGELLINE INSENSITIVE 2), which activates another RLK, BAK1 (BRASSINOSTEROID INSENSITIVE 1 (BRI1)- ASSOCIATED RECEPTOR KINASE 1). BAK1 phosphorylates FLS2 and forms a complex with FLS2. This receptor complex further phosphorylates the receptor-like cytoplasmic kinase BIK1 (BOTRYTIS-INDUCED KINASE 1) and induce a burst of calcium (Ca^{2+}) in the cytosol. In addition, it increases in reactive oxygen species (ROS) levels via plasma membrane-localized NADPH (REDUCED NICOTINAMIDE ADENINE DINUCLEOTIDE PHOSPHATE) oxidase named RBOHD (RESPIRATORY BURST OXIDASE HOMOLOG D). Further, PTI also activates mitogen-activated protein kinases (MAPKs) cascades and other cellular protein kinases, which then regulate transcription factors and modulate defense genes expression and synthesize defense hormones and antimicrobial metabolites. A complex of signaling regulations contribute to disease resistance (Bigeard et al., 2015; Zipfel, 2009).

To counter PTI, bacteria pathogens use secretion system to deliver effectors into the host cell (Asai and Shirasu, 2015). These effectors have been shown to target host cell defense signaling components and can affect metabolic processes to facilitate propagation of pathogen (Dou and Zhou, 2012). In turn plants have evolved to recognize effectors via

resistance (*R*) proteins. Most *R* genes encodes NB-LRR proteins that contain nucleotide binding (NB) and leucine rich repeat (LRR) domains (Eitas and Dangl, 2010). Most known NB-LRR proteins are localized in the cytosol. A given effector in the host cell is detected by a corresponding NB-LRR protein, resulting in the effector triggered immunity (ETI) (Elmore et al., 2011). ETI is a much stronger immune response compared to PTI and is often associated with drastically increased ROS production, and hypersensitive response (HR) at the infection site, as a result, ETI limits pathogen from spreading and achieves disease resistance (Tsuda and Katagiri, 2010) (Figure 1.1).

1.3 Systemic acquired resistance (SAR)

In response to a pathogen attack, at the infection site (leaves), plants activate PTI and/or ETI to defend themselves (Yuan et al., 2021). In the meantime, local infected leaves produce a yet unknown signal(s), which is mobilized to distal (or systemic) uninfected leaves through the vascular system, resulting in increased disease resistance to subsequent infections. This phenomenon is termed systemic acquired resistance (SAR) (Durrant and Dong, 2004; Fu and Dong, 2013; Mishina and Zeier, 2007). SAR is a broad-spectrum resistance, and it strikes a balance response between defense and growth upon pathogen infections, making it a desired disease control approach (Gao et al., 2014a; Kachroo and Kachroo, 2020). The SAR signaling involves signal generation at the local infection site (local leaves), signal transport from local to distal leaves and signal perception in the distal leaves (Kachroo and Kachroo, 2020) (Figure 1.2).

1.4 SAR signals

The last three decades have seen significant progress in understanding SAR. Several plant metabolites are capable of inducing resistance in distal leaves when applied to the local leaves, suggesting they are potential SAR signals. These signals include salicylic acid (SA), methyl salicylate (MeSA), azelaic acid (AzA), glycerol-3-phosphate

(G3P), the non-protein amino acid pipecolic acid (Pip) and N-hydroxy-pipecolic acid (NHP), free radicals nitric oxide (NO) and ROS, NAD^+ and pinene volatiles (Chanda et al., 2011; Gaffney et al., 1993; Hartmann et al., 2018; Jung et al., 2009; Lim et al., 2016; Lim et al., 2020; Navarova et al., 2012; Park et al., 2007; Riedlmeier et al., 2017; Wang et al., 2014; Wang et al., 2019; Wang et al., 2018; Wendehenne et al., 2014).

1.4.1 Salicylic acid (SA)

Plants defective in SA accumulation and signaling are SAR compromised, suggesting SA is critical for SAR (Cao et al., 1997; Gaffney et al., 1993). SA is an important hormone involved in the regulation of plant growth, development, and responses to biotic and abiotic stresses. In plants, SA can be synthesized via ICS (ISOCHORISMATE SYNTHASE) or PAL (PHENYLALANINE AMMONIA LYASE) catalyzed reactions. Biotrophic pathogen infection greatly induces SA production. In *Arabidopsis*, mutant analysis revealed that two ICS proteins *ICS1* and *ICS2* both contribute to SA biosynthesis, with ICS1 accounting for 90% pathogen-induced SA accumulation. Meanwhile, the basal and pathogen induced SA levels in *Arabidopsis* PAL quadruple mutant (retained 10% PAL activity) plants were reduced to 25% or 50% of WT levels, respectively (Peng et al., 2021; Zhang and Li, 2019). In soybean (*Glycine max*) plants, the ICS- and PAL- pathways function collectively and both pathways are required for pathogen induced SA biosynthesis (Shine et al., 2016). In tobacco (*Nicotiana tabacum*) plants, tobacco mosaic virus (TMV) infection dramatically induced the expression of *PAL* and the corresponding PAL enzymatic activity, in contrast, TMV inoculated plants did not induce *ICS1* or show higher ICS activity. This suggested that SA in tobacoo-TMV pathosystem may be mainly produced through the PAL pathway (Peng et al., 2021). Together, these findings suggest that both ICS and PAL pathways contribute to pathogen induced SA accumulation.

SA levels in plants are tightly regulated because of its important roles in multiple physiological processes (Rivas-San Vicente and Plasencia, 2011). Some of the important positive regulators involved in maintaining SA levels include EDS1 (ENHANCED DISEASE SUSCEPTIBILITY 1), PAD4 (PHYTOALEXIN DEFICIENT 4) (ETI components), TGA transcription factors TGA1/TGA4 (binds to TGACG motif), SARD1 and CBP60g (CALMODULIN-BINDING PROTEIN 60g). On the contrary, calmodulin

(CaM)-binding transcription activators (CAMTA) CAMTA1, CAMTA2 and CAMTA3 act redundantly and negatively regulate SA biosynthesis possibly by inhibiting SARD1 and CBP60g's transcription (Sun et al., 2020). In addition, WRKY transcription factor WRKY70 was implicated in the repression of SARD1 and shown to negatively control SA levels in absence of pathogen infection (Li et al., 2006; Zhou et al., 2018). SA levels are also regulated via its conversion into various chemical derivatives and these modifications include hydroxylation, glycosylation, methylation, and amino acid conjugation. These chemical modifications can contribute to SA homeostasis and affect SA mediated defense responses (Peng et al., 2021).

1.4.2 Methyl salicylate (MeSA)

MeSA (methyl salicylate) is a volatile SA derivative. Tobacco grafting experiments showed that SAR was abolished when SA methyl transferase (converts SA to MeSA) was silenced in primary infected leaves. Protein mutagenesis analysis revealed that the MeSA esterase activity of SABP2 (SALICYLIC AICD BINDING PROTEIN 2), which converts MeSA into SA, was required for SAR signal perception in systemic tissues. In addition, MeSA treatment of lower leaves induced SAR in upper untreated leaves, suggesting MeSA is a SAR signal in tobacco plants (Park et al., 2007).

1.4.3 Pipecolic acid (Pip) and N-hydroxy-pipecolic acid (NHP)

Like SA, the non-protein amino acid pipecolic acid (Pip) and its derivative N-hydroxy-pipecolic acid (NHP) have recently been discovered to play important roles in SAR and local defense (Cecchini et al., 2015). Pip levels are significantly induced by pathogen infection and *Arabidopsis* plants impaired in Pip biosynthesis are not able to activate potent SAR. Aminotransferase AGD2-LIKE DEFENSE RESPONSE PROTEIN1 (ALD1) catalyzes a committed step in the Pip biosynthesis pathway, which converts L-Lysine into ketoacid ε-amino-α-ketocaproic acid (KAC) (Navarova et al., 2012). KAC undergoes spontaneous intramolecular cyclization and isomerization to form dehydro-pipecolic acid (2,3-DP), which is then converted to Pip by SARD4 (SAR-DEFICIENT4) encoded reductase. Pip is oxidized to NHP by the flavin-containing monooxygenase FMO1 (FLAVIN-DEPENDENT MONOOXYGENASE1) in the presence of FAD (flavin adenine dinucleotide), NAD(P)H and molecular oxygen (Hartmann and Zeier, 2019; Hartmann et

al., 2018). NHP is proposed to be the active product of the pipecolate pathway during SAR. Interestingly, NHP has been shown to undergo glycosylation and yield to an NHP-hexose conjugate, which negatively regulates NHP levels and thereby inhibiting NHP mediated SAR (Cai et al., 2021; Holmes et al., 2021). Recent reports found that Pip confers SAR by inducing free radicals such as nitric oxide (NO) and reactive oxygen species (ROS) in plants (Lenk et al., 2019; Wang et al., 2018).

1.4.4 Nitric oxide (NO)- reactive oxygen species (ROS)- azelaic acid (AzA)-glycerol-3-phosphate (G3P) cascade

NO is a gaseous molecule that has versatile roles in plant growth, development, flowering and stress responses (Wilson et al., 2008). NO is believed to exert its function by modulating target gene expression and posttranslational modification (Leitner et al., 2009). It was recently reported that NO levels in *Arabidopsis* regulate SAR in a dose-dependent manner because SAR was inhibited in plants accumulating high levels of NO or those unable to synthesize or accumulate NO. Further investigation showed that NO, together with ROS, confer plants SAR by facilitating the biosynthesis of SAR signal AzA (a C9 dicarboxylic acid) (Wang et al., 2014). AzA was discovered by screening metabolites that showed increased accumulation in the petiole exudates of pathogen-infected plants as compared to mock-treated plants. Exogenous AzA treatment can induce SAR in *Arabidopsis* and this SAR inducing activity is dependent on the lipid transfer proteins DIR1 (DEFECTIVE IN INDUCED RESISTANCE) and AZI1 (AZELAIC ACID INDUCED 1) (Jung et al., 2009). DIR1 and AZI1 proteins operate in a feedback loop with glycerol-3-phosphate (G3P), which also serves as a precursor for *de novo* biosynthesis of glycerolipids. Notably, G3P induces SAR is not associated with activation of the SA pathway. DIR1 protein contributes to G3P induced SAR by assisting G3P transport via phloem system. DIR1 and AZI1 interact with each other and G3P can restore SAR in the *azi1* mutant (Chanda et al., 2011; Yu et al., 2014). These findings suggest G3P functions downstream of AzA pathway. Growing evidence found G3P also acts downstream of the Pip pathway because G3P can also restore SAR in Pip deficient *ald1* mutant plants. Together, it was proposed that plant SAR operates in two parallel signaling branches, one

is controlled by SA, the other is regulated by the Pip-NO/ROS-AzA-G3P cascade (Wang et al., 2018).

Currently, studies focused on SAR signal transport have just started. A major recent breakthrough discovered that SA is mainly transported via the apoplastic pathway. In contrast, the preferred transport rout for AzA and G3P is the symplastic pathway, where the transport is regulated by PDLP1 (PLASMODESMATA LOCALIZING PROTEIN 1) and PDLP5 (PLASMODESMATA LOCALIZING PROTEIN 5) (Lim et al., 2016; Lim et al., 2020).

SAR signal perception in distal (systemic) tissues is another area where more investigations are needed. Unlike the local infection site, distal tissues are expected to receive much lower concentration of defense signals. Therefore, the signaling events in the distal tissues are likely to be different from the local tissues. Nonetheless, it was found that SABP2 (SALICYLIC ACID BINDING PROTEIN 2) (Park et al., 2007) and an intact plant cuticle in distal tissues are indispensable in SAR signal perception (Xia et al., 2009). Notably, a kinase encoded by *SnRK2.8* (*SNF1-RELATED PROTEIN KINASE 2.8*), which phosphorylates the master SA regulator NPR1 (NONEXPRESSER OF PATHOGENESIS-RELATED GENES 1) in distal leaves, is also required for SAR (Lee et al., 2015).

My study reported in this dissertation is focused on three objectives. The first is to understand how NO regulates SAR. The second is to dissect how GSNOR1 regulates HR cell death and local resistance in *Arabidopsis* plants. The third is to investigate how NOX1 regulates chloroplast-nucleus retrograde defense signaling.

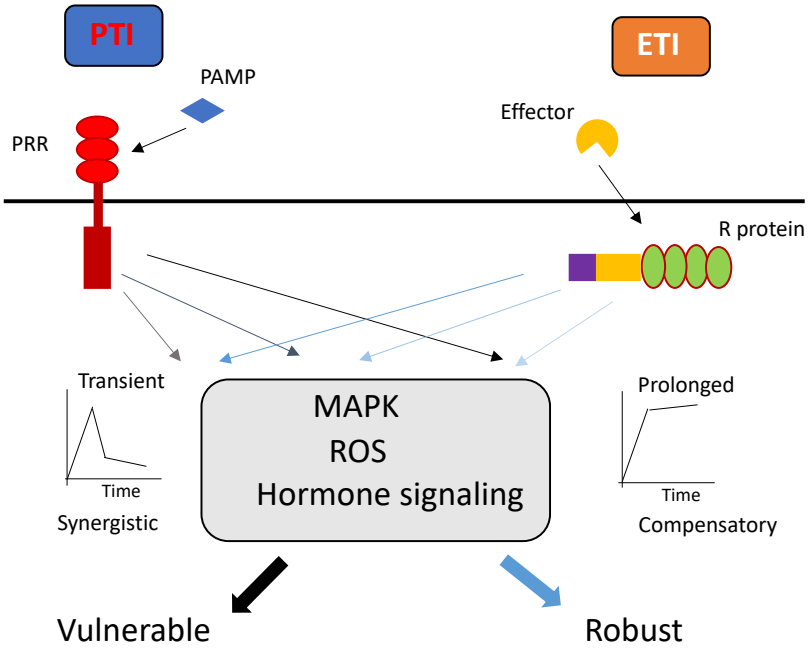

Figure 1.1 PTI and ETI signaling in plant immune system

The PTI is activated when a PAMP is recognized by a PRR. The ETI is triggered when an effector is recognized by an R protein. PTI and ETI share lots of signaling components such as MAP kinases, ROS and hormones. It is proposed that PTI and ETI may utilize these components at different levels or time points. In general, PTI activated defense responses are transient and synergistic, but ETI induced defense responses are more prolonged and compensatory. These features make PTI relative vulnerable to pathogenic perturbations but ETI relative robust to both pathogenic and genetic perturbations (adapted from Tsuda and Katagiri, 2010).

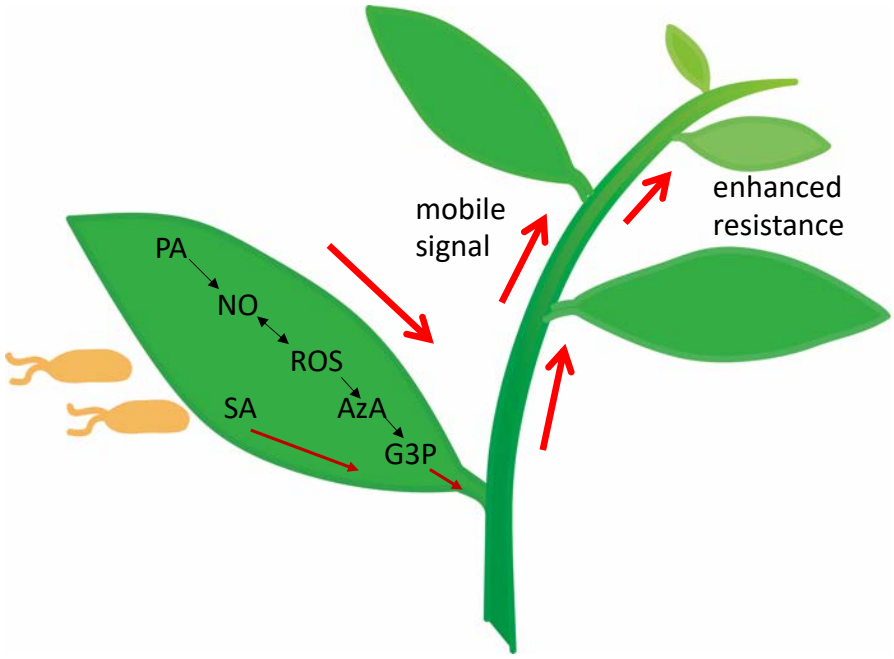

Figure 1.2 A simplified diagram showing SAR signals and their interactions

Pathogen attack (avirulent) induces the accumulation of SA and Pip in the local leaves. Pip confers plant SAR by promoting NO production. NO and ROS operate in a feedback loop and facilitate the biosynthesis of AzA. AzA functions upstream of G3P in the local leaves. SAR signals SA, G3P, AzA, and Pip can be detected in the petiole exudate collected from leaves inoculated with avirulent pathogen. Red arrows indicate transport of SA, G3P, and Pip from local to distal leaves (Modified from Wang et al., 2018).

CHAPTER 2. METHODS

2.1 Plant growth conditions and plant materials used

Plants were grown in walk-in chambers at 22°C, 65% relative humidity, and a photoperiod of 14 hours. Cool white fluorescent bulbs (Sylvania, FO96/841/XP/ECO) were used in the chambers and the photon flux density of the day period was 106.9 µmoles m-2 s-1 (measured using a digital lightmeter, Phytotronics Inc.). Seeds were sowed on autoclaved PRO-MIX soil (Premier Horticulture Inc.). Soil was fertilized once with Scotts Peters 20-10-20 peat lite special general fertilizer which contained 8.1% ammoniacal nitrogen and 11.9% nitrate nitrogen (Scottspro.com). Deionized or tap water was used to irrigate plants. Arabidopsis mutants and transgenic lines used in this study were listed in Table 2.1.

2.2 DNA extraction and genotyping analysis

For small scale DNA extraction, 10-20 mg leaf tissue were frozen in liquid nitrogen, ground with an autoclaved nucleotide-free plastic pestle and suspended in 200 µL of DNA extraction buffer containing 200 mM Tris-HCl pH 8.0, 25 mM EDTA, 1% (w/v) SDS and 250 mM NaCl. The homogenate was extracted with 100 µL of phenol: chloroform: isoamyl alcohol (25:24:1) and centrifuged at 6,000 x g for 10 min. One hundred fifty µL of the upper phase was transferred to a new microfuge tube, precipitated with 115 µL of isopropanol, mixed by inversion and centrifuged to collect DNA pellet (6,000 x g for 10 min). The pellet was air dried and re-suspended in 50-100 µL of sterile milli-Q water. Genotyping was conducted via PCR (polymerase chain reaction) using gene specific primers (Table 2.2).

2.3 Pathogen infection

Bacterial pathogens used in this study include the *Pseudomonas syringe* pv. *tomato* (*Pst*) virulent strain DC3000 (carrying pVSP61 empty vector), Pst avirulent strains *avrRpm1* (carrying pVSP61-AvrRpm1 construct) and *avrRpt2* (carrying pVSP61-AvrRpt2 construct). The bacterial stock was first streaked on King's B agar plates containing 25

μg/mL of rifampicin and 50 μg/mL of kanamycin and incubated at 29 °C for two days. A single bacterial colony was cultured for 12-16 h in 10 mL King's B broth medium (containing 25 μg/mL of rifampicin and 50 μg/mL of kanamycin) (King's B 1 L broth: 20 g of peptone, 10 mL of glycerol, 1.5 g of K_2HPO_4, 1.5 g of $MgSO_4$ and pH was adjusted to 7.5; for plates, 15 g agar was added). The cultured cells were centrifuged at 1000 × g for 5 min, washed once with 10 mM $MgCl_2$ and resuspended in 10 mM $MgCl_2$. The bacterial concentration was measured by a spectrophotometer (A600) and the cells were suspended at a concentration of 10^5-10^7 CFU (colony-forming units)/mL. For plant inoculation, bacterial suspension was infiltrated into the abaxial surface of the leaf using a needle-less syringe.

For SAR assay, three lower leaves of plants were infiltrated with 10 mM $MgCl_2$ (mock) or 1 × 10^7 CFU/mL *avrRpm1*. Two days later, three distal leaves of mock or avrRpm1 treated plants were inoculated with 1 × 10^5 CFU/mL DC3000. DC3000 growth was monitored at 0 and 3 dpi (day post inoculation). To measure bacterial growth, twelve leaf discs (three discs combined as one repeat) were collected and homogenized with 10 mM $MgCl_2$ solution and 1/10 (for 0 dpi) or $1/10^5$ (for 3 dpi) of the homogenate was plated on King's B plates and bacterial colonies were counted manually.

2.4 Petiole exudate and apoplastic fluid collection

Plants were first inoculated with mock (10 mM of $MgCl_2$) or 10^6 *avrRpm1*, 8~10 h later, inoculated leaves were excised from the plants at the lower end of petioles. The leaves were first rinsed in 50% (v/v) ethanol and then washed twice with 1mM EDTA solution (pH 8.0, in water). Approximately 10 washed leaves were then transferred (petioles down) into opened lid microcentrifuge tubes filled with collection solution (1 mM EDTA, 100 μg/mL of ampicillin in water, pH 8.0). The tubes were kept inside a glass container to prevent excessive evaporation and the glass container was placed inside of the plant growth chamber. The plant exudates were collected for 2 days, followed by freeze drying and were re-suspended in 200 μL of water and filtered through a 0.45 μm microcentrifuge filter (Spin-X centrifuge tube filter, Costar, 0.45 μm nylon, 2 mL tube, CN: 8170). The protein concentration of the petiole exudate was estimated using the Bradford assay (Bradford,

1976). Apoplastic fluid collection was carried out as described before (Villiers and Kwak, 2013).

2.5 G3P, AzA, SA, Pip and NHP quantifications

For G3P quantification, 10 mg of lyophilized leaf tissue was frozen and ground in liquid nitrogen in a 1.5 mL microfuge tube using sterile plastic pestles. The ground leaf powder was suspended in 1 ml of G3P extraction buffer (80% ethanol, 25 mM NaH2PO4 ,1 mM sodium orthovanadate and 10 mM sodium pyrophosphate), 4 µg of adonitol was added as an internal standard. The extract was boiled immediately for 5 min and centrifuged at 6,000 × g for 10 min. The supernatant was then transferred to a 13 x 100 mm glass tube and dried under a stream of nitrogen gas. The dry pellet was resuspended in 200 µl of water and transferred to a new 1.5 mL microfuge tube and centrifuged at 6,000 × g for 20 min to remove chlorophyll. The supernatant was transferred to a GC vial, dried under nitrogen gas, suspended in 75 µl of acetonitrile and derivatized with 75 µl of MSTFA (N-Methyl-N-(trimethylsilyl) trifluoroacetamide) (containing 1% TCMS (2,2,2-Trifluoro-N-methyl-N-(trimethylsilyl)-acetamide, chlorotrimethylsilane)) at 65 °C for 1 h. The derivatized reactions were analyzed by gas chromotography-mass spectrometry (GC-MS). AzA quantification were carried out as described earlier (Chanda et al., 2011). SA and SA glucoside were extracted and measured as described before (Chandra-Shekara et al., 2006). Pip quantification was carried out using GC-MS as described before (Yu et al., 2020).

For total NHP quantification, 10 mg lyophilized leaf tissue was ground using liquid nitrogen in a 1.5 mL microfuge tube and suspended in 1 ml of 80% methanol containing 1 µg of anisic acid as an internal standard. The extract was vortexed at 4 °C for 10 min and centrifuged at 6,000 × g for 10 min. The supernatant was then transferred to a 13 x 100 mm glass tube and dried under a stream of nitrogen gas. The dry pellet was resuspended in 200 µl of 50 mM Phosphate buffer (pH 5.0), transferred to a fresh 1.5 mL microfuge tube and centrifuged at 6,000 × g for 20 min to remove chlorophyll. The supernatant was transferred to a GC vial and reacted with 15 units of β -galactosidase at 30 °C for 1 h. The reaction was then dried under nitrogen gas, suspended in 50 µl of acetonitrile and derivatized with 50 µl of MSTFA (containing 1% TCMS) at 65 °C for 1 h. NHP levels were quantified using GC-MS.

2.6 Amino acids extraction and quantifications

For amino acids extraction, 100 mg of fresh leaf tissue was frozen and ground in liquid nitrogen in a 1.5 mL microfuge tube using sterile plastic pestles. The ground leaf powder was extracted with 1 ml of chloroform: methanol: water solution (1: 2.5 :1, volume). The supernatant was transferred to a 13 x 100 mm glass tube, and the pellet was re-extracted with 1 ml of chloroform: methanol: water solution. The supernatants were combined and 200 ng of anisic acid was added as an internal standard. The extract was dried under a stream of nitrogen gas. The dry pellet was resuspended in 200 µl of water and transferred to a new 1.5 mL microfuge tube and centrifuged at 6,000 × g for 20 min to remove chlorophyll. The supernatant was transferred to a GC vial, dried under nitrogen gas, suspended in 75 µl of acetonitrile and derivatized with 75 µl of MTBSTFA (N-Methyl-N-tert-butyldimethylsilyltrifluoroacetamide) (containing 1% TCMS) at 110 °C for 2 h. The derivatized reactions were analyzed by GC-MS.

2.7 Fatty acid analysis

Fatty acid (FA) extraction was carried out by placing 50 mg leaf tissue in 2 ml of 3% H_2SO_4 in methanol. After 30 min of incubation at 80°C, 1 ml of hexane with 0.001% butylated hydroxytoluene (BHT) was added. The hexane phase was then transferred to vials for GC analysis. One-microliter samples were analyzed by GC on an Agilent 0.25 mm x 50 m FAME column and quantified using flame ionization detection. For quantification of FAs, leaves (50 mg) were extracted together with an internal standard 17:0 (Sigma-Aldrich), and the FA levels were calculated based on the detected peak areas corresponding to the FA retention time relative to the areas of the internal standard.

2.8 Galactolipid analysis

Thin layer chromatographic (TLC) analysis of galactolipids of MGDG (monogalactosyldiacylglycerol) and DGDG (digalactosyldiacylglycerol) was carried out as described before (Gao et al., 2014b; Yu et al., 2013). For MGDG and DGDG recovery from TLC plates, 0.005% primulin in 80% acetone in water was sprayed on the TLC and bands were visualized under long wave UV light. The MGDG and DGDG bands were

scraped off the TLC plates and eluted with approximately 10 ml of the TLC developing solvent mixture acetone: toluene: water (90:30:7.5, by vol). A small portion of the eluted galactolipids was used for quantification and the remaining portion was dried under a stream of nitrogen gas and re-constituted in 1 ml of acetone. For MGDG and DGDG quantification, ~300 mg of Arabidopsis leaf tissue was suspended in 600 µl of chloroform: methanol: formic acid (20:10:1, by vol), vortexed vigorously for 5 min followed by addition of 300 µl of 0.2 M H_3PO_4 and the samples were revortexed for additional 1 min. After a brief centrifugation for 1 min at 6,000 × g, the lower phase was transferred to a glass test tube and the upper phase was re-extracted with 300 µl of chloroform. The extract was combined and dried under a stream of nitrogen gas. The samples were reconstituted in 1 ml of chloroform and 100 µl was loaded on a TLC plate prepared as described earlier (Gao et al., 2014b; Yu et al., 2013). The MGDG and DGDG bands were scraped and added to a glass test tube containing 20 µg of triheptadecanoin in 100 µl of chloroform: methanol (2:1, by vol). To this 500 µl of 4.8% sodium methoxide was added and the samples were shaken for 40 min at 150 rpm. The samples were mixed with 1 ml of hexane: MTBE (96:4, v/v) and 600 µl of 0.9% KCl, centrifuged at 500 × g for 1 min followed by the transfer of the upper layer to a GC vial. The samples were dried, resuspended in 400 µl of hexane and the FA content was analyzed using GC equipped with a FAME (0.25mm x 50 m) column.

2.9 Chemical treatments

SA, G3P, AzA and Pip treatments were carried out by using 500, 100, 1000 and 1000 µM solutions, respectively. SA was prepared and diluted in water. AzA and Pip stocks were prepared in methanol and diluted in water. All dilutions were freshly prepared before performing biological experiments. G3P was dissolved and diluted in water.

DETA-NONOate ((Z)-1-[N-(2-aminoethyl)-N-(2-ammonioethyl) amino] diazen-1-ium-1,2-diolate), Sulfo-NONOate (Hydroxydiazenesulfonic acid 1-oxide), H2O2 and aromatic amino acids were prepared and diluted in water at desired concentrations.

2.10 RNA extraction, reverse transcription and quantitative real-time PCR

Small-scale extraction of RNA from two or three leaves (per sample) was performed with the TRIzol reagent (Thermo Fisher Scientific), following the manufacturer's instructions. Reverse transcription (RT) and first-strand complementary DNA synthesis were carried out using SuperScript II (Thermo Fisher Scientific). Quantitative real-time PCR was carried out as described before (Zhang et al., 2009). Each sample was run in triplicate, and ACTIN2 (At3g18780) expression levels were used as an internal control for normalization. Cycle threshold values were calculated by SDS 2.3 software.

2.11 Protein extraction and immunoblot analysis

Proteins were extracted in buffer containing 50 mM Tris-HCl (pH 7.5), 10% glycerol, 150 mM NaCl, 10 mM $MgCl_2$, 5 mM EDTA, 5 mM DTT (dithiothreitol), and 1× protease inhibitor cocktail (Sigma-Aldrich). Protein concentration was measured by the Bio-Rad protein assay (Bio-Rad). For Ponceau S staining, polyvinylidene difluoride membranes were incubated in Ponceau S solution (40% methanol (v/v), 15% acetic acid (v/v), and 0.25% Ponceau S). The membranes were distained using deionized water. Proteins (~50 μg) were fractionated on an 8 to 12% SDS–polyacrylamide gel electrophoresis gel and subjected to immunoblot analysis using GFP or MYC antibody. Immunoblots were developed using an enhanced chemiluminescence (ECL) detection kit (Roche)

2.12 Trypan blue staining

The leaves were vacuum infiltrated with trypan blue staining solution (10 mg of trypan blue in 10 ml of acidic phenol, 10 ml of glycerol, and 20 ml of sterile water). The samples were placed in a water bath (65°C) for 10 min and incubated at room temperature for 8-12 h. The samples were de-stained using chloral hydrate (25 g/10 ml sterile water; Sigma-Aldrich), mounted on slides and observed for cell death with a compound microscope. The samples were photographed using an AxioCam camera (Zeiss, Germany).

2.13 Hydrogen peroxide staining (DAB staining)

The leaves were placed in 6-well plates containing 2-5 mL of DAB (3,3'-diaminobenzidine) staining solution (1 mg/mL of DAB, 200 mM of Na_2HPO_4, pH 3.0, 1 μL/mL of Tween 20,). A gentle vacuum was applied in order to penetrate staining solution into leaf tissues. The plates were incubated at room temperature for 6-8 h on an orbital shaker set at 150 rpm (Varion Inc., model T, New Jersy, USA). Staining solution was discarded and de-staining solution containing ethanol: acetic acid: glycerol (3:1:1) was added to the leaves and the plates were boiled in a water bath for 5~10 min. The leaf samples were mounted on slides using glycerol and photographed using an AxioCam camera (Zeiss, Germany).

2.14 Conductivity (Ion leakage) assays

Electrolyte leakage was measured in ~4-week-old plants. Leaves were infiltrated with $MgCl_2$ or *avRpm1* (10^6 CFU/ml). After inoculation, ~5 leaf discs (diameter, 7 mm) per plant were removed with a cork borer, floated in distilled water for ~30 min, and subsequently transferred to tubes (8 leaf discs per tube) containing 5 ml of distilled water. Conductivity of the solution was determined with a National Institute of Standards and Technology (NIST) traceable digital conductivity meter (Fisher Scientific) at the indicated time points. Standard deviation (SD) was calculated from four replicate measurements per genotype per experiment.

2.15 GSNOR1-pGWB5 vector construction and generation of transgenic plants

GSNOR1 full-length CDS was amplified from Col-0 cDNA and cloned into pGWB5 (Martin et al., 2009). The construct was introduced into Agrobacterium tumefaciens strain MP90. Transgenic Arabidopsis plants expressing 35S-GSNOR1 were generated in the *gsnor1* background using the floral dip transformation method (Clough and Bent, 1998).

2.16 Confocal microscopy

For confocal imaging, samples were scanned on an Olympus FV3000 microscope (Olympus, Tokyo, Japan). Water-mounted sections of leaf tissue were examined by

confocal microscope equipped with lasers spanning the spectral range of 405-633 nm. GFP and RFP was excited using 488, and 543 nm laser, respectively.

2.17 NO staining

For NO root staining, Arabidopsis roots were incubated in a solution containing 0.1 mM $CaCl_2$, 10 mM KCl and 10 mM MES-Tris (incubating solution, pH 5.6) for 1 h, and stained with 10 μM DAF-2 DA (4,5-diaminofluorescein diacetate, molecular probe) for 45 min, then washed twice with incubating solution. Roots were observed under Olympus FV3000 laser-scanning confocal microscope using 488 nm laser (He et al., 2004).

For NO leaf staining, Arabidopsis leaves were infiltrated with 10 μM DAF-2DA (prepared with the incubating solution), these leaves were transferred into the 10 μM DAF-2DA staining solution and incubated for 1 h with gentle swing, leaf discs were washed twice with incubating solution and observed under Olympus FV3000 laser-scanning confocal microscope using 488 nm laser (He et al., 2004; Mandal et al., 2012).

2.18 Protoplast ^{14}C-SA transport assays

Protoplasts were prepared as described before (Lim et al., 2020), quantified using a hemocytometer, and suspended at a concentration of 10^6/ml. For 14C-SA transport assays, 200 μl of freshly prepared protoplast were incubated with 2 μM ^{14}C-SA for 1 h, the protoplasts were pelleted by centrifuging at 100 × g for 3 min and the supernatant was transferred to a plastic vial (used for liquid scintillation counting). The protoplast pellets were washed and centrifuged for 3 min for four times with W5 buffer (154 mM NaCl, 125 mM $CaCl_2$, 5 mM KCl, 2 mM MES (2-(N-morpholino) ethanesulfonic acid), pH 5.7) and the supernatants were all combined into one plastic vial. Radio activity in the protoplast and the supernatants were measured by using a liquid scintillation counter.

2.19 D7-FAM transport assays

The 6-carboxyfluorescein (FAM) tagged D7 RNA (D7-FAM, synthesized by Integrated DNA Technologies or Eurofins Genomics) was dissolved in RNase free water. The abaxial surface of three-week-old Arabidopsis leaves was infiltrated with 5-10 μM D7-

FAM. The plants were then kept in a growth chamber with 14 h light and 10 h dark photoperiods and the infiltrated (local) and un-infiltrated (distal) leaves were analyzed by confocal microscopy using 488 nm laser (Shine et al., 2022, In press).

2.20 Statistics and reproducibility

For pathogen assays, about 16 plants/genotype/treatment were analyzed in a single experiment. At least three to four technical replicates/genotype/treatment were plated. For metabolite quantification, around 12 plants/genotype/treatment were analyzed in each experiment. Experiments were repeated at least two to three times with a different set of plants. Unless otherwise mentioned, error bars indicate SD.

Table 2.1 Seed materials used in this study

No.	Mutants and transgenic lines	References
1	Columbia-0 (Col-0)	Kachroo et al., 2003
2	*gsnor1* (*gsnor1-3*)	Feechan et al., 2005
3	*par2-1*	Chen et al., 2009
4	35S-GSNOR1-GFP (*gsnor1*)	This study
5	35S-AZI1-MYC	Pitzschke et al., 2014
6	35S-DIR1-GFP	From Stephen B Ryu (Korea)
7	35S-AZI1-MYC (*gsnor1*)	This study
8	35S-DIR1-GFP (*gsnor1*)	This study
9	*tga1 tga4*	This study
10	*mod1*	Lim et al., 2020
11	*camta2/3*	Kim et al., 2013
12	*camta1/2/3*	Kim et al., 2013
13	*wrky70*	Li et al., 2006
14	*gsnor1 cmata2/3*	This study
15	*gsnor1 camta1/2/3*	This study
16	*gsnor1 wrky70*	This study
17	*sid2*	Kachroo et al., 2005
18	*gsnor1 sid2*	This study
19	*gsnor1 npr1*	This study
20	*gsnor1 ald1*	This study
21	*gsnor1 rbohD*	This study
22	Nossen (Nö)	Kachroo et al., 2001
23	*ssi2*	Kachroo et al., 2001
24	*ald1*	Návarová et al., 2012
25	*fmo1*	Návarová et al., 2012
26	*ssi2 sid2*	Kachroo et al., 2005
27	*ssi2 ald1*	This study
28	*ssi2 fmo1*	This study
29	*ssi2 gsnor1*	This study
30	*nox1*	He et al., 2004
31	*ssi2 nox1*	This study
32	*act1*	Kachroo et al., 2003
33	*nox1 camta1/2/3*	This study

Table 2.2 List of primers used in this study

Primer name	Primer sequence	Use
gsnor1-s-LP	ACATTGATGTGTCTCTGGGC	Genotyping
gsnor1-s-RP	GACAAAGAGCAGTGTAGAGG	Genotyping
GSNOR1-qRT-2F	GGTCTCTTTCCTTGTATTCTAG	qPCR
AZI1-qRT (Fwd)	TCCGGAAACAGCTGTCCTAT	Genotyping
MYC-tag Rev	CAAGTCTTCCTCGGAGATTAGCTT	Genotyping
GFP-Fwd (~350 bp)	ATGGTGAGCAAGGGCGAGGAG	Genotyping
GFP-Rev (~350 bp)	ATGCGGTTCACCAGGGTGTCG	Genotyping
tga1-1(SALK_028212)-LP	AAACCTGGATTCATGGTTTCC	Genotyping
tga1-1(SALK_028212)-RP	GTGTCCCCTCTGGTTTCTTTC	Genotyping
TGA1-qRT-Fwd	ACGAACCTGTCCATCAATTCGG	qPCR
TGA1-qRT-Rev	CCATGGGAAGTATCCTCTGACACG	qPCR
tga4-1(SALK_127923C)-LP	TGCTGAAGTTTTCCACATTCC	Genotyping
tga4-1(SALK_127923C)-RP	GACACATTTTGTTCCACCGAG	Genotyping
TGA4-qRT-Fwd	AAAGTCGTTTGCGCAAGAAAGC	qPCR
TGA4-qRT-Rev	AGCATTGGTATCTACTCCGTTCCC	qPCR
SARD1-qRT-Fwd	CCTCAACCAGCCCTACGTTA	qPCR
SARD1-qRT-Rev	TAGTGGCTCGCAGCATATTG	qPCR
CBP60g-RT-Fwd	AGAAGAATTGTCCGAGAGGAG	qPCR
CBP60g-RT-Rev	GGCGAGTTTATGAAGCACAG	qPCR
SALK_008187(camta1)LP	CAGGTTCCATGATTGGAAAAC	Genotyping
SALK_008187(camta1)RP	ACTCAGATCGGTTAGGGTTCG	Genotyping
SALK_007027(camta2)LP	GGAACCTCCACTTCTCCAAAC	Genotyping
SALK_007027(camta2)RP	CCCTGTTAACGTCAGAGCATC	Genotyping
SALK_001152(camta3)LP	TGAAAACCTGATGAATCCGAG	Genotyping
SALK_001152(camta3)RP	TGTTTGGGCAAACAGAAGTTC	Genotyping
Salk_025198/WRKY70RP	CAAACCACACCAAGAGGAAAG	Genotyping
Salk_025198/WRKY70-LP	GGTGTTACACGTGTGGTTTCC	Genotyping
sid2 CAPS Fwd (MfeI)	CTGTTGCAGTCCGAAAGACGA	Genotyping
sid2 CAPS Rev (MfeI)	CTAGAGCTGATCTGATCCCGA	Genotyping
SID2 Real time Fwd	CCAATTGACCAGCAAATCGGAGCA	qPCR
SID2 Real time Rev	CGTTTCCGTTTCCGTTTCCGTTCT	qPCR
ssi2 dCAPS Fwd	TTGGTGGGGGACATGATCACAGAAGA	Genotyping
ssi2 dCAPS Rev	AAGTAGGACTAGCACCTGTTTCATCC	Genotyping
Salk_007673 (ald1) LP	GTTATTTGCTCTGGAATAGGC	Genotyping
Salk_007673 (ald1) RP	TTTTAAATGGAACGCAAGGAG	Genotyping

ALD1-qRT-Fwd	GGATTGGCATGCCTTTCTTC	qPCR
ALD1-qRT-Rev	TGAACCCACAAGTATGGAGC	qPCR
Salk_026163 (fmo1) LP	ATTATTGGGTGTGGGGCTTACC	Genotyping
Salk_026163 (fmo1) RP	CTGCTTTGGACGTATCCTACG	Genotyping
FMO1-qRT-Fwd	CTTGGCTTGAGTTTCCAA	qPCR
FMO1-qRT-Rev	CCACATTGAACGTAGCTCTG	qPCR
nox1-Genotyping-Fwd	TCTCGTTCTGATGGCTCCTGTG	Genotyping
nox1-Genotyping-Rev	GTGTAACCGGTGATACTCTCGCC	Genotyping
act1-CAPS Fwd (BsmF I)	GCCATCAAGTGTTCATCTACT	Genotyping
act1-CAPS Rev (BsmF I)	GGAAGTCATACAAGGTTGCTA	Genotyping
ADT1-qRT-Fwd	GCTTCCTAAACCGCTAACTG	qPCR
ADT1-qRT-Rev	GCTGTCTCACTATATGCACCT	qPCR
ADT2-qRT-Fwd	AACCTCACAAAGATTGAAAGCC	qPCR
ADT2-qRT-Rev	GCCATAGATGCTTCAAAGTCC	qPCR
ADT3-qRT-Fwd	ATCATTGTCTCATTGCTCTTCC	qPCR
ADT3-qRT-Rev	GTATCATCAACAGCTTCACGAG	qPCR
ADT4-qRT-Fwd	ATCTCAAGTTCCGATCAACAG	qPCR
ADT4-qRT-Rev	AACGACTCCGACCTATAACC	qPCR
ADT5-qRT-Fwd	GTTGATTTAAGCCTTGTTCCGT	qPCR
ADT5-qRT-Rev	ACGAAGAGTAGATCCATGAGAC	qPCR
ADT6-qRT-Fwd	GAGAAATCTGATAGCAATCCGT	qPCR
ADT6-qRT-Rev	GGAACACCTTGATAAGCGAC	qPCR

CHAPTER 3. CHARACTERIZATION THE ROLE OF S-NITROSOGLUTATHIONE REDUCTASE 1 (GSNOR1) IN SYSTEMIC ACQUIRED RESISTANCE

3.1 Introduction

Nitric oxide (NO) is present in various tissues and organs in mammals and has been recognized as an important signaling molecule in the nervous system, immune system, cardiovascular system and endocrine system. Studies of NO in plants emerged more recently and it was found that NO has crucial regulatory roles in diverse physiology processes including growth, development and stress responses (Domingos et al., 2015). Current findings suggest NO executes its physiological roles mainly through posttranslational modifications, including tyrosine nitration, metal nitrosylation, and S-nitrosylation. While a number of proteins modified through tyrosine nitration and metal nitrosylation have been reported, NO-mediated protein S-nitrosylation has been the most studied in plants. S-nitrosylation is a redox-based protein modification by covalently adding a nitrogen monoxide group to the reactive thiols of a cysteine residue, which regulates protein activities through changing protein conformation, stability, cellular localization and affecting protein-protein interactions (Sami et al., 2018).

In mammals, NO biosynthesis is mainly dependent on NITRIC OXIDE SYNTHASE (NOS), which catalyzes conversion of L-arginine to L-citrulline (Fukuto and Wink, 1999) and generates NO as a byproduct. In plants, even though animal NOS inhibitors appear to affect NO production, currently no canonical NOS gene has been identified. Details regarding NO biosynthesis in plants are still lacking, but genetic and pharmacological studies suggest that NITRATE REDUCTASE (NR) and NOA1 (NO ASSOCIATED 1) proteins play important roles in controlling NO biosynthesis in plants (Desikan et al., 2002; Guo et al., 2003; Gupta et al., 2011).

NO is a free radical, as it has an unpaired electron, which makes NO a highly reactive molecule. NO can react with the superoxide anion (O2-) and other biologic molecules to form NO derived reactive nitrogen species (RNS), including ONOO-, S-nitrosothiols (such as S-Nitrosoglutathione, GSNO), nitroxyl (HNO), nitrosonium cation (NO+), higher

oxides of nitrogen (Martinez and Andriantsitohaina, 2009). GSNO is formed when NO reacts with glutathione (GSH), and this reaction is believed to be reversible and independent of enzyme activity. GSNO is the active cellular molecule that mediates protein S-nitrosylation in both plants and animals. GSNO is relatively more stable compared to NO and can be transported throughout the cells and thereby mediating NO function and serve as a major bioactive NO reservoir across different living organisms. GSNO breakdown is catalyzed by the conserved GSNO reductase (GSNOR) (Feng et al., 2019). It has been shown that GSNOR function is associated with blood pressure regulation and stress responses in animals. In plants, GSNOR proteins were shown to be involved in immune responses, hormone signaling, growth and development (Feechan et al., 2005; Ohtani et al., 2018; Shi et al., 2015; Wang et al., 2015).

In *Arabidopsis*, there is a single copy of the GSNOR1 (GSNO REDUCTASE 1) gene and Arabidopsis gsnor1 mutant plants have altered disease resistance to different pathogens (Feng et al., 2019). Likewise, silencing of the GSNOR1 gene in tomato affects their defense response (Rusterucci et al., 2007), suggesting GSNOR1 likely plays a conserved role in different plants. Upon pathogen infection, the gsnor1 plants accumulate significantly less SA compared to wild type (WT) plants (Feechan et al., 2005). NON-EXPRESSOR OF PATHOGENESISRELATED 1 (NPR1) is a SA co-receptor and acts as a master regulator of SA-induced defense responses (Cao et al., 1997; Fu et al., 2012; Zavaliev et al., 2020). NPR1 was reported to be a target of GSNO-mediated S-nitrosylation and this post-translational modification regulates NPR1 protein conformation and subcellular localization thereby controlling NPR1-mediated defense signaling (Tada et al., 2008). In addition, transcription factor TGA1, an important signaling component of the SA pathway, is also subjected to GSNO-mediated S-nitrosylation during defense response (Lindermayr et al., 2010). These findings strongly suggest that GSNOR1 regulates the SA pathway.

Previous work from the Kachroo lab showed that NO confers plants SAR in a dose dependent manner (Wang et al., 2014). In this study I investigated the role of GSNOR1 in

Arabidopsis SAR. I show that GSNOR1 regulates SA and Pip biosynthesis and that higher NO levels in gsnor1 plants may regulate SAR by modulating SA transport.

3.2 Results

3.2.1 The *gsnor1* mutant plants are compromised in SAR

Earlier studies suggest *Arabidopsis gsnor1* mutant plants accumulate high levels of NO and the plants become susceptible to various pathogens (Feechan et al., 2005). It was also reported that *gnsor1* mutant is compromised in *avrRpt2* induced SAR (Wang et al., 2014). To further understand the role of GSNOR1 in SAR, I first tested SAR in two widely used GSNOR1 loss of function mutants *gsnor1-3* and *par2-1* (Chen et al., 2009; Feechan et al., 2005). For SAR assays, the lower three leaves of WT and *gsnor1* plants were infiltrated with $MgCl_2$ (mock) or avirulent pathogen *avrRpm1*. Two days later three upper leaves of these plants with virulent pathogen DC3000. Leaves were sampled at 0-and 3-day post inoculation (dpi) and monitored for DC3000 growth. Results show that while *avrRpm1* inoculation significantly increased plant resistance to DC3000 in WT plants (Col-0), the colony count between Mock and *avrRpm1* treatment for both *gsnor1-3* and *par2-1* were not statistically different, indicating that *gsnor1-3* and *par2-1* were compromised in SAR (Fig. 3.1A). To further confirm that the SAR phenotype was associated with mutation in *GSNOR1*, I transformed full length *GSNOR1* into *gsnor1-3* mutant plants. Expression of *GSNOR1* restored the *gsnor1* morphology (Fig. 3.1B) and these plants showed normal SAR (Fig. 3.1C). Together, these results suggest *GSNOR1* is required for SAR.

3.2.2 AzA/G3P pathway is not affected in the *gsnor1* plants

SAR requires two parallel branches, one of which is controlled by SA, and the other involving Pip-NO/ROS-AzA/G3P signaling cascade (Gao et al., 2014a; Kachroo and Kachroo, 2020; Shine et al., 2019). Because the *gsnor1* plants accumulate high levels of NO it was possible that they are upregulated in other downstream components like ROS, AzA or G3P. NO and ROS positively contribute to AzA production by facilitating the cleavage of the C9 double bond in C18 fatty acids (Wang et al., 2014). As shown before

(Chen et al., 2020; Olah et al., 2020), the *gsnor1* accumulated higher levels of NO than WT (Fig. 3.2A). In contrast, they accumulated WT like levels of H_2O_2, both when challenged by mock or pathogen infection (*avrRpm1*) (Fig. 3.2B). Likewise, *gsnor1* plants accumulated normal levels of AzA and G3P before and after pathogen infection (Figs. 3.2C and D). Since G3P operates in a feedback loop with AZI1 and DIR1 proteins, I next assayed levels of AZI1-MYC and DIR1-GFP proteins in the *gsnor1* plants. These genotypes were obtained by crossing *gsnor1* with *35S-AZI1-MYC* (Col-0 background) (Pitzschke et al., 2014), and *35S-DIR1-GFP* (Col-0 background) plants (From Stephen B Ryu (Korea)). Protein gel blot analysis with MYC and GFP antibodies showed that the levels of AZI1-MYC and DIR1-GFP proteins expressed in WT and *gsnor1* background were comparable (Figs. 3.2E and F). Furthermore, the localization of DIR1-GFP protein was not altered in *gsnor1* as compared in WT background (Fig. 3.2G). Together, these results suggest that increased accumulation of NO does not affect SAR components that act downstream of NO. Overexpression of AZI1 or DIR1 protein in the *gsnor1* background or exogenous application of AzA or G3P was unable to confer SAR in *gsnor1* plants (Fig. 3.2H and I). These results suggested that defective SAR phenotype of *gsnor1* plants was not associated with AZI1, DIR1, AzA or G3P.

3.2.3 The *gsnor1* plants are defective in SA transport

Consistent with earlier work (Feechan et al., 2005), the pathogen inoculated *gsnor1* plants accumulated considerably less SA and SA glucoside (SAG) than the WT plants in the infected leaves (Figs. 3.3A and B). SA levels are regulated by the transcription factors SARD1 and CBP60g, which regulate expression of *ICS1*, that encodes the SA biosynthesis enzyme ISOCHORISMATE SYNTHASE. Notably, the *avrRpm1* inoculated *gsnor1* plants showed reduced expression of *SARD1* and *CBP60g* genes (Figs. 3.3C and D), which explains reduced expression of *ICS1* and thereby lower SA levels in the infected leaves after pathogen inoculation (Fig. 3.3E). SARD1/CBP60g also regulate expression of *ALD1* (Sun et al., 2015), which encodes the AMINOTRANSFERASE that catalyzes biosynthesis of Pip (Navarova et al., 2012). As predicted, the *gsnor1* plants showed significantly lower expression of *ALD1* after pathogen infection (Fig. 3.3F), which in turn correlated with

reduced levels of Pip (Fig. 3.3G) as well as N-hydroxy Pip (NHP) that is derived from Pip (Hartmann et al., 2018) (Fig. 3.3H). Consistently, the expression of NHP biosynthesis gene FMO1 was also reduced in *gsnor1* plants (Fig. 3.3I). To determine if reduced levels of SA, Pip or NHP contributed to defective SAR in *gsnor1* plants, I assayed SAR after localized exogenous application of SA, Pip and NHP. Exogenous localized application of SA, Pip or NHP conferred SAR on WT but not on *gsnor1* plants (NHP may confer partial SAR on *gsnor1* plants) (Figs. 3.3J and K). This suggested that the SAR defect in the *gsnor1* plants was not related to accumulation of SA, Pip or NHP in the local leaves.

To determine if the SAR defect in the *gsnor1* plants was associated with transport of SAR associated metabolites, I next assayed transport of SA, G3P, Pip and NHP by quantifying levels of these metabolites in the petiole exudate (PEX) collected from mock- and pathogen (*avrRpm1*)-inoculated plants. The *gsnor1* plants transported WT like levels of G3P (Fig. 3.3L). NHP was not detected in the PEX, and Pip PEX levels showed inconsistent results. Notably, compared to WT, PEX SA levels in the *gsnor1* plants were significantly lower (Fig. 3.3M). Moreover, the pathogen inoculated *gsnor1* plants accumulated significantly reduced levels of SA in the apoplastic compartment (Fig. 3.3N) and in the cuticular wax (Fig. 3.3O). Earlier work found that although the *pad4* mutant accumulates significantly less SA than WT plants in the infected leaves upon pathogen infection, the pathogen induced SA accumulation in PEX were comparable in WT and *pad4* plants, suggesting that the apoplastic transport of SA precedes accumulation of SA in the cytosol in infected leaves (Lim et al., 2020). We predicted that *gsnor1* plants may be defective in SA apoplastic transport. To test this, I assayed SA transport in WT and *gsnor1* plants after localized application with cold or ^{14}C-SA. Both these assays showed significantly reduced transport of SA in the *gsnor1* plants (Figs. 3.3P and Q). Since accumulation of Pip in the distal leaves is dependent on normal transport of SA and G3P (Wang et al., 2018), I next quantified Pip levels in the distal tissues of WT and *gsnor1* plants. Consistent with their reduced transport of SA, the *gsnor1* plants accumulated significantly less Pip in the distal leaves (Fig. 3.3R). Since SA transport is governed by the water potential, it was possible that reduced SA transport in the *gsnor1* plants was caused by a defect in water potential. However, the *gsnor1* plants showed WT-like water potential (Fig. 3.3S). In addition, the *gsnor1* leaves were not permeable to the hydrophilic dye

toluidine blue (Fig. 3.3T), suggesting the presence of a normal cuticle. Together, these results suggest that defective transport of SA in the *gsnor1* plants was not associated with water potential or cuticular permeability.

3.2.4 The *gsnor1* plants are competent in generation of SAR signal

Earlier work has shown that impaired transport of SA in *acp4* and *mod1* plants does not affect generation of the SAR signal (Lim et al., 2020). To test if this was also the case for *gsnor1* plants, I assayed signal generation and perception by evaluating SAR inducing activity of PEX collected from Col-0 and *gsnor1* plants on both genotypes. PEX collected from *Pst avrRpm1* inoculated WT or *gsnor1* plants was able to confer SAR on Col-0 plants but not on *gsnor1* (Fig. 3.4A). This suggested that *gsnor1* plants were competent in generation of the SAR signal but were unable to perceive it. Consistent with these results, the *gsnor1* plants showed normal levels of the recently discovered RNA based SAR signal, which undergoes phased cleavage in response to pathogen infection to generate small RNAs which then travel to distal tissues to confer SAR (Shine et al., 2022, accepted manuscript) (Fig. 3.4B). A fluorescein (FAM) labelled small RNA (D7-FAM) was used to evaluate transport and local application of this RNA showed normal distribution to distal tissues (Fig. 3.4C). This result is in line with SAR based bioassays and further reinforce our conclusion that SA transport does not impair transport of the small RNA SAR signal.

3.2.5 Increased NO levels attenuate transport of SA to distal leaves

The fact that exogenous application of NO donor at or above 300 μM inhibits SAR (Wang et al., 2014), together with the result that *gsnor1* plants accumulate elevated levels of NO prompted the suggestion that higher NO levels might affect SA transport. To test this assumption, I first assayed uptake of ^{14}C-SA into the protoplasts prepared from Col-0 leaves. The freshly prepared protoplasts were incubated with various concentrations of NO donor DETA-NONOate or N_2O donor Sulfo-NONOate and ^{14}C-SA, followed by three washes before quantifying ^{14}C-SA levels in the protoplasts. The untreated and Sulfo-NONOate treated protoplasts showed similar transport that was ~2-times higher than that see in DETA-NONOate treated protoplasts (Fig. 3.5A). Incubation of DETA-NONOate

with SA did not alter SA levels or structure (Fig. 3.5B and C), suggesting that reduced import of SA in DETA-NONOate treated protoplasts was not due to any chemical alteration of ^{14}C-SA. Unlike NO donor, protoplasts treated with H_2O_2 showed normal transport and uptake of ^{14}C-SA (Fig. 3.5D). Next, I assayed SA transport in Col-0 leaves pre-treated with DETA-NONOate or Sulfo-NONOate for 12 h prior to inoculation with *Pst avrRpm1*. Leaves inoculated with mock ($MgCl_2$) and *Pst avrRpm1* were used as controls and PEX collected from leaves were assayed for SA levels. The DETA-NONOate pretreated leaves showed a significant reduction in SA levels compared to pathogen inoculated or Sulfo-NONOate pretreated leaves (Fig. 3.5E). Together, these results suggested that high levels of NO attenuates SA transport and was likely responsible for impaired SAR in the *gsnor1* plants.

Earlier work has shown that the *gsnor1* plants are partially insensitive to SA and unable to induce normal levels of the SA marker gene *PR-1* (Tada et al., 2008). Indeed, exogenous application of SA induced much lower levels of *PR-1* transcript in the *gsnor1* plants (Fig. 3.5F). To determine if the partial insensitivity of *gsnor1* plants to exogenous SA could be related to their defect in SA transport, I sprayed Col-0 and *gsnor1* plants with 500 µM SA and then monitored total- and wax- SA levels 24 h post treatments. Although, Col-0 and *gsnor1* plants accumulated similar levels of exogenous SA on their leaves, much of the applied SA was retained in the cuticular wax in the *gsnor1* plants (Figs. 3.5G, H and I). To reconfirm this result, I assayed *PR-1* gene expression in Col-0 and *gsnor1* plants after soil drench with SA. The soil drench treatment was able to distribute exogenous SA via the vasculature throughout the plants and induce normal *PR-1* expression in *gsnor1* plants (Figs. J, K and L). Importantly, soil drench with SA increased Pip levels in distal leaves (Fig. 3.5M) and restored SAR in the *gsnor1* plants (Fig. 3.5N), thus reconfirming an important role for SA transport in SAR.

Since elevated NO levels contributed to attenuated SA transport, I next performed an epistatic analysis between *gsnor1* and genes involved in NO biosynthesis/accumulation. The NO biosynthesis and accumulation in plants is governed by NIA (NITRATE REDUCTASE) and NOA1 proteins, respectively (Desikan et al., 2002; Guo et al., 2003). Surprisingly, the *gsnor1 noa1* double mutants showed *gsnor1*- and *noa1*-like morphology

and accumulated elevated levels of NO (Fig. 3.5O). To determine if this could be due to redundancy between NOA1- and NIA-dependent pathways, I generated *gsnor1 noa1 nia2* triple mutant plants. Notably, the *gsnor1 noa1 nia2* plants showed a developmental phenotype and poor seed set (Fig. 3.5O). Importantly, the triple mutant plants also accumulated elevated levels of NO (Fig. 3.5P). Consistent with their elevated NO levels, the *gsnor1 noa1* plants showed impaired SA transport (Fig. 3.5Q) and compromised SAR (Fig. 3.5R). Together, these results suggested that high levels of NO in *gsnor1* plants are not regulated by NOA1, NIA2.

3.2.6 GSNOR1 is epistatic to CAMTA and WRKY70

SA biosynthesis is positively regulated by SARD1/CBP60g as well as the TGA transcription factors TGA1 and TGA4. However, in contrast to *SARD1/CBP60g,* the *gsnor1* plants expressed WT like levels of *TGA1* and *TGA4* in infected leaves after pathogen infection (Figs. 3.6A and B), suggesting that TGA1/4 factors were not associated with compromised induction of SA levels in the *gsnor1* plants. Furthermore, even though *tag1 tga4* double mutant plants accumulated considerably less SA after pathogen infection (Figs. 3.6C and D), they transported WT like levels of SA to PEX (Fig. 3.6E). Thus, compromised SAR phenotype of *tga 1 tga4* (Fig. 3.6F) is not associated with transport of SA.

In contrast to TGA1/4, CAMTA transcription factors and WRKY70 negatively regulate SARD1 expression, and thereby SA and Pip biosynthesis (Sun et al., 2018; Sun et al., 2020; Zhou et al., 2018). Thus, it was possible that a mutation in *GSNOR1* increases *CAMTA* and *WRKY70* expression, and increased levels of these proteins in turn causes repression of *SARD1*. However, WT like levels of *CAMTA3* transcripts were observed in the *gsnor1* plants (Fig. 3.6G). There are six *CAMTA* isoforms in *Arabidopsis* which are thought to act redundantly (Bouche et al., 2002; Doherty et al., 2009; Kim et al., 2013). Of these a mutation in *camta 2/3* double or *camta 1/2/3* triple mutants shows constitutive defense and increased levels of SA and Pip (Kim et al., 2020; Sun et al., 2020). To determine if mutations in *CAMTA* and *WRKY70* can upregulate *SARD1* expression and thereby transport of SA and SAR phenotype in *gsnor1* plants, I created *gsnor1 camta1/2/3*

and *gsnor1 wrky70* mutants. Interestingly, *gsnor1* was epistatic to *camta1/2/3* and suppressed *camta1/2/3* induced cell death, H_2O_2-, SA-, Pip, NHP-levels and *camta1/2/3* stunted morphology (Figs. 3.6H, I and J). Likewise, *gsnor1* was epistatic to *wrky70*, and suppressed *wrky70*-induced constitutive SA and Pip biosynthesis (Figs. 3.6K and L). The *camta1/2/3* and *gsnor1 camta1/2/3* plants accumulated elevated levels of NO (Fig. 3.6M) and showed reduced transport of SA into PEX (Fig. 3.6N). Likewise, *gsnor1 wrky70* plants remained impaired in SA transport (Fig. 3.6O). Importantly, *gsnor1 camta1/2/3* and *gsnor1 wrky70* remained compromised in SAR (Figs. 3.6P and Q). Together, these results suggest that the *gsnor1* mutation was epistatic to *camta1/2/3* and *wrky70* and that a *gsnor1*-derived component played a major role in regulation of *SARD1* and *CBP60g* expression, and thereby *SARD1/CBP60g*-mediated regulation of SA and Pip biosynthesis.

3.3 Discussion

The last decade has seen several major breakthroughs in the SAR field with several chemicals identified and organized into two parallel branches (Gao et al., 2014a; Kachroo and Kachroo, 2020; Shine et al., 2019). One of these branches is regulated by SA and other by Pip-NO-ROS-AzA-G3P (Chen et al., 2020; Olah et al., 2020; Wang et al., 2018). These chemical signals are also known to undergo multiple non-linear interactions as well as cross-talk among the components of the two branches. In this study, I characterized SAR in *gsnor1* plants, which accumulate elevated levels of NO and show compromised SAR (Wang et al., 2014). High NO levels were not associated with increased accumulation of ROS, AzA or G3P, which function downstream of NO in the SAR pathway. Likewise, *gsnor1* plants accumulated WT like levels of AZI1 and DIR1 proteins, which operate in a feedback loop with G3P (Yu et al., 2013). Moreover, localized application of AzA or G3P were unable to confer SAR on *gsnor1* plants.

Surprisingly, high NO levels in the *gsnor1* plants were associated with impaired transport of SA into apoplast, PEX and eventually partitioning of SA into cuticular wax during pathogen infection. Recent work has reformed our view regarding the importance of SA transport in SAR (Lim et al., 2020), a notion that was discounted in an earlier study that assayed SA transport and SAR in wild-type and salicylate hydroxylase (NahG)

expressing tobacco (Vernooij et al., 1994). The grafting study relied on quantification of SA from leaves, which was unable to detect changes in a background of high basal SA. Moreover, this study did not account for the fact that SA was transported via the apoplast (Lim et al., 2016) and that cytosolically localized NahG will not be able to degrade SA present in the apoplastic compartment. Characterization of mutants impaired in cuticle permeability showed that increased transpiration in these mutant plants reduces hydrostatic pressure which in turn impairs distal transport of SA (Lim et al., 2020). A normal cuticle and water potential in *gsnor1* plants suggests that impaired SA transport was not caused by physiological changes that affect hydrostatic pressure in the apoplastic compartment. Instead, impaired SA transport in *gsnor1* plants was likely due to NO-mediated repression of the putative plasma membrane localized transporter that transports SA in a pH-dependent manner (Lim et al., 2020). Indeed, high NO levels, that are ineffective in conferring SAR (Wang et al., 2014), impaired SA transport into protoplasts and out of leaves. These results further support an important role for SA transport in SAR. When delivered via soil drench, SA was able to induce normal SAR in the *gsnor1* plants. This suggests that at least a portion of the SA delivered via soil drench is transported into the cells possibly via the symplastic route or xylem.

Soil drench with SA also normalized *PR-1* expression in the *gsnor1* plants. In contrast, whole plant spray application with SA was unable to induce WT like expression of *PR-1* in the *gsnor1* plants ((Tada et al., 2008) and this study). These results may be caused by NO-mediated nitrosylation of NPR1, which was thought to retain NPR1 in the cytosol and consequently unable to induce transcription of SA-NPR1 responsive genes in the nucleus (Kinkema et al., 2000; Tada et al., 2008). However, results based on soil drench and retention of sprayed SA in the cuticular wax of *gsnor1* leaves suggests that the inability of SA to localize NPR1 to nucleus (Tada et al., 2008) and induce *PR-1* gene expression in *gsnor1* plants may be due to a defect in *gsnor1* plants' ability to internalize sprayed SA.

In addition to SA, the *gsnor1* plants were unable to induce normal levels of Pip after pathogen infection. This in turn was associated with their inability to induce normal expression of *SARD1* and *CBP60g* transcription factors, which regulate expression of genes associated with SA (*ICS1*) and Pip (*ALD1*) biosynthesis. Interestingly, *gsnor1* was

epistatic to *camta1/2/3* and *wrky70* transcription factors, which negatively regulate *SARD1* and *CBP60g* expression and thereby SA and Pip levels. A mutation in three of the six *CAMTA* isoforms, which act redundantly in Arabidopsis, or *WRKY70*, increased *SARD1/CBP60g* expression and thereby SA and Pip levels. The *camta 1/2/3* triple mutant plants showed an autoimmune response that was associated with stunted morphology, constitutive cell death and elevated ROS levels. These phenotypes of *camta1/2/3* plants were restored to wild-type-like phenotypes in *camta ald1* and *camta fmo1* plants (Kim et al., 2020), suggesting that the autoimmune phenotype of *camta 1/2/3* plants was associated with elevated Pip and NHP levels. Interestingly, the *gsnor1* mutation was also able to suppress the autoimmune phenotypes of *camta1/2/3* even though they accumulated significantly higher levels of Pip and NHP. Together, these results suggest that the *gsnor1*-mediated suppression of the autoimmune phenotype in *camta 1/2/3* plants is likely associated with other factors besides Pip and NHP and perhaps the *gsnor1* mutation suppresses autoimmune response by targeting components downstream of NHP. Notably, both *camta 1/2/3* and *gsnor1 camta 1/2/3* plants accumulated elevated levels of NO, suggesting that high levels of NO in *camta 1/2/3* are not responsible for their autoimmune phenotype.

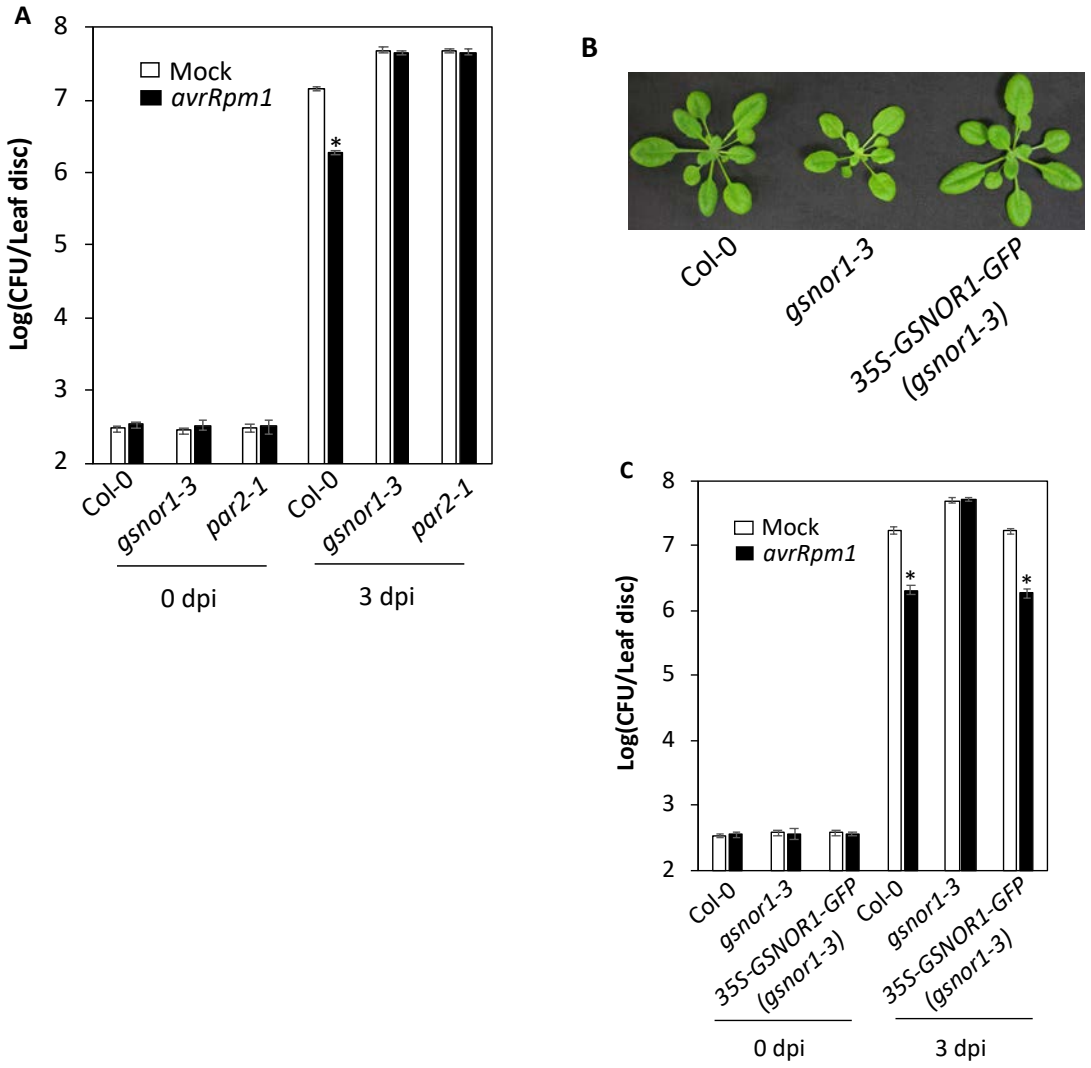

Figure 3.1 The *gsnor1* mutants are compromised in SAR

(A) SAR response in distal leaves of Col-0, *gsnor1-3* and *par2-1* plants. The virulent pathogen (DC3000) was inoculated 48 hours after local Mock (10 mM $MgCl_2$) or *avrRpm1* infiltration. Leaves were sampled at 0- or 3- dpi to measure bacterial populations. Error bars indicate SD (n = 4). CFU, colony-forming units. Asterisks denote a significant difference between *avrRpm1* and Mock (10 mM $MgCl_2$) treated leaves (t test, $P < 0.05$). The experiment was repeated twice with similar results. **(B)** The morphology of indicated genotype of plants. **(C)** SAR response in distal leaves of Col-0, *gsnor1-3* and 35S-GSNOR1-GFP (*gsnor1-3*) plants. The virulent pathogen (DC3000) was inoculated 48 hours after local Mock (10 mM $MgCl_2$) or *avrRpm1* infiltration. Leaves were sampled at 0- or 3- dpi to measure bacterial populations. Error bars indicate SD (n = 4). CFU, colony-forming units. The "*" denotes a significant

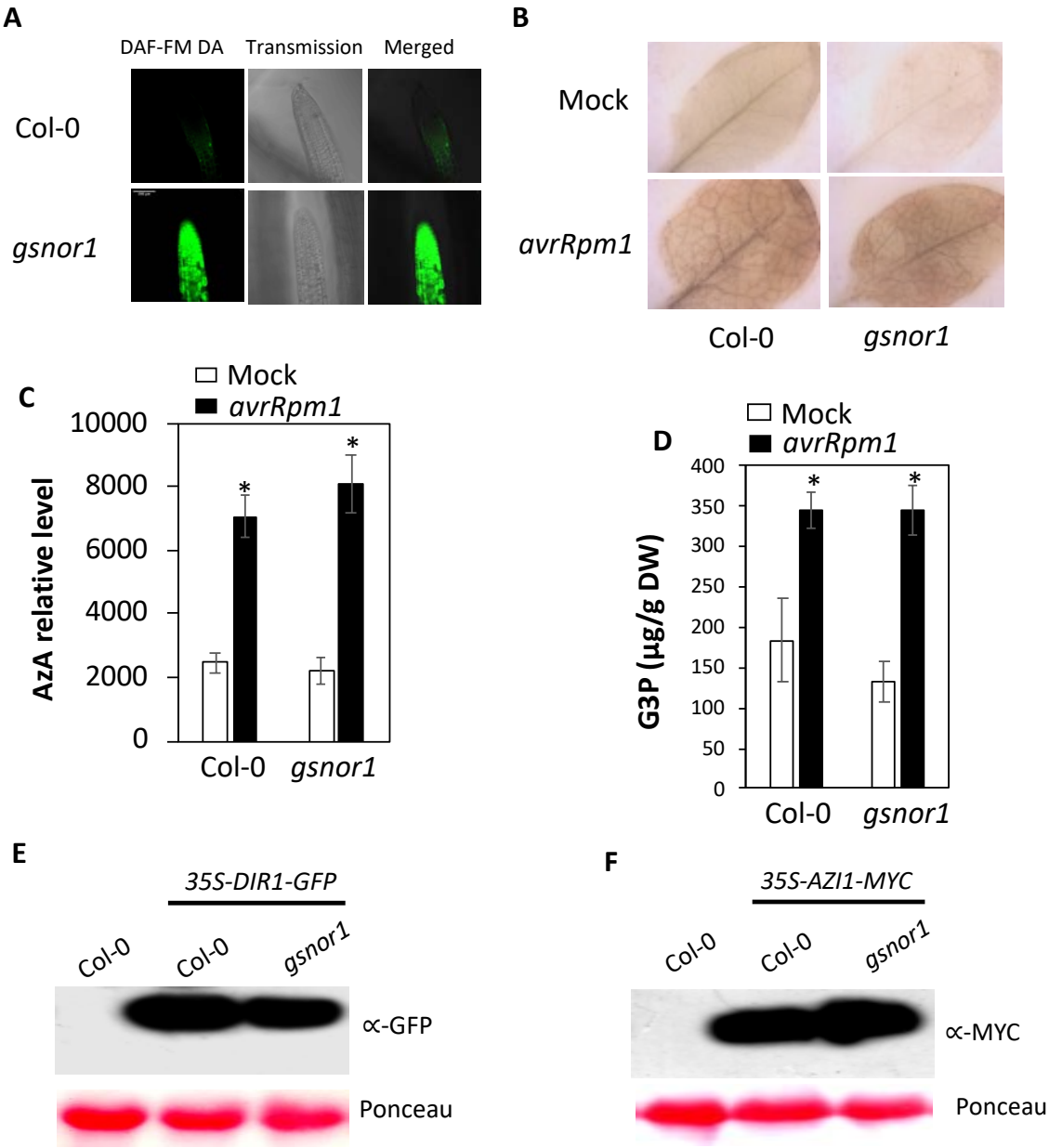

Figure 3.2 AzA/G3P pathway is not affected in the *gsnor1* plants

(A) Root NO staining in Col-0 and *gsnor1* plants. See method for detailed protocol. Scale bar, 200 µm. DAF-FM DA, 4-amino-5-methylamino-2′,7′-difluorofluorescein diacetate. **(B)** H_2O_2 detected by DAB staining in Col-0, and *gsnor1* plants after Mock (10 mM $MgCl_2$) or *avrRpm1* inoculation (16 hpi). **(C)** AzA and **(D)** G3P levels in Col-0 and *gsnor1* plants after Mock or *avrRpm1* inoculation (16 hpi). DW, dry weight. Error bars indicate SD (n = 4). The "*" denotes a significant difference with Mock treatment (10 mM $MgCl_2$) (t test, $P < 0.01$). **(E)** Western blot analysis of DIR1-GFP protein levels in 35S-DIR-GFP (Col-0) or 35S-DIR-GFP (*gsnor1*) plants. **(F)** Western blot analysis of AZI1-MYC protein levels in 35S-AZI1-MYC (Col-0) or 35S-AZI1-MYC (*gsnor1*) plants. The experiment was repeated twice with similar results.

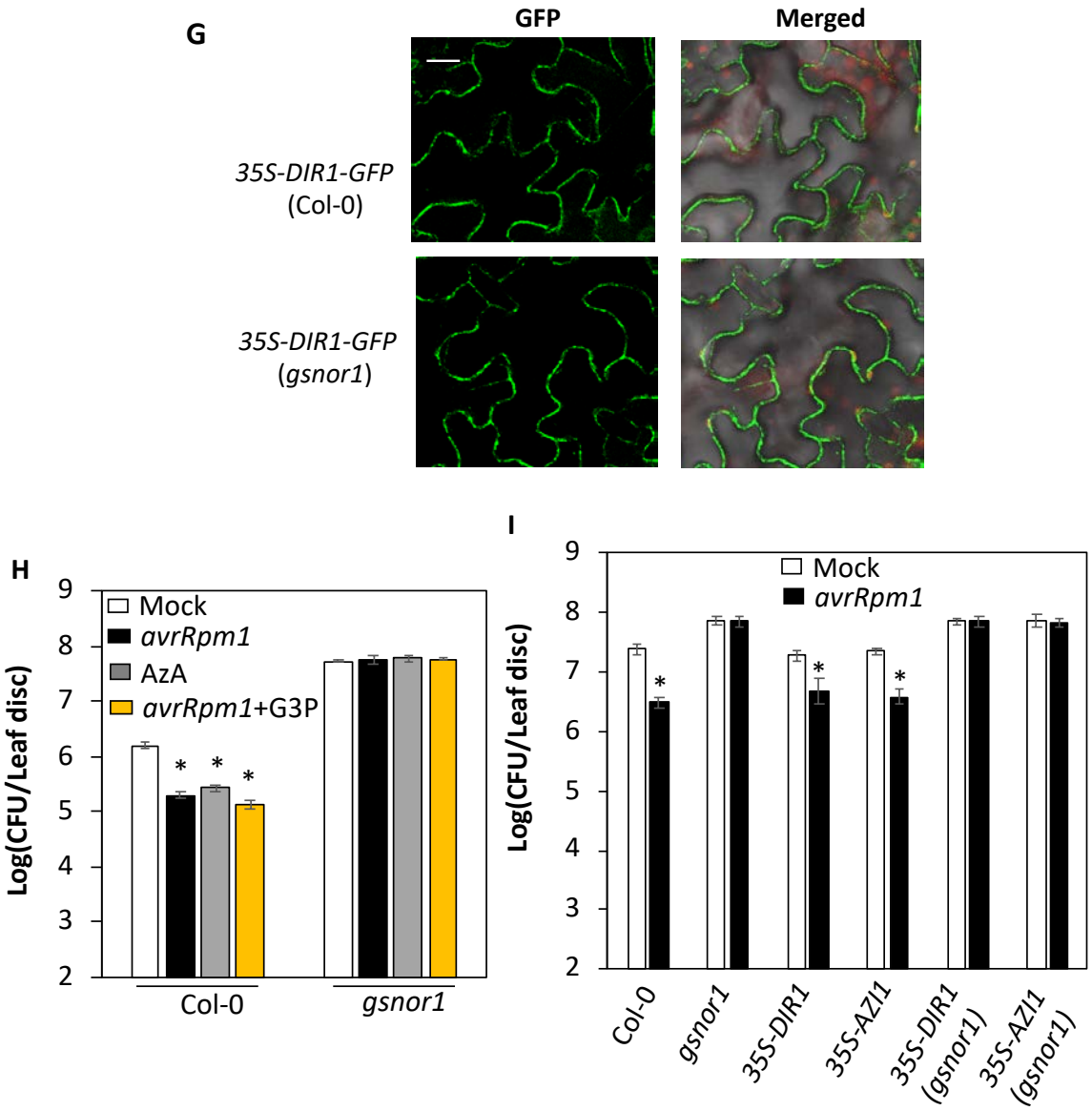

Figure 3.2 (Continued) AzA/G3P pathway is not affected in the *gsnor1* plants

(**G**) DIR1-GFP protein detected by confocal microscope. Scale bar, 10 µm. **(H)** SAR response in distal leaves of Col-0 and *gsnor1* plants locally infiltrated with Mock (10 mM $MgCl_2$), *avrRpm1*, 1 mM AzA, or *avrRpm1*+0.1 mM G3P. The virulent pathogen (DC3000) was inoculated 48 hours after local treatments. Leaves were sampled at 3 dpi to measure bacterial populations. Error bars indicate SD (n = 4). The "*" denotes a significant difference with Mock treatment (10 mM $MgCl_2$) (t test, $P < 0.01$). **(I)** SAR response in distal leaves of indicated genotype of plants locally infiltrated with Mock (10 mM $MgCl_2$) or *avrRpm1*. The virulent pathogen (DC3000) was inoculated 48 hours after local treatments. Leaves were sampled at 3 dpi to measure bacterial populations. Error bars indicate SD (n = 4). "*" denotes a significant difference with Mock treatment (10 mM $MgCl_2$) (t test, $P < 0.05$).

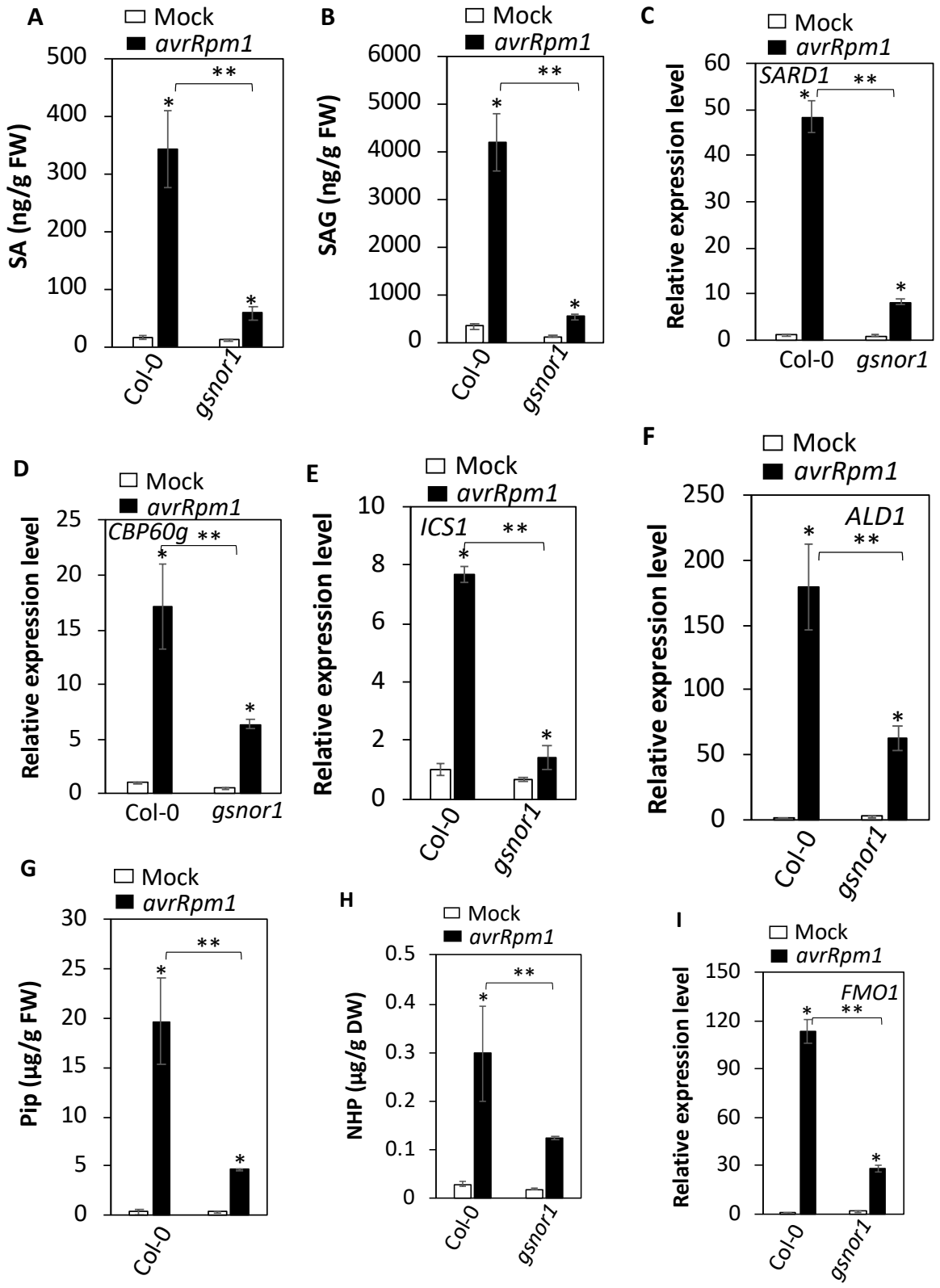

Figure 3.3 The *gsnor1* plants are defective in SA transport

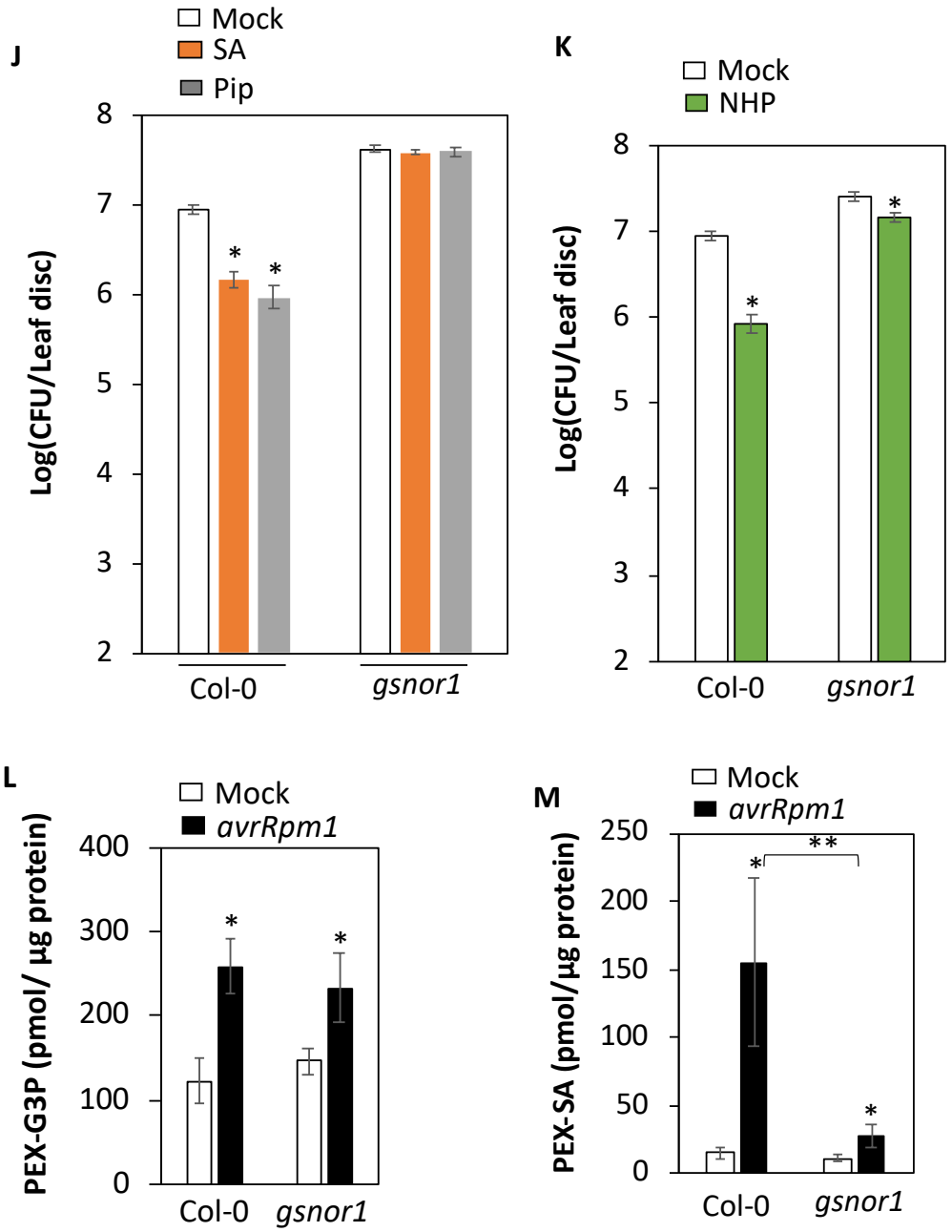

Figure 3.3 (Continued) The *gsnor1* plants are defective in SA transport

(A) SA and **(B)** SAG levels in infiltrated leaves of Col-0 and *gsnor1* plants after Mock (10 mM $MgCl_2$) or *avrRpm1* inoculation. Error bars indicate SD (n = 4). The "*" denotes a significant difference with Mock treatment (10 mM $MgCl_2$) (t test, $P < 0.01$). The "**" denotes a significant difference between two genotypes (t test, $P < 0.01$).

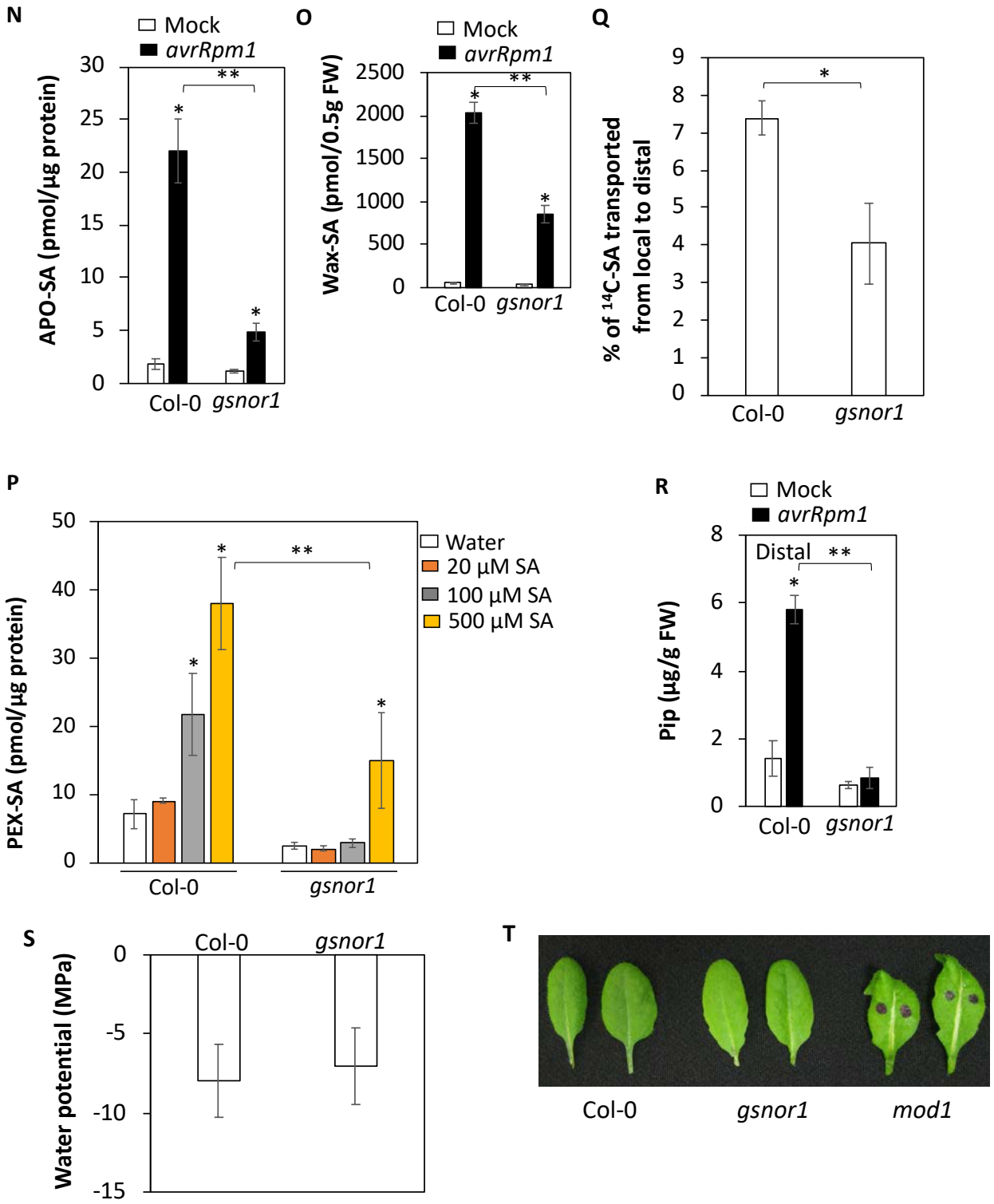

Figure 3.3 (Continued) The *gsnor1* plants are defective in SA transport

Figure 3.3 (Continued) The *gsnor1* plants are defective in SA transport

(C) *SARD1* and **(D)** *CBP60g* and **(E)** *ICS1* and **(F)** *ALD1* and **(I)** *FMO1* expression levels in Col-0 and *gsnor1* plants after Mock (10 mM $MgCl_2$) or *avrRpm1* inoculation. Error bars indicate SD (n = 4). The "*" denotes a significant difference with Mock treatment (10 mM $MgCl_2$) (t test, $P < 0.01$). The "**" denotes a significant difference between two genotypes (t test, $P < 0.01$). **(G)** Pip and **(H)** NHP levels in infiltrated leaves of Col-0 and *gsnor1* plants after Mock (10 mM $MgCl_2$) or *avrRpm1* inoculation. Error bars indicate SD (n = 4). The "*" denotes a significant difference with Mock treatment (10 mM $MgCl_2$) (t test, $P < 0.01$). The "**" denotes a significant difference between two genotypes (t test, $P < 0.01$). **(J)** SAR response in distal leaves of Col-0 and *gsnor1* plants after locally treated with Mock (water), 500 μM SA or 1 mM Pip. The virulent pathogen (DC3000) was inoculated 48 hours after local treatments. Leaves were sampled at 3 dpi to measure bacterial populations. Error bars indicate SD (n = 4). The "*" denotes a significant difference with Mock treatment (10 mM $MgCl_2$) (t test, $P < 0.01$). **(K)** SAR response in distal leaves of Col-0 and *gsnor1* plants after locally treated with Mock (water) or 100 μM NHP. The virulent pathogen (DC3000) was inoculated 48 hours after local treatments. Leaves were sampled at 3 dpi to measure bacterial populations. Error bars indicate SD (n = 4). The "*" denotes a significant difference with Mock treatment (10 mM $MgCl_2$) (t test, $P < 0.05$). **(L)** Petiole exudate G3P and **(M)** SA in Col-0 and *gsnor1* plants after Mock (10 mM $MgCl_2$) or *avrRpm1* inoculation, PEX were collected 10 h after Mock or *avrRpm1* treatments for a duration of 48 h. Error bars indicate SD (n = 4). The "*" denotes a significant difference with Mock treatment (10 mM $MgCl_2$) (t test, $P < 0.01$). The "**" denotes a significant difference between two genotypes (t test, $P < 0.01$). **(N)** Apoplastic SA and **(O)** Wax SA in Col-0 and *gsnor1* plants after Mock (10 mM $MgCl_2$) or *avrRpm1* inoculation. Error bars indicate SD (n = 4). The "*" denotes a significant difference with Mock treatment (10 mM $MgCl_2$) (t test, $P < 0.01$). The "**" denotes a significant difference between two genotypes (t test, $P < 0.01$). **(P)** PEX SA in Col-0 and *gsnor1* plants after locally infiltrated with water, 20 ~500 μM SA. PEX-SA were collected the same as Mock or *avrRpm1* treated plants. Error bars indicate SD (n = 4). The "*" denotes a significant difference with Mock treatment (Water) (t test, $P < 0.01$). The "**" denotes a significant difference between two genotypes (t test, $P < 0.01$). **(Q)** ^{14}C-SA transport after locally infiltrated with 20 μM ^{14}C-SA. Error bars indicate SD (n = 4). "*" denotes a significant difference with between *gsnor1* and WT (Col-0) plants (t test, $P < 0.01$). **(R)** Pip levels in distal leaves of Col-0 and *gsnor1* plants 2 days after locally infiltrated with Mock (10 mM $MgCl_2$) or *avrRpm1* (10^7 CFU). **(S)** Water potential in leaves of Col-0 and *gsnor1* plants under normal condition. **(T)** Toluidine blue staining of Col-0, *gsnor1* and *mod1* plants. The leaves were stained on their adaxial surface for 5 min. These experiments were repeated at least twice with similar results.

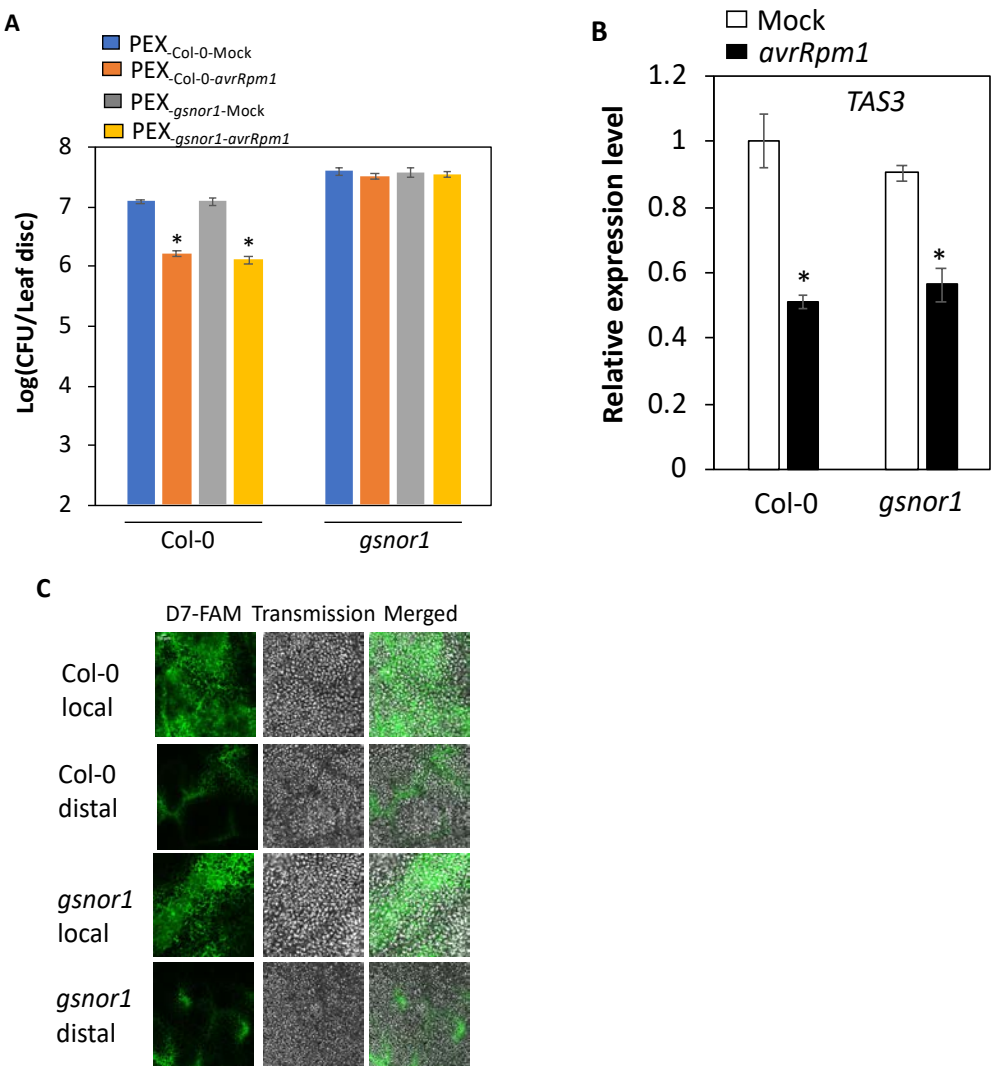

Figure 3.4 The *gsnor1* plants are competent in generation of the SAR signal

(A) SAR response in Col-0 and *gsnor1* plants infiltrated with PEX collected from Col-0 or gsnor1 plants that were treated either with Mock (10 mM $MgCl_2$) or *avrRpm1*. The virulent pathogen (DC3000) was inoculated 48 hours after local treatments. Leaves were sampled at 3 dpi to measure bacterial populations. Error bars indicate SD (n = 4). The "*" denotes a significant difference with Mock treatments ($PEX_{\text{-Col-0-Mock}}$ or $PEX_{\text{-}gsnor1\text{-Mock}}$) (t test, $P < 0.01$). The experiment was repeated twice with similar results. **(B)** *TAS3* expression levels in Col-0 and *gsnor1* plants with Mock or *avrRpm1*. Error bars indicate SD (n = 4). The "*" denotes a significant difference with Mock (10 mM $MgCl_2$). The experiment was repeated twice with similar results. **(C)** TAS3 siRNA D7 transport (labeled with FAM) from local to distal leaves. Leaf fluorescence was observed under confocal microscopy using 488 nm laser. Scale bar, 50 µm.

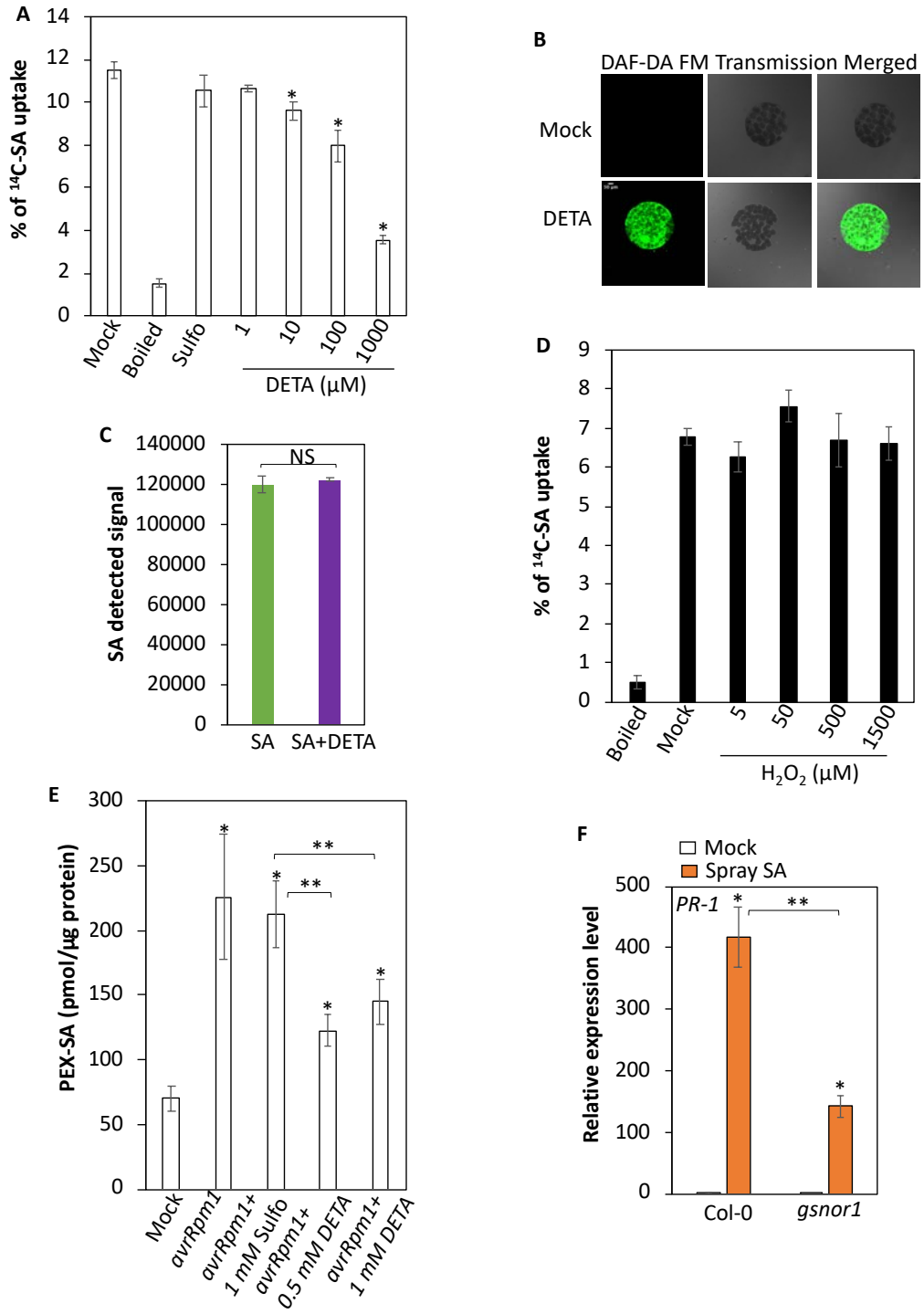

Figure 3.5 Increased NO levels attenuate transport of SA to distal leaves

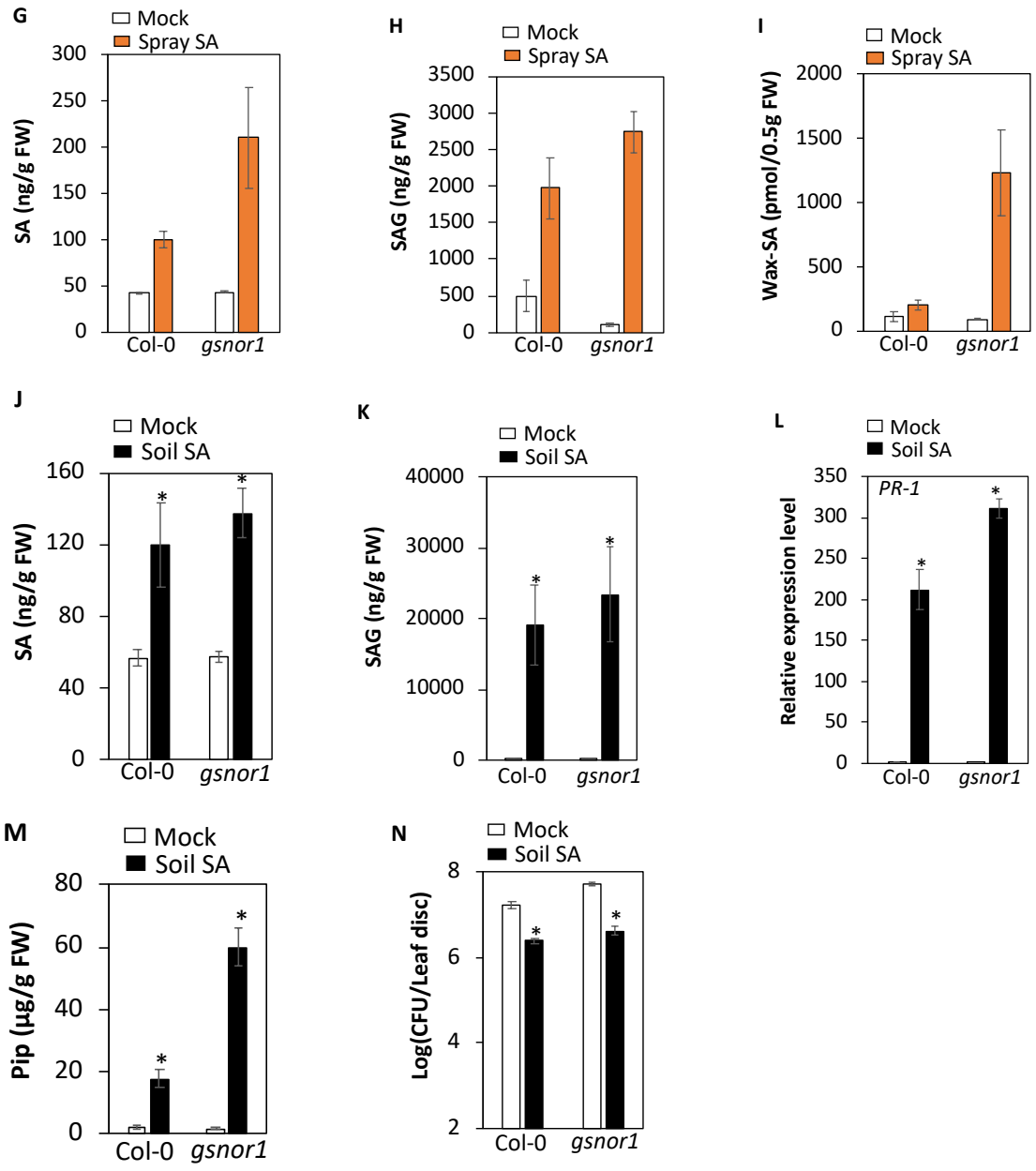

Figure 3.5 (Continued) Increased NO levels attenuate transport of SA to distal leaves

(A) NO donor DETA (DETA-NONOate, release NO) induced NO accumulation in protoplast prepared from WT (Col-0) plants. Protoplast was incubated with 1 mM DETA for 1 h under room temperature and was analyzed using confocal microscope. **(B)** SA relative levels determined by GC-MS after incubating 100 ng of SA standard with or without 1 mM DETA. SA standard (100 ng) was incubated with 1 mM DETA or water for 1 h and then derivatized with MTBSTFA for GC-MS analysis. Error bars indicate SD (n = 4). NS, no significant difference.

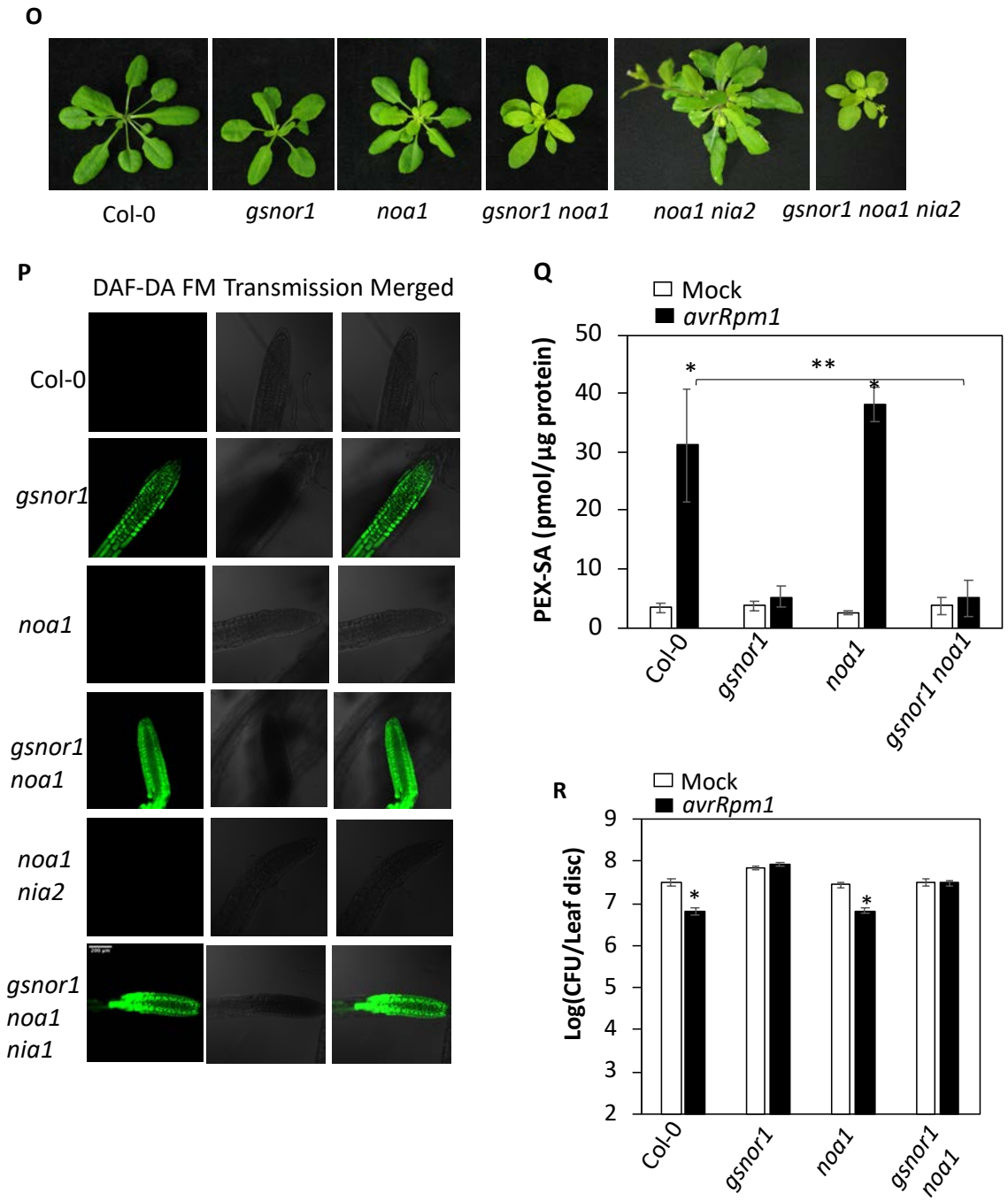

Figure 3.5 (Continued) Increased NO levels attenuate transport of SA to distal leaves

Figure 3.5 (Continued) Increased NO levels attenuate transport of SA to distal leaves

(C) Freshly prepared protoplasts (Col-0) were incubated with ^{14}C-SA and NO donor DETA or negative control Sulfo (Sulfo-NONOate, release N_2O) for 1 h and checked for ^{14}C-SA uptake. Sulfo concentration was 100 μM. Boiled, boiled protoplast. Error bars indicate SD (n = 4). The "*" denotes a significant difference with Mock treatment (t test, P < 0.01). **(D)** Freshly prepared protoplasts (Col-0) were incubated with ^{14}C-SA and different concentrations of H_2O_2 or Mock (water) for 1 h and checked for ^{14}C-SA uptake. Boiled, boiled protoplast. Error bars indicate SD (n = 4). **(E)** PEX SA levels in Col-0 plants treated with Mock (water), *avrRpm1*, Sulfo+*avrRpm1* or DETA+*avrRpm1*. Sulfo or DETA was infiltrated 12h prior to *avrRpm1* inoculation. Error bars indicate SD (n = 4). The "*" denotes a significant difference with Mock treatment. The "**" denotes a significant difference between two treatments (t test, P < 0.01). **(F)** *PR-1* expression, **(G)** SA, **(H)** SAG and **(I)** Wax SA in leaves of Col-0 and *gsnor1* plants 24h after 500 μM SA spray. FW, fresh weight. Error bars indicate SD (n = 4). The "*" denotes a significant difference with Mock treatment, The "**" denotes a significant difference between WT and *gsnor1* plants. **(J)** SA, **(K)** SAG, **(L)** *PR-1* expression and **(M)** Pip levels in leaves of Col-0 and *gsnor1* plants 24h after soil drench with water or 500 μM SA. Error bars indicate SD (n = 4). The "*" denotes a significant difference with Mock treatment (t test, P < 0.01). **(N)** Leaf response to DC3000 infection after root soil drench with Mock (water) or 500 μM SA. The virulent pathogen (DC3000) was inoculated 48 hours after soil drench. Leaves were sampled at 3 dpi to measure bacterial populations. Error bars indicate SD (n = 4). The "*" denotes a significant difference with Mock treatments (t test, P < 0.01). **(O)** Morphology of indicated genotype of plants under same growth conditions. **(P)** Root NO levels of indicated genotype plants measured by DAF-DA FM under confocal microscope. **(Q)** PEX SA levels of indicated genotype of plants treated with Mock (10 mM $MgCl_2$) or *avrRpm1*. Error bars indicate SD (n = 4). The "*" denotes a significant difference with Mock treatment, The "**" denotes a significant difference between two plant genotypes (t test, P < 0.01). **(R)** SAR response in distal leaves of indicated genotype plants after locally treated with Mock (10 mM $MgCl_2$) or *avrRpm1*. The virulent pathogen (DC3000) was inoculated 48 hours after local treatments. Leaves were sampled at 3 dpi to measure bacterial populations. Error bars indicate SD (n = 4). The "*" denotes a significant difference with Mock treatment (10 mM $MgCl_2$) (t test, P < 0.01). The experiment was repeated twice with similar results.

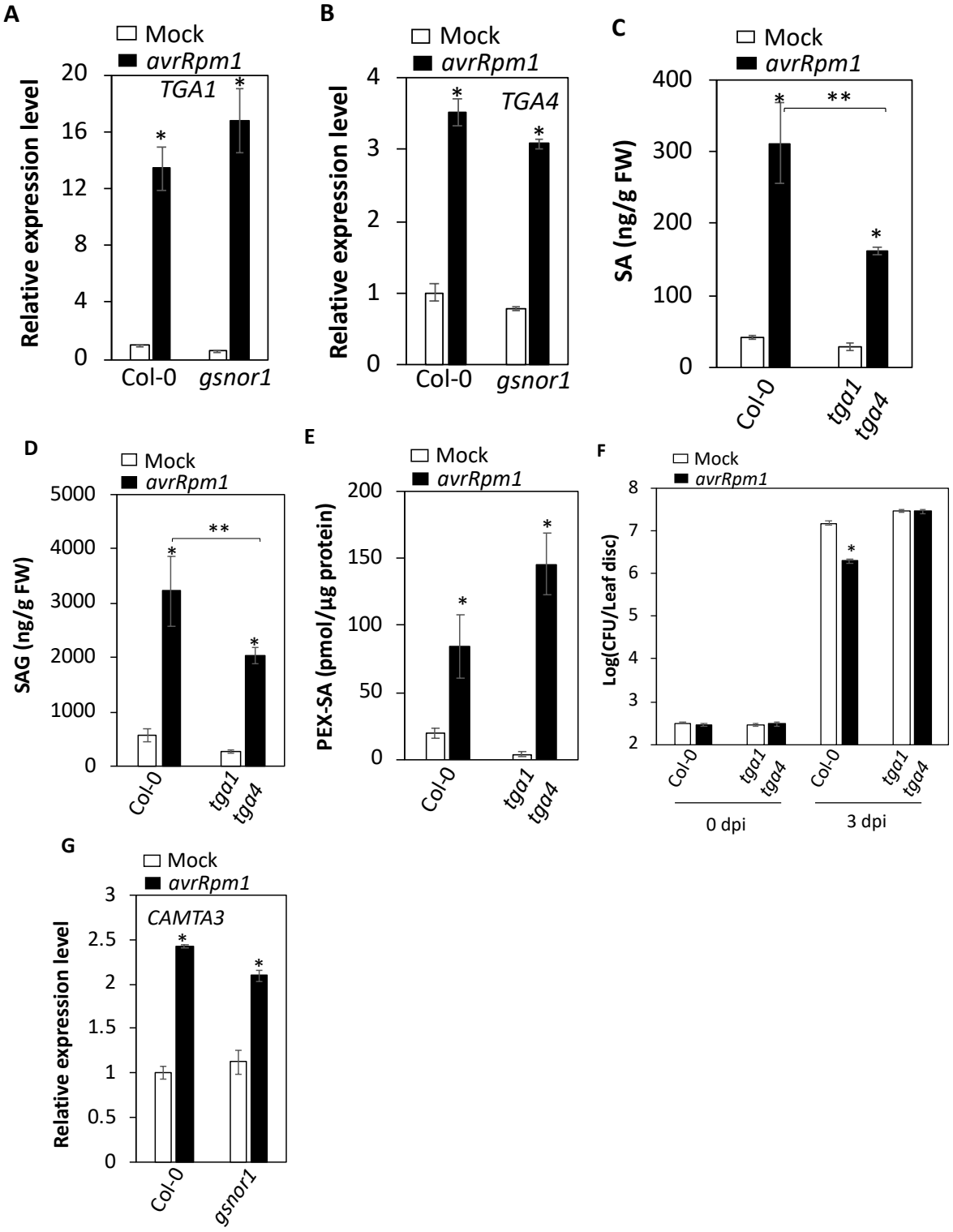

Figure 3.6 GSNOR1 is epistatic to CAMTA and WRKY70

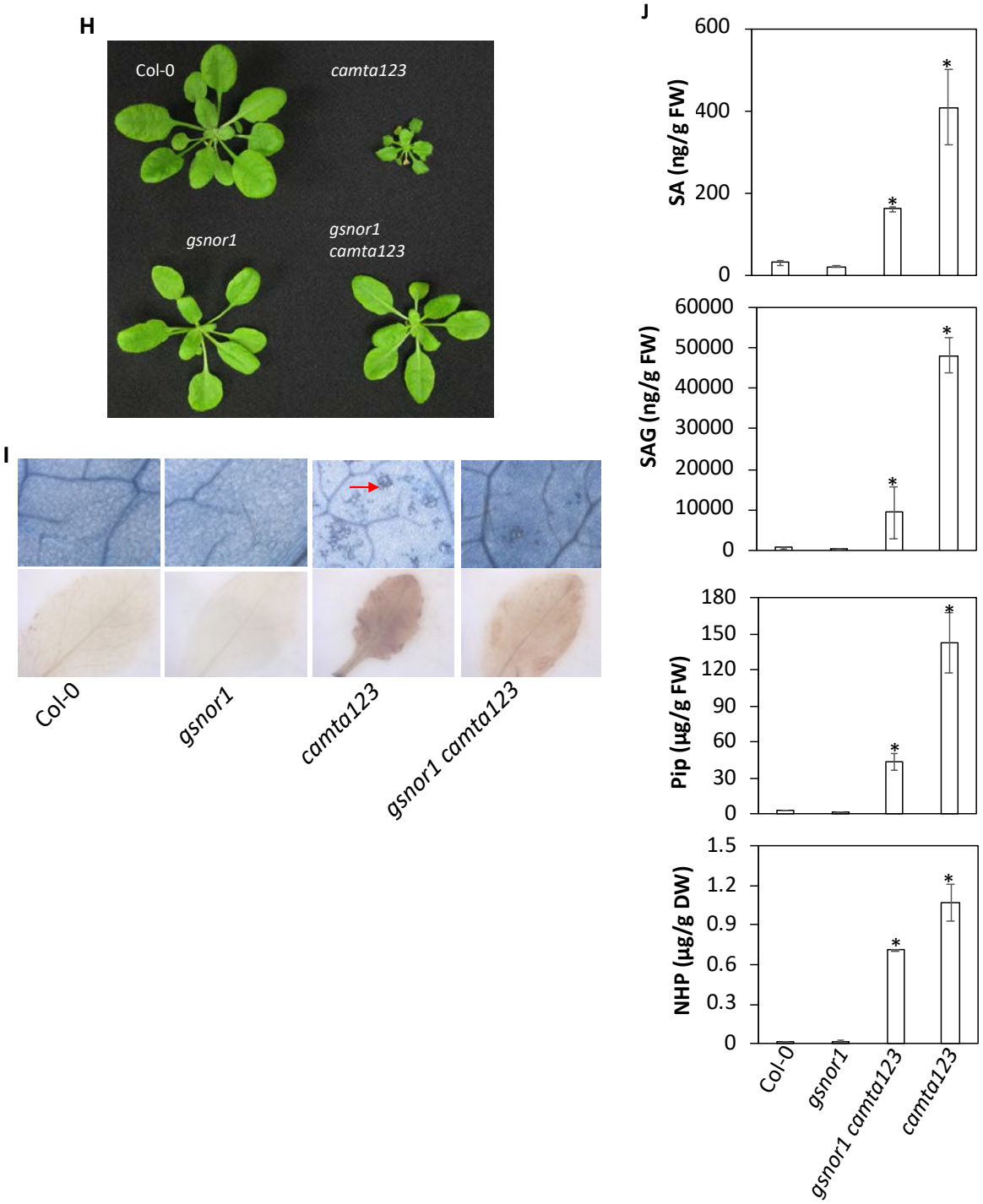

Figure 3.6 (Continued) GSNOR1 is epistatic to CAMTA and WRKY70

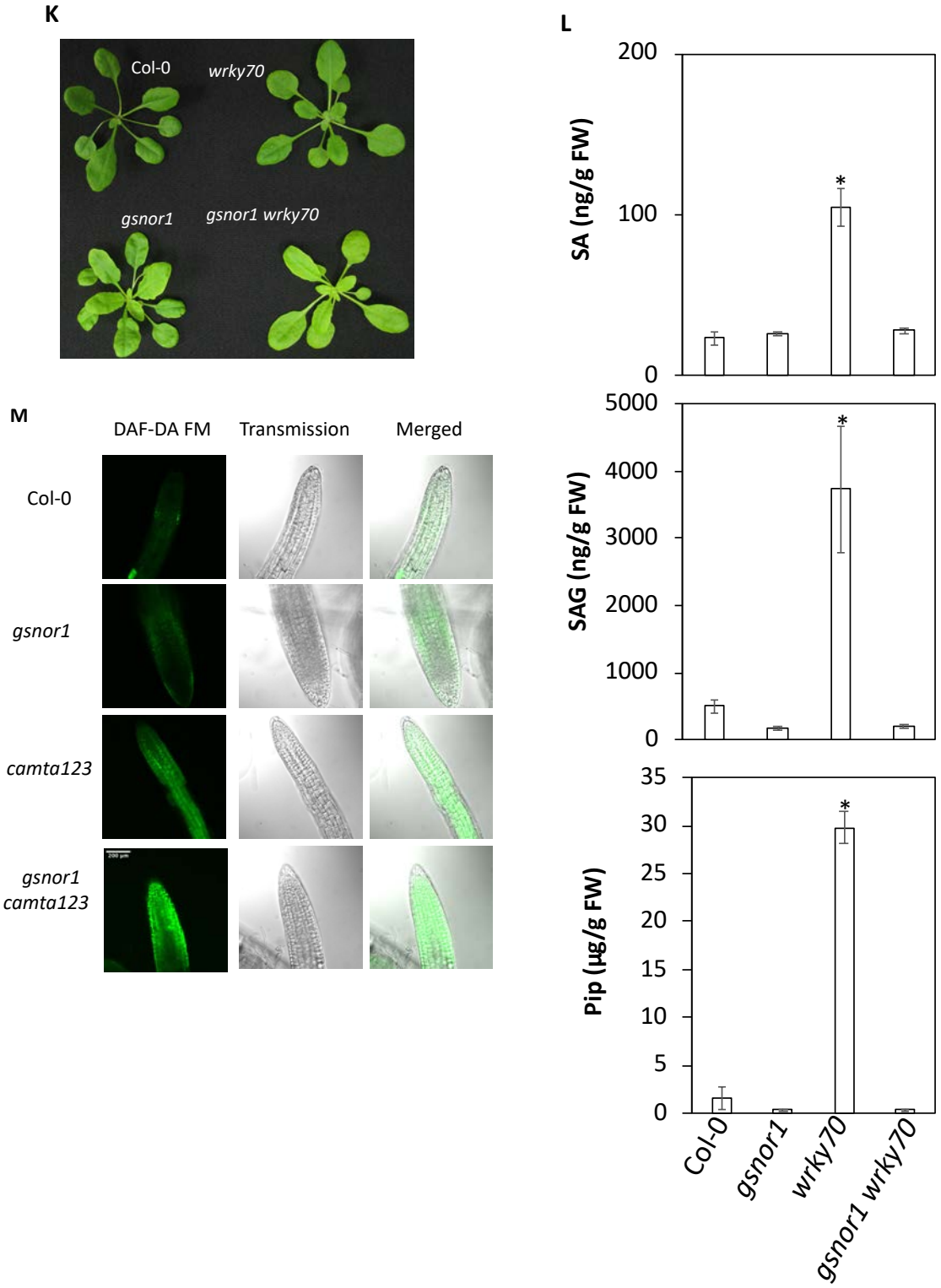

Figure 3.6 (Continued) GSNOR1 is epistatic to CAMTA and WRKY70

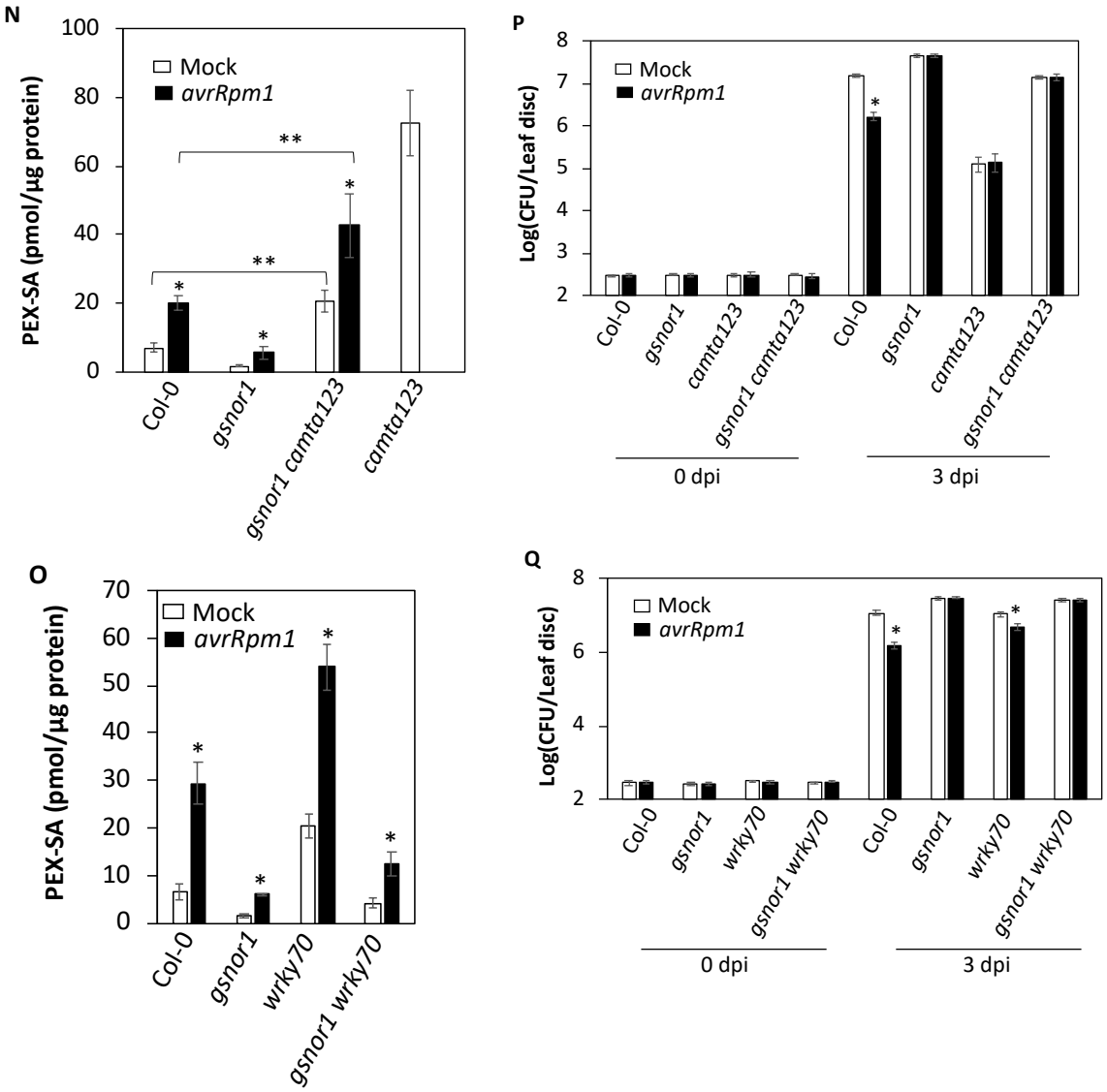

Figure 3.6 (Continued) GSNOR1 is epistatic to CAMTA and WRKY70

Figure 3.6 (Continued) GSNOR1 is epistatic to CAMTA and WRKY70

(A) *TGA1* and **(B)** *TGA4* expression levels in infiltrated leaves of Col-0 and *gsnor1* plants 16 h after Mock (10 mM $MgCl_2$) or *avrRpm1* inoculation. Error bars indicate SD (n = 4). The "*" denotes a significant difference with Mock treatment (10 mM $MgCl_2$) (t test, $P < 0.01$). **(C)** SA and **(D)** SAG levels in infiltrated leaves of Col-0 and *tga1 tga4* plants after Mock (10 mM $MgCl_2$) or *avrRpm1* inoculation. Error bars indicate SD (n = 4). The "*" denotes a significant difference with Mock treatment (10 mM $MgCl_2$) (t test, $P < 0.01$). The "**" denotes a significant difference between Col-0 and *tga1 tga4* plants (t test, $P < 0.05$). FW, fresh weight. **(E)** PEX-SA levels in Col-0 and *tga1 tga4* plants after Mock (10 mM $MgCl_2$) or *avrRpm1* inoculation. Error bars indicate SD (n = 4). The "*" denotes a significant difference with Mock treatment (10 mM $MgCl_2$) (t test, $P < 0.01$). **(F)** SAR response in distal leaves of in Col-0 and *tga1 tga4* plants locally infiltrated with Mock (10 mM $MgCl_2$) or *avrRpm1*. The virulent pathogen (DC3000) was inoculated 48 hours after local treatments. Leaves were sampled at 3 dpi to measure bacterial populations. Error bars indicate SD (n = 4). The "*" denotes a significant difference with Mock treatment (10 mM $MgCl_2$) (t test, $P < 0.01$). **(G)** *CAMTA3* expression levels in infiltrated leaves of Col-0 and *gsnor1* plants 16 h after Mock (10 mM $MgCl_2$) or *avrRpm1* inoculation. **(H)** Morphology of Col-0, *gsnor1*, *camta123* and *gsnor1 camta123* plants. **(I)** Leaf cell death stained with trypan blue (top panel) and H_2O_2 stained with DAB (bottom panel) in indicated genotype of plants. Arrow points to death cells stained by the dye. **(J)** SA, SAG, Pip and NHP levels in leaves of indicated genotype of plants without treatments. FW, fresh weight; DW, dry weight. **(K)** Morphology of Col-0, *gsnor1*, *wrky70* and *gsnor1 wrky70* plants. **(L)** SA, SAG and Pip levels in leaves of Col-0, *gsnor1*, *wrky70* and *gsnor1 wrky70* plants without treatments. FW, fresh weight. **(M)** Root NO levels of indicated genotype of plants measured by DAF-DA FM under confocal microscope. **(N** and **O)** PEX SA levels of indicated genotype of plants after Mock ($MgCl_2$) or *avrRpm1* inoculation. Error bars indicate SD (n = 4). The "*" denotes a significant difference with Mock treatment (10 mM $MgCl_2$) (t test, $P < 0.01$). The "**" denotes a significant difference between two genotypes of plants (t test, $P < 0.05$). **(P** and **Q)** SAR response in distal leaves of indicated genotype of plants after locally treated with Mock ($MgCl_2$) or *avrRpm1*. The virulent pathogen (DC3000) was inoculated 48 hours after local treatments. Leaves were sampled at 3 dpi to measure bacterial populations. Error bars indicate SD (n = 4). The "*" denotes a significant difference with Mock treatment (10 mM $MgCl_2$) (t test, $P < 0.01$). The experiment was repeated twice with similar results.

CHAPTER 4. DISSERCTING GSNOR1-REGULATED HYPERSENSITIVE RESPONSE AND LOCAL RESISTANCE IN ARABIDOPSIS

4.1 Introduction

I discussed the role of GSNOR1 in SAR earlier in this thesis. Notably, it has been found that GSNOR1 is also a central player in regulating local resistance (Feechan et al., 2005). In plants, local microbial invasion could result in a number of diverse defense responses. These include SA biosynthesis, reactive nitrogen and oxygen species (RNS and ROS respectively) burst, which act together to modulate hypersensitive response cell death during ETI (effector triggered immunity) (Wang and Chu, 2020). As previously discussed, GSNOR1 governs the decomposition of GSNO (a major bioactive RNS species) and the *Arabidopsis gsnor1* plants over accumulate GSNO. RNS and ROS share many similarities in biochemical properties, and they are often intertwined in regulating physiological processes (such as cell death).

It has been suggested that pathogen induced ROS burst is mainly controlled by the plasma membrane localized RBOHs (RESPIRATORY BURST OXIDASE HOMOLOGUES) protein (encoding NADPH oxidase) (Torres and Dangl, 2005). Among the ten RBOH proteins in Arabidopsis, RBOHD is believed to play a major role in producing ROS (e.g.H_2O_2) (Kadota et al., 2015). Notably, RBOHD protein was shown be S-nitrosylated by GSNO during ETI (Yun et al., 2011). It was proposed that cell death is positively regulated by increased levels of SA and GSNO at early stage of ETI, while GSNO at later stage negatively affects RBOHD protein activity thereby decreasing RBOHD synthesized ROS and as a result, limiting cell death development. Indeed, *Arabidopsis gsnor1* mutant show an accelerated cell death in response to *P. syringae avrB* or *avrRpm1* infection. In plants, APX (ASCORBATE PEROXIDASE) catalyzes the electron transfer from ascorbate to H_2O_2 to scavenge H_2O_2, resulting in the production of dehydroascorbate and water. APX proteins are critical in maintaining ROS homeostasis and they are presented in various cellular compartments including cytosol, chloroplast, peroxisome and mitochondria. It has been reported that during heat shock and H_2O_2 induced programed cell death, the tobacco cytosolic APX (cAPX) is S-nitrosylated by

GSNO, which decreases cAPX activity and promotes cAPX degradation (de Pinto et al., 2013). In another example, the rice *NOE1* (*NITRIC OXIDE EXCESS 1*) gene encodes a catalase which is also important in scavenging H_2O_2 in the cell. The loss-of-function mutant *noe1* caused accumulation of H_2O_2 and triggered constitutive cell death. Importantly, the cell death caused by loss-of-function in *NOE1* was dramatically alleviated by reducing GSNO levels via overexpressing rice *GSNOR* gene, suggesting GSNO plays a role in regulating cell death in rice (Lin et al., 2012).

Plant hormones often exist at very low concentration within the cell and play signaling roles in all aspects of growth and development in plants, including plant defense. Although SA is known to play a prominent role in defense, other hormones have also been found to influence disease resistance. For instance, jasmonic acid (JA) positively regulate plant's resistance to necrotrophic pathogens *Alternaria brassicicola* and *Botrytis cinereal* through an antagonistic crosstalk with SA. Phytohormone brassinosteroids (BRs) are a class of polyhydroxysteroids mainly involved in promoting plant growth. BRs are perceived by the plasma membrane localized kinase BRI1 (BRASSINOSTEROID INSENSITIVE 1) and co-receptor BAK1 (BRASSINOSTEROID ASSOCIATED KINASE 1). Recent studies reveal that BAK1 is a crucial signal transduction component in PTI. In addition, ABA, a hormone involved in regulating seed germination, dormancy and abiotic stress responses, also has an impact on disease resistance by regulating stomatal closure (Robert-Seilaniantz et al., 2011).

In addition to hormones, plants also produce low molecular weight secondary metabolites with antimicrobial activity to fight against pathogen infections. These antimicrobial secondary metabolites are collectively known as phytoalexins. Camalexin is one of the most well studied phytoalexins. Camalexin biosynthesis is significantly induced by the necrotrophic fungi *A. brassicicola* and *B. cinereal*, as well as the hemi-biotrophic bacteria model *P syringae*. The camalexin biosynthesis deficient mutant *pad4* becomes highly susceptible to *A. brassicicola* and *B. cinereal*. Notably, the biosynthesis of camalexin was suggested to be controlled by mitogen-activated protein kinase (MAPK) cascades (Ahuja et al., 2012).

The genome of Col-0 ecotype *Arabidopsis* is known to encode hundreds of resistance (R) proteins, which recognize corresponding effector(s) secreted by avirulent (Avr) pathogen(s) upon infection. The R-Avr interaction triggers a hypersensitive response (HR) and cause localized cell death to restrict pathogen spread. R proteins are generally divided into two functionally distinct subfamilies: TIR-NB-LRR (denoted as TNL) and CC-NB-LRR (denoted as TNL), respectively (TIR: interleukin 1 receptors domain; NB-LRR: nucleotide-binding, leucine-rich repeat) (Eitas and Dangl, 2010). Previously, Yun et al. reported that the increases in NO levels in the *gsnor1* mutant positively regulates HR development upon avirulent *P. syringae* infection (Yun et al., 2011). Their conclusion was based on the observation that the *gsnor1* plants displayed an accelerated HR in response to *avrRpm1* (recognized by CNL subfamily R protein RPM1 (RESISTANCE TO P. SYRINGAE PV MACULICOLA 1)) and *avrRps4* (recognized by TNL subfamily R protein RPS4 (RESISTANT TO P. SYRINGAE 4)).

Here in this study, I investigated the role of GSNOR1 in HR and local immunity. I show that the GSNOR1-modulated HR depends on the individual characteristics of host-pathogen interaction and SA deficiency is not the only factor affecting disease susceptibility in *gsnor1* plants.

4.2 Results and discussion

4.2.1 The *gsnor1* mutant shows different HR phenotypes in different *R*-Avr interactions

To test if GSNOR1 is involved in HR regulation during ETI, WT (Col-0) and *gsnor1* plants were first inoculated with *avrRpm1* and HR development was recorded at two different time points (24 and 48 hpi). Indeed, HR cell death was evident at a much earlier time point in *gsnor1* than WT plants. Also, the intensity of HR in *gsnor1* was markedly stronger in *gsnor1* than WT plant (Fig. 4.1A). These results are consistent with earlier report (Yun et al., 2011). Interestingly, the HR was delayed in *gsnor1* at early time point (16 h) compared to WT plants when they were inoculated with *avrRpt2* (recognized by CNL subfamily R protein RPS2) (Fig. 4.1B). Cell death often leads to the collapse of the cell membrane thus electrolytes such as K^+ ions leak out of the cell during HR. The

amount of electrolytes leaked from infected tissues thus can be used to estimate the extent of cell death in the tissue. To further validate my finding, I conducted electrolytes leakage assays as a proxy to measure cell death in WT and *gsnor1* plants upon *avrRpm1* or *avrRpt2* infection. Notably, electrolytes leakage was consistently higher in *gsnor1* than WT plants upon *avrRpm1* infection (Fig. 5.1B). In contrast, the *gsnor1* mutant suffered less electrolytes leakage than WT plants in response to *avrRpt2* infection at 12 and 16h post infection but similar levels of electrolytes leakage at 24 h (Fig. 4.1C). Together, these data imply that *gsnor1*-mediated HR phenotypes may be related to the specific R-Avr interaction.

4.2.2 The HR phenotypes in *gsnor1* mutant are independent of SID2, NPR1, ALD1 and RBOHD

As we showed earlier that SA and Pip biosynthesis are compromised in *gsnor1* plants and NO may have connections with ROS. We asked if SA, Pip or ROS may play a role in HR regulation in *gsnor1* plants. I crossed *gsnor1* with *sid2*, *npr1*, *ald1* and *rbohD* and isolated *gsnor1 sid2*, *gsnor1 npr1*, *gsnor1 ald1* and *gsnor1 rbohD* homozygous double mutants. I then tested HR in these plants by inoculating them with *avrRpm1* or *avrRpt2*. Importantly, these mutants showed similar HR phenotypes as seen in *gsnor1* plants (Fig. 4.2), suggesting that SID2, NPR1, ALD1 and RBOHD likely do not regulate HR modulated by GSNOR1.

4.2.3 SA induction pattern can be altered by different *R*-Avr interactions

Earlier studies showed that *gsnor1* mutant is compromised in SA biosynthesis (Feechan et al., 2005; Yun et al., 2016). As *gsnor1* plants show opposite HR phenotypes over a limited time period in response to *avrRpm1* and *avrRpt2*, we asked if SA production could be different when *gsnor1* plants were challenged by *avrRpm1* or *avrRpt2*. I tested this by measuring SA levels in WT and *gsnor1* plants after *avrRpm1* or *avrRpt2* infection. Interestingly, SA levels were significantly lower in *gsnor1* than in WT plants at both early (16 hpi) and later stage (40 hpi) of *avrRpm1* infection (results showed in chapter 3, Figure 3.3A, B and unpublished results). In contrast, SA levels were lower in *gsnor1* than in WT plants at early (16 hpi) but became higher in *gsnor1* than in WT plants at later (40 hpi)

stage of *avrRpt2* infection (Fig. 4.3A and B). Furthermore, *PR-1* expression patterns were consistent with SA levels in WT and *gsnor1* plants upon *avrRpm1* or *avrRpt2* infection (Fig. 4.3C). Collectively, these results indicate SA biosynthesis in *gsnor1* plants may be regulated by R-Avr interaction.

4.2.4 SA is not the only factor that affects local resistance in *gsnor1* plant

It has been shown that the *gsnor1* mutant becomes highly susceptible to *P. syringae* due to its deficiency in SA biosynthesis. We asked if additional factors could contribute to *gsnor1* plant's susceptibility. To test this, I crossed *gsnor1* with the SA deficient mutant *sid2* (*salicylic acid induction deficient 2*) plants and isolated the homozygous *gsnor1 sid2* double mutant. I next measured disease resistance in WT, *gsnor1*, *sid2* and *gsnor1 sid2* plants after DC3000 and *avrRpt2* infection. It was found that *gsnor1 sid2* were more susceptible than either of the *gsnor1* or *sid2* single mutants upon both DC3000 and *avrRpt2* infection (Fig. 4.4A and B), suggesting additional factors beyond SA further contribute to susceptibility in *gsnor1* plants.

I found that *gsnor1* plants were also more susceptible than WT plants when inoculated with *Colletotrichum higginsianum* (Fig. 4.4C). Phytoalexin camalexin has been suggested to confer plants resistance to C. *higginsianum*. Camalexin biosynthesis is also induced by avirulent *P. syringae* infection. I measured camalexin levels in WT and *gsnor1* plants after *avrRpm1* infection. Notably, camalexin production after *avrRpm1* infection was severely compromised in *gsnor1* compared to WT plants (Fig. 4.4D). Together, these data indicate that multiple defects exist in the NO overaccumulation *gsnor1* mutant and cautions should be taken while interpreting results obtained from this mutant.

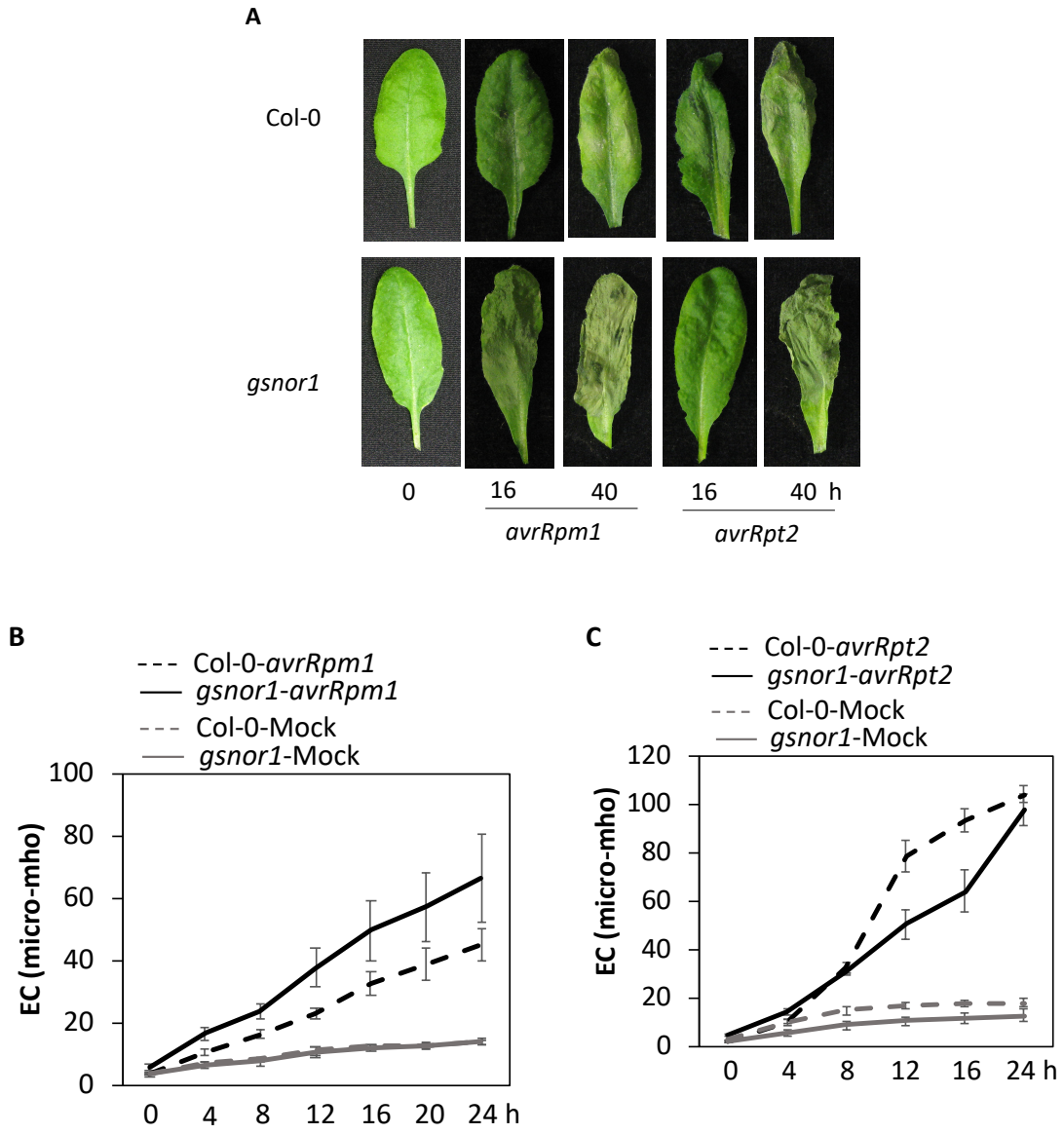

Figure 4.1 The *gsnor1* mutant shows different HR phenotypes in different *R*-Avr interactions

(A) Leaf HR symptoms in Col-0 and *gsnor1* plants in response to Mock (10 mM $MgCl_2$), *avrRpm1* or *avrRpt2* inoculation (Concentration 5 x 10^5). **(B)** Ion leakage in Col-0 and *gsnor1* plants in response to Mock (10 mM $MgCl_2$) or *avrRpm1* inoculation (Concentration 5 x 10^5). The error bars indicate standard deviation (SD) (n = 4). **(C)** Ion leakage in Col-0 and *gsnor1* plants in response to Mock (10 mM $MgCl_2$) or *avrRpt2* inoculation (Concentration 5 x 10^5). The error bars indicate standard deviation (SD) (n = 4). The experiment was twice with similar results.

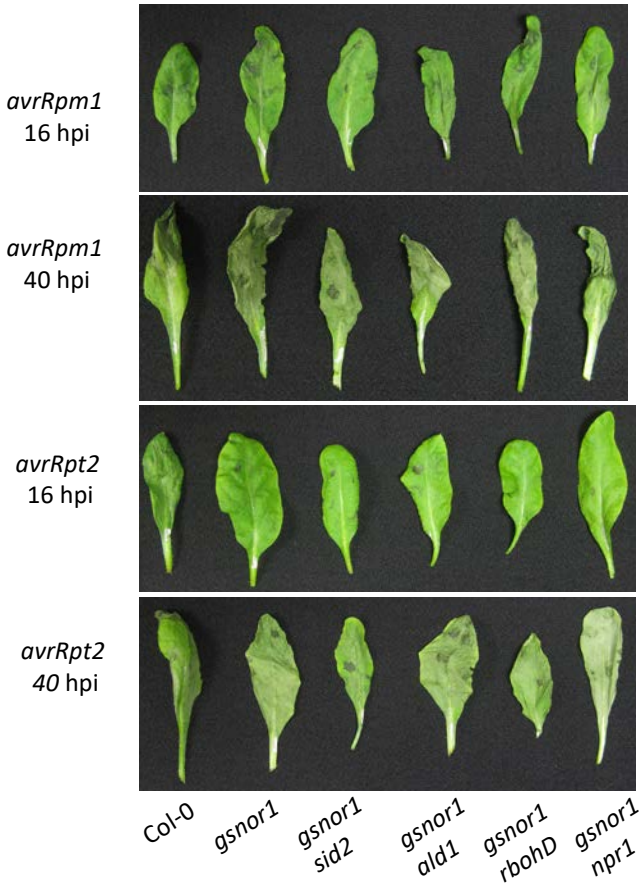

Figure 4.2 GSNOR1 regulates HR phenotype independent of SID2, ALD1, RBOHD or NPR1

Leaf HR symptoms in Col-0, *gsnor1, gsnor1 sid2, gsnor1 ald1*, *gsnor1 rbohD and gsnor1 npr1* plants in response to *avrRpm1* or *avrRpt2* infection (Concentration 5 x 10^5).

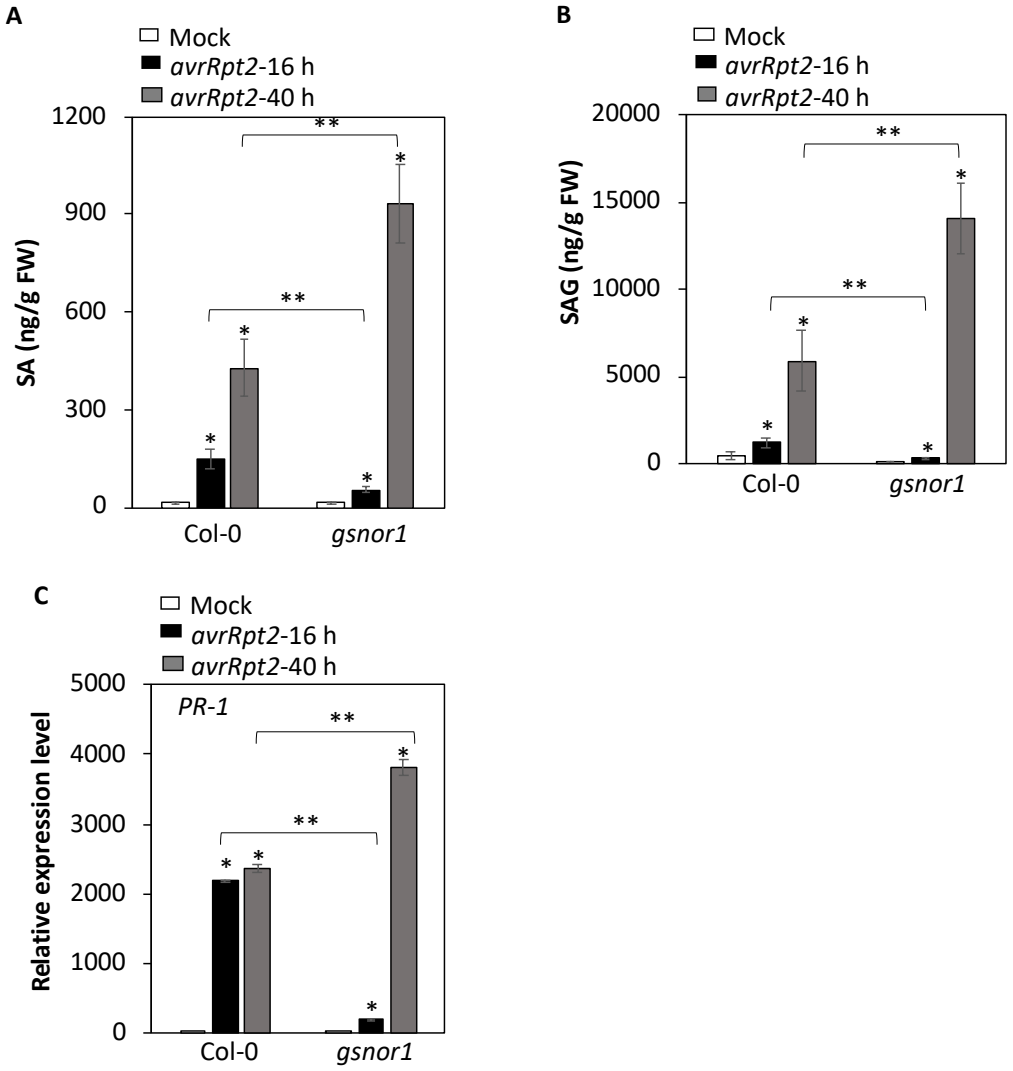

Figure 4.3 SA induction pattern in *gnsor1* plants can be altered by different R-Avr interactions

(A) SA and **(B)** SAG levels in Col-0 and *gsnor1* plants in response to Mock (10 mM $MgCl_2$) or *avrRpt2* inoculation. FW, fresh weight. Error bars indicate SD (n = 4). "*" denotes a significant difference with Mock treatment (t test, P < 0.01), "**" denotes a significant difference between two genotypes (t test, P < 0.01). **(C)** *PR-1* gene expression levels in Col-0 and *gsnor1* plants in response to Mock (10 mM $MgCl_2$) or *avrRpt2* inoculation. Error bars indicate SD (n = 4). "*" denotes a significant difference with Mock treatment (t test, P < 0.01), "**" denotes a significant difference between two genotypes (t test, P < 0.01).

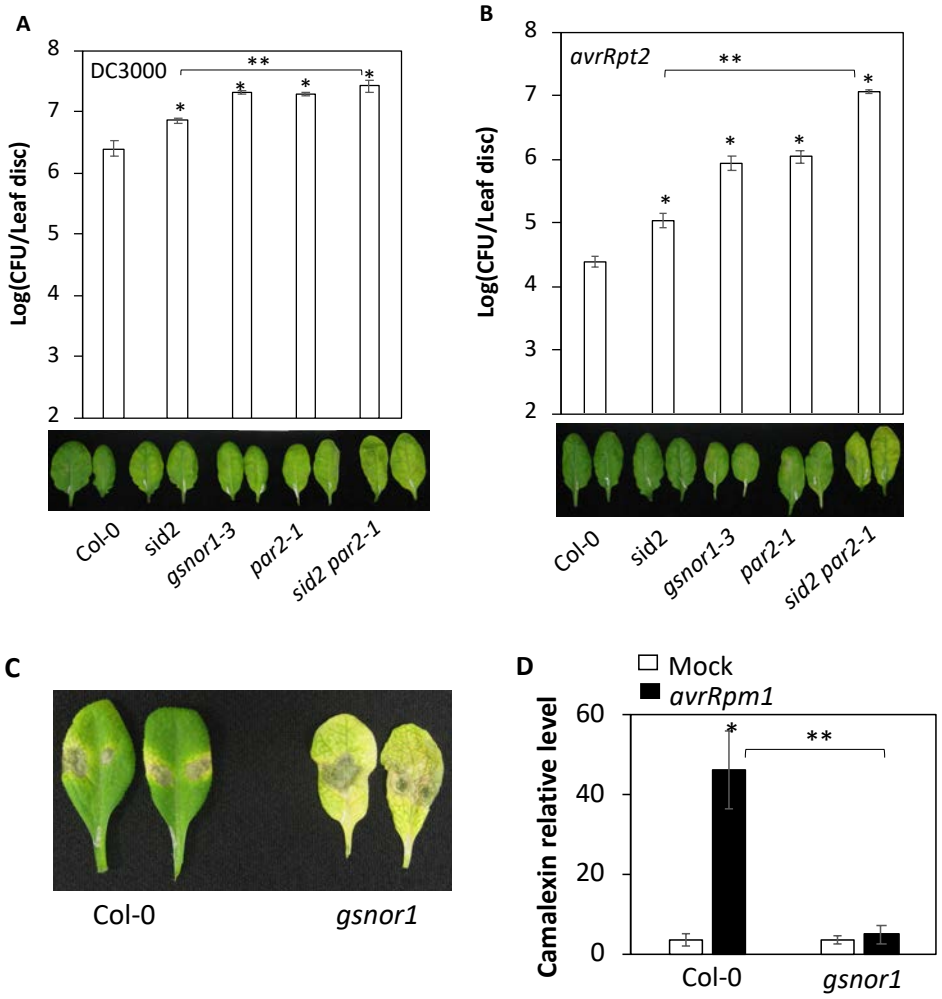

Figure 4.4 SA is not the only factor that affects local resistance in *gsnor1* plants

(A) Local leaf response to DC3000 infection in indicated genotype of plants. Bottom panel showed the leaf symptoms. **(B)** Local leaf response to *avrRpm1* in indicated genotype of plants. Bottom panel showed the leaf symptoms. **(C)** Leaf symptoms (5 dpi) showing response to *Colletotrichum higginsianum* infection in Col-0 and *gsnor1* plants. **(D)** Camalexin levels in Col-0 and *gsnor1* plants in response to Mock (10 mM $MgCl_2$) or *avrRpm1* inoculation. Error bars indicate SD (n = 4). "*" denotes a significant difference with Mock treatment (t test, $P < 0.01$), "**" denotes a significant difference between two genotypes (t test, $P < 0.01$). The experiment was repeated at least two times with similar results.

CHAPTER 5. NOX1 REGULATES SSI2-MEDIATED DEFENSE SIGNALING IN *ARABIDOPSIS*

5.1 Introduction

Salicylic acid (SA) plays a central role in plant defense. NPR1 acts as a key SA co-receptor and controls the expression of the *pathogenesis-related* (*PR*) genes and systemic acquired resistance (SAR) (Cao et al., 1997; Fu et al., 2012; Wang et al., 2020). The recessive *ssi2* (*suppressor of salicylic acid insensitivity 2*) mutant was isolated in a screen for the suppressor of *npr1* (Kachroo et al., 2001; Shah et al., 2001). The *SSI2* gene encodes a soluble chloroplast stearoyl-ACP (acyl-carrier-protein) desaturase, which preferentially desaturates 18:0-ACP between carbons 9 and 10 to synthesize 18:1-ACP, as a result, the *ssi2* plants contain markedly higher levels of stearic acid (18:0) and significantly lower levels of oleic acid (18:1) (Kachroo et al., 2003a). The *ssi2* plants show a dwarf morphology, constitutively express PR proteins, exhibit spontaneous cell death on mature leaves and display an increased resistance to biotrophic pathogens such as *Peronospora parasitica* and *P. syringae* but an elevated susceptibility to the necrotrophic pathogen *Botrytis cinereal* (Nandi et al., 2005). In higher plants, de novo fatty acid (FA) biosynthesis occurs exclusively in the plastids. During this process, the acetyl-CoA undergoes carboxylation and elongation catalyzed by key enzymes acetyl-CoA carboxylase (ACCase) and FA synthase (FAS) complex to produce saturated 16- or 18-carbon FAs (16:0 and 18:0). The FAS complex includes the small cofactor ACYL CARRIER PROTEIN (ACP). ACP proteins bind to growing FA chains via a thioester (form FA-ACPs such as 16:0-ACP and 18:0-ACP) during the biosynthesis cycles (Lim et al., 2017). De novo synthesized 18:1-ACP can either remain in the plastids or is exported into the cytoplasm as a CoA thioester (18:1- CoA). In both locations, 1-acyl-sn-glycerol 3-phosphate (lyso-PA) can be formed through the acylation of 18:1 with glycerol-3-phosphate (G3P). Lyso-PA is a key molecule because it serves as the building block for chloroplast membrane lipids such as monogalactosyldiacylglycerol (MGDG), digalactosyldiacylglycerol (DGDG) and sulfolipid (SL); and extrachloroplast lipids including phosphatidylinositol (PI), phosphatidylcholine (PC) and phosphatidylethanolamine (PE) (Kunst et al., 1988). Extensive previous studies demonstrated that the autoimmunity activated in *ssi2* plants is

associated with reduced levels of 18:1 in the chloroplast. This conclusion is supported by several lines of evidence. First, several genes that encode proteins involved in 18:1 metabolism regulation play a role in *ssi2*-activated signaling. These genes include *ACT1* (encodes a G3P acyltransferase, catalyzes the acylation of 18:1 with G3P), *GLY1* (encodes a G3P dehydrogenase, generates G3P from dihydroxyacetone phosphate (DHAP)) and *ACP4* (encodes an acyl carrier protein, 18:1-ACP4 is the preferred substrate for ACP4) (Kachroo et al., 2003a; Kachroo et al., 2004; Xia et al., 2009). A knock-out mutation in any of the three genes reduces 18:1 consumption by either limiting substrates (G3P) or decreasing (diminishing) acyltransferase activity, resulting in increased levels of 18:1 in the chloroplast. Consistently, the *ssi2 act1*, *ssi2 gly1* and *ssi2 acp4* plants all show WT like phenotypes because although the *ssi2* mutation reduces 18:1 level, it does not eliminate it. Therefore, any reduction on the drain on plastid levels of 18:1, due to the mutations mentioned above, replenish 18:1 amounts and thereby WT like phenotypes. Second, glycerol is known to be phosphorylated by GLI1 (a glycerol kinase) to form G3P in the cytoplasm. Notably, exogenous glycerol application on WT plants increases G3P levels, leading to a reduction in total 18:1 levels, and results in *ssi2*-like phenotypes such as cell death and enhanced disease resistance to pathogen such as *P. syringae* (Kachroo et al., 2004). These findings present strong connections between 18:1 levels and defense signaling. Third, the Arabidopsis genes *FAD2* (*FATTY ACID DESATURASE 2*) encodes an endoplasmic reticulum (ER) localized FA desaturase, which converts 18:1 to 18:2. A mutation in *FAD2* markedly increases 18:1 levels in the *ssi2* background but, strikingly, the *ssi2 fad2* plants still show a *ssi2* like phenotype (Kachroo et al., 2003). In contrast, another similar functioned FA desaturase FAD6 resides on the plastid envelop, a mutation in FAD6 also greatly increases 18:1 levels in the *ssi2* background, and partially restores *ssi2* activated phenotypes (Kachroo et al., 2003). The discrepancy between *fad2* and *fad6* suggests the levels of 18:1 in subcellular compartments may be critical for *ssi2* mediated signaling. Fourth, a recent study found 18:1 physically binds to the nitric oxide biosynthesis related protein NOA1 (NITRIC OXIDE ASSOCIATED 1) and facilitate the degradation of NOA1 in a protease-dependent manner. The reduction of 18:1 levels in *ssi2* plants thus leads the accumulation of NOA1 protein, resulting in increased NO production in the chloroplast and ultimately activates NO mediated defense signaling (Mandal et al., 2012).

These results suggest that NO functions downstream of 18:1 in *ssi2* activated defense signaling.

Arabidopsis *NOX1* (*NO OVERPRODUCER 1*) (or *CUE1* (*CHLOROPHYLL A/B BINDING*, *CAB*) *PROTEIN UNDEREXPRESSED* 1, or *PHOSPHOENOLPYRUVATE/PHOSPHATE TRANSLOCATOR* (*PPT*)) gene encodes a transporter protein localized in the plastid envelope membrane (He et al., 2004; Knappe et al., 2003; Li et al., 1995). Earlier studies suggested NOX1 catalyzes the transport of phosphoenolpyruvate (PEP) and inorganic phosphate (Pi) across the inner envelope membrane of plastids. The *nox1* plants are defective in expression of several light-regulated genes and display a reticulate pattern with veins greener than the interveinal regions of leaves. The *Arabidopsis* genome encodes another NOX1 like protein PPT2, which shares 52% identical amino acids with NOX1. Interestingly, although NOX1 and PPT2 both showed transport activities for Pi and PEP when heterologously expressed in yeast cells, because PPT2 protein has a different tissue expression pattern than NOX1, overexpressing PPT2 in the *nox1* background only partially reversed *nox1* morphology. Conversely, overexpressing a PLASTID-TARGETED PYRUVATE ORTHOPHOSPHATE DIKINASE (PPDK) from the C4 plant *Flaveria trinervia* was found to increase PEP levels in the *nox1* background and thereby almost completely rescued the *nox1* mutant phenotype. Plastids from C3 plants rely on PEP supplied from the cytosol as a substrate for the shikimate pathway reactions, through which plants produce all three aromatic amino acids and diverse downstream products such as tocopherol, phenylpropanoids and lignin. However, it was found that the *nox1* mutant only contained slightly lower levels of PEP in the light compared to WT plants. Moreover, among the three aromatic amino acids, only phenylalanine (Phe) levels showed a decline by 40%, while tyrosine (Tyr) and tryptophan (Trp) levels were not less in *nox1* as compared to WT plants under different growth conditions (Knappe et al., 2003; Voll et al., 2003). These data suggest the levels of PEP and its downstream products in subcellular compartment may play a role in NOX1 regulated signaling.

The *nox1* mutant contains high levels of NO. This NO overaccumulation has been suggested to regulate flowering time, development and defense response in *nox1* plants (He et al., 2004). However, the underlying mechanism of how *nox1* affects NO production remains largely unknown.

In this chapter, I show that *ssi2* plants constitutively accumulate high levels of Pip but abolishing Pip biosynthesis does not significantly alter *ssi2* defense and morphological phenotypes. However, a mutation in *NOX1* can reverse most autoimmune phenotypes presented in the *ssi2* background. Moreover, unlike *ssi2* suppressors *act1*, *acp4* and *gly1*, which normalizes *ssi2* phenotypes by increasing 18:1 levels, the *ssi2 nox1* plants continue to accumulate low levels of 18:1. Also different from *noa1*, which restore *ssi2* phenotypes by inhibiting NO production, the *nox1* mutant itself accumulates excess amount of NO, and the *ssi2 nox1* plants remain to contain high levels of NO. I further show that exogenous Phe but not PEP, Tyr or Trp is able to rescue *ssi2 nox1* back to *ssi2*- like defense phenotype. All these unique features indicate NOX1 plays a novel role in *ssi2* activated signaling. I also discuss the differences between *nox1* and *gsnor1*, *ssi2* and *camta1/2/3* plants.

5.2 Results

5.2.1 The *ssi2* plants show activated Pip biosynthesis and this activation is dependent on ALD1

Previous studies show *ssi2* plants constitutively accumulate SA and express PR-1 proteins (Nandi et al., 2005). Interestingly, a mutation in *ICS1* (*ISOCHORISMATE SYNTHASE 1*) or overexpressing *nahG* (a bacterial gene that encodes an SA hydroxylase) could block SA biosynthesis in *ssi2* background but neither of them can fully normalize *ssi2* morphology and defense phenotypes, suggesting additional factor may be involved in regulating *ssi2* signaling (Kachroo et al., 2005). We speculated that *ssi2* may also affect Pip levels in plants. I therefore determined Pip levels in *ssi2* plants. Notably, *ssi2* plants indeed accumulate a 30~40 folds increase in Pip levels compared to the WT plants (Fig. 5.1A). To test if the increase in Pip levels in *ssi2* plants is associated with Pip biosynthesis, I quantified the expression levels of *ALD1 (AGD2-LIKE DEFENSE RESPONSE PROTEIN*

1) because ALD1 regulates a key step in Pip biosynthesis (Navarova et al., 2012). Consistently, *ALD1* transcript levels were drastically elevated in *ssi2* compared to WT plants (Fig. 5.1B). NHP is the downstream signaling metabolite derived from Pip. To extend our findings related to Pip, I next measured NHP levels in *ssi2* plants. As expected, we found *ssi2* plants indeed contained about 30 times higher NHP than the WT plants (Fig. 5.1C). Similar to *ALD1*, *FMO1 (FLAVIN-DEPENDENT MONOOXYGENASE 1),* which encodes a pipecolate N-hydroxylase that converts Pip to NHP, was also highly expressed in *ssi2* plants (Fig. 5.1D). To further test if ALD1 is responsible for Pip biosynthesis in *ssi2* plants, I crossed *ssi2* with *ald1* plants thus generate the *ssi2 ald1* double mutant. Importantly, Pip levels in *ssi2 ald1* were completely restored to levels seen in *ald1* plants (Fig. 5.1E). Together, these results suggest Pip biosynthesis is induced in *ssi2* plants and this induction is dependent on ALD1.

5.2.2 The morphology and cell death phenotypes of *ssi2* are not associated with increased levels of Pip

The stunted morphology of *ssi2* plants is not caused by the increased SA accumulation because despite *ssi2 sid2* and *sid2 nahG* plants contained less than WT levels of SA, the size of *ssi2 sid2* and *sid2 nahG* plants were only slightly bigger than *ssi2* plants, indicating SA does not play a decisive role in regulating *ssi2* plant size (Kachroo et al., 2005; Shah et al., 2001). As we found *ssi2* plants also over accumulate Pip and its derivative NHP, we asked if Pip or NHP modulate(s) plant size in *ssi2*. I crossed *ssi2* with *ald1* or *fmo1* plants and generated homozygous *ssi2 ald1*, *ssi2 fmo1* double mutant plants. Interestingly, compared to the *ssi2* single mutant, *ssi2 ald1* and *ssi2 fmo1* plants showed slightly increased morphology, but they were still significantly smaller than the WT plants (Fig. 5.2A).

To assess how ALD1 and FMO1 affect auto cell death activated in *ssi2* plants. I monitored cell death in *ssi2 ald1* and *ssi2 fmo1* via trypan blue staining. As expected, no microscopic indicators of cell death were observed in WT, *sid2*, *ald1* and *fmo1* plants, while the *ssi2* plants showed extensive cell death. Notably, significant cell death developed in *ssi2 ald1* and *ssi2 fmo1* plants (Fig. 5.2B). These data correlate with the morphology

phenotypes seen in these plants, which collectively, suggesting that the morphology and cell death phenotypes presented in *ssi2* plants are likely not associated with increased levels of Pip (or NHP).

5.2.3 A mutation in the *NOX1* gene reverses *ssi2* morphological phenotypes

As mentioned earlier, *NOX1* encodes a chloroplast PEP/Pi transporter protein. It has also been reported that the *nox1* plants constitutively accumulate NO and the plants become more susceptible to both virulent and avirulent *P. syringae* pathogens. In contrast, in the *ssi2* plants, it was suggested that the increased levels of NO in *ssi2* chloroplasts positively regulate *ssi2* plants' resistance to virulent and avirulent *P. syringae* infection. Considering that *ssi2* activated defense signaling requires signal transport from the chloroplast to the nucleus, we suspect that NOX1 might play a role in *ssi2* activated defense signaling. To address this possibility, I crossed *nox1* with *ssi2* and isolated a homozygous *ssi2 nox1* double mutant from the F2 progeny. As previously discussed, *ssi2* plants have a stunted morphology while the *nox1* mutant shows a reticulate leaf pattern, additionally, *nox1* plants are also smaller in size than WT plants but are bigger than *ssi2* plants. To our surprise, the F2 progeny derived from *ssi2* × *nox1* cross mainly exhibited three morphology types, these were WT, *ssi2* and *nox1* like morphologies. I used mutant specific primers and genotyped ~100 F2 plants covering all three morphology types. The *ssi2 nox1* double mutant plants were isolated and it is interesting that all these plants looked like *nox1* and the other plants were either like WT or *ssi2* (Fig. 5.3).

5.2.4 The *nox1* mutation does not alter 18:1 levels in the *ssi2* background

Because SSI2 modulates 18:1 levels and most previously characterized *ssi2* suppressors rescue *ssi2* phenotypes by increasing 18:1 levels in *ssi2* plants. We asked if *nox1* would affect 18:1 levels in *ssi2* plants. To test this possibility, I first examined levels of 18:1 and its precursor 18:0 in *ssi2 nox1*, *ssi2*, *nox1* and WT plants. Notably, *ssi2* and *ssi2 nox1* plants were shown to contain similarly lower levels of 18:1 but higher levels of 18:0 compared to WT and *nox1* plants, suggesting *nox1* mutation does not affect 18:1 levels in *ssi2* plants (Figs. 5.4A and B). Detailed fatty acid (FA) profile analysis found that the *nox1* mutant contained normal levels of major FAs, which include C16 and C18-FAs (Fig.

5.4C). In *Arabidopsis* plastids, a portion of C16 and C18-FAs are incorporated into the galactolipid biosynthesis pathway to produce membrane lipids such as MGDG and DGDG. It is worth noting that, despite the *nox1* mutant exhibiting a normal total FA profile, it did contain lower levels of MGDG and DGDG, suggesting NOX1 is involved in plastid metabolism regulation (Figs. 5.4D and E). Together, these data indicate that although *nox1* rescue the *ssi2* morphology, it does not do this by altering 18:1 levels.

5.2.5 The *nox1* mutation reverses *ssi2* triggered defense phenotypes

The *ssi2* mutant exhibits enhanced resistance to *P. syringae* through SA dependent and independent pathways (Kachroo et al., 2003b; Shah et al., 2001). We sought to understand if *nox1* affects *ssi2* defense phenotypes. To test if the *nox1* mutation affects SA biosynthesis in *ssi2* plants, I first measured leaf SA levels in *ssi2*, *nox1*, *ssi2 nox1* and WT plants. Consistent with previous reports, *ssi2* contained high levels of free SA and bound SA (SA-glucoside, SAG), and *nox1* showed WT like basal levels of SA and SAG. However, the SA and SAG levels in *ssi2 nox1* were similar to those levels seen in WT plants (Figs. 5.5A and B). I earlier showed *ssi2* plants also constitutively accumulate Pip. It was later found that *ssi2 nox1* plants contained WT like levels of Pip (Fig. 5.5C). Moreover, the expression levels of SA pathway marker gene *PR-1* in *ssi2 nox1* were greatly reduced compared to *ssi*2 plants, albeit they were still higher than in WT plants (Fig. 5.5D). These results imply that the *nox1* mutation is able to largely block activation of the SA pathway in *ssi2* plants. The autoimmunity triggered by the *ssi2* mutation leads to constitutive cell death and H_2O_2 production, which are independent of the SA pathway. To determine if *nox1* could restore the cell death and H_2O_2 overaccumulation phenotypes seen in *ssi2* plants. I did trypan blue and DAB staining to examine cell death and H_2O_2 levels, respectively. The results showed that the *ssi2* plants contained widely distributed dead cells and high levels of H_2O_2 in absence of pathogen attack, but the *ssi2 nox1* plants were devoid of dead cells and produce less H_2O_2 than *ssi2* plants (Figs. 5.5E and F). These data demonstrate that *nox1* mutation suppress SA independent autoimmunity such as constitutive cell death and H_2O_2 overaccumulation in *ssi2* plants. Further, to test if *nox*1 mutation compromise heightened disease resistance in *ssi2*, I inoculated *ssi2*, *nox1*, *ssi2 nox1* and WT plants with virulent DC3000 and avirulent *avrRpm1* pathogen to evaluate

basal and *R* gene mediated resistance in these plants respectively. As expected, the *nox1* plants showed increased susceptibilities while *ssi2* plants displayed significantly elevated resistance to both DC3000 and *avrRpm1* infection, in contrast, *ssi2 nox1* plants supported more bacteria (DC3000 and *avrRpm1*) growth in their leaves compared to WT plants, similar to those seen in *nox1* plants (Figs. 5.5G and H). Collectively, these data suggest that *nox1* may reverses *ssi2* defense phenotypes through both SA dependent and independent pathways.

5.2.6 Exogenous Phe treatments reconstitute *ssi2* like phenotypes in *ssi2 nox1* plants

Previous reports suggest NOX1 is involved in PEP (and/or Pi) transport therefore *nox1* mutant might be defective in the biosynthesis of PEP derived metabolites including three aromatic amino acids (Tyr, Trp and Phe, collectively denoted as "TTP") in plants. Importantly, exogenous application of the three aromatic amino acids to *nox1* plants can rescue their reticulate leaf phenotype, demonstrating the importance of at least one of these aromatic amino acids in *nox1* mediated signaling (Streatfield et al., 1999). We asked what potential role PEP and TTP amino acids may play in *nox1* mediated rescue of *ssi2* phenotypes. To answer if PEP and TTP affect *nox1* and *ssi2 nox1* phenotypes, I grew *ssi2*, *nox1*, *ssi2 nox1* and WT plants on ½ MS plates supplied with or without additional 0.5 mM PEP or 0.5 mM TTP (aromatic amino acids combination). Notably, 0.5 mM PEP treatments seemed to uniformly inhibit plant growth as all four genotype of plants were reduced in size as compared to their counterparts grown on ½ MS plates without PEP, but the morphology of these plants were not different with or without PEP, suggesting exogenous PEP likely could not rescue *nox1* and *ssi2 nox1* morphological phenotypes. However, I found that adding 0.5 mM TTP in the ½ MS plates was able to restore the reticulate leaf phenotype seen in nox1 and *ssi2 nox1* plants (Fig. 5.6A).

Because *ssi2* plants accumulate high levels of Pip but *ssi2 nox1* plants contain WT like levels of Pip, we sought to use high Pip levels as a defense activation marker in the *ssi2* background. Indeed, *ssi2* plants grown on ½ MS plates continue to show constitutive Pip accumulation, albeit these Pip levels are lower than soil grown *ssi2* plants. Consistently, *ssi2 nox1* plants grown on ½ MS plates produce WT like levels of Pip. We measured Pip levels in *ssi2*, *nox1*, *ssi2 nox1* and WT plants grown on ½ MS plates with or

without 0.5 mM PEP or 0.5 mM TTP. Compared with mock treatment (PEP and TTP not added), adding 0.5 mM PEP in the ½ MS plates did not change Pip levels in plants assayed (WT, *ssi2*, *ssi2 nox1*) (Fig. 5.6B). Conversely, 0.5 mM TTP treatment significantly increased Pip levels in *ssi2 nox1* plant, suggesting that TTP may reactivate defense signaling in *ssi2 nox1* plants (Fig. 5.6C). To test if the defense reactivation in *ssi2 nox1* plants require all three aromatic amino acids or there is a single, individual amino acid that is responsible for the process, I again grew *ssi2*, *nox1*, *ssi2 nox1* and WT plants on ½ MS plates, and, in addition, supplied these plates with 0.5 mM Tyr, 0.5 mM Trp, 0.5 mM Phe or a combination of 0.5 mM of combinations of two amino acids (Tyr+Trp, Tyr+Phe and Trp+Phe). I measured Pip levels in these plants. Notably, Pip levels were rescued in *ssi2 nox1* plants when Phe alone or in combination was included in the media (Fig. 5.6D). These data reveal that, of the TTP, likely only Phe plays an important role in *nox1* governed *ssi2* signaling.

5.2.7 The *ssi2* mutant contains high levels of Phe whereas *nox1* is deficient in Phe biosynthesis and Phe is involved in plant defense

Consistent with previous report, I found that Phe levels were induced by avirulent *avrRpm1* infection (data not shown). We suspected that Phe levels may be important in *ssi2* mediated signaling. I next measured Phe levels in *ssi2*, *nox1*, *ssi2 nox1* and WT plants. Notably, our results showed that compared to the WT plants, *ssi2* retained about 2~4-fold levels of Phe, and *nox1* contained less than 50% levels of Phe, whereas Phe levels in *ssi2 nox1* were comparable or less than in WT plants (Fig. 5.7A). Phe can be synthesized from arogenate by ADT (AROGENATE DEHYDRATASE). The *Arabidopsis* genome encodes six *ADT* genes (Chen et al., 2016). To test if ADT are involved in Phe accumulation in *ssi2*, I measured the expression levels of *ADT* genes in *ssi2* and WT plants. The expression levels of *ADT1*, *ADT2*, *ADT5*, *ADT6* were similar between *ssi2* and WT plants, *ADT3* expression levels were somehow reduced in *ssi2* plants. However, the expression levels of *ADT4* were increased by 5 folds in *ssi2* as compared to WT plants (Fig. 5.7B). It was previously reported that overexpressing *ADT4* could dramatically increase Phe levels in *Arabidopsis* (Aoi et al., 2020). These data indicate that *ssi2* may increase Phe accumulation by up-regulating *ADT4* expression.

To understand the biological function of Phe, I sought to exogenously provide *ssi2*, *nox1*, *ssi2 nox1* and WT plants with Phe and test if this treatment could affect their phenotypes. To do this, I grew *Arabidopsis* plants in soil and supplied them with 0.5 mM Phe through either leaf infiltration or soil drench. Intriguingly, unlike plants grown on ½ MS plates, neither leaf infiltration nor soil drench of Phe could recover leaf Pip levels in *ssi2 nox1* plants, suggesting Phe may have not been effectively taken up by the plants grown in soil. To determine if the leaves of soil grown plants can take up Phe from soil via the root system, I irrigated WT plants with different concentrations of Phe. Results seemed to suggest higher concentrations (20 mM) of Phe, applied as a soil drench, did increased leaf Phe levels (data not shown). We asked if Phe levels could affect plant resistance. To test this, I soil drenched *ssi2*, *nox1*, *ssi2 nox1* and WT plants with 0 (control) or 20 mM Phe, and inoculated plants with virulent DC3000 one day after Phe treatments. Notably, compared to the control, 20 mM Phe soil drench drastically enhanced resistance to DC3000 in WT plants, and an increase in resistance were also evident in *nox1* and *ssi2 nox1* plants, although these are weaker than WT. Since *ssi2* plants were already highly resistant to DC3000, Phe soil treatments did not appear to further upregulate its resistance (Fig. 5.7C). Phe can serve as a precursor for SA biosynthesis in plants, I therefore measured SA levels in *ssi2*, *nox1*, *ssi2 nox1* and WT plants with or without 20 mM Phe soil drench. To our surprise, Phe soil treatments did not appear to affect SA levels in these plants (Figs. 5.7D and E). Together, these data reinforce the idea that Phe may play an important role in *ssi2* mediated defense signaling.

5.2.8 The *nox1* plants are less sensitive to glycerol induced reduction of 18:1 levels

Previous studies reveal that exogenous application of glycerol on *Arabidopsis* leaves can lower 18:1 levels in plants, and thus mimic *ssi2* phenotypes in WT plants. We sought to take advantage of glycerol treatments to generate a low 18:1 environment in the *nox1* plants and investigate how *nox1* plants respond to 18:1 level change. Consistent with the fact that *ssi2 nox1* plants contains *ssi2*-like levels of 18:1, exogenous glycerol application reduced 18:1 levels in *nox1* like it did in the WT plants, as a control, the *act1* mutant did not show reduced 18:1 levels after glycerol treatment because it lacked the G3P

ACETYLTRANSFERASE capable of forming the ester linkage of 18:1 with G3P (derived from glycerol) (Fig. 5.8A). Because lowering 18:1 levels can induce cell death in plants, I found that exogenous glycerol induced significant cell death on WT plants, which was evident through the yellowish appearance of the treated leaves and cell death measured via trypan blue staining assay, however, the leaf appearance of *nox1* plants were not significantly different with or without glycerol treatment, neither did *nox1* leaves show microscopic cell death after glycerol treatment. The *act1* plants behaved as expected since their leaves did not present a difference with or without glycerol treatment (Figs. 5.8B and C).

Lowering 18:1 levels has also been shown to induce SA biosynthesis in plants. I measured SA levels in WT, *act1* and *nox1* plants after glycerol treatment. Indeed, in WT plants, exogenous glycerol application increased free SA levels by 2~3 fold and SAG levels by more than 50 folds, which reflected a similar SA/SAG pattern seen in *ssi2* plants. Notably, no increase of SA and SAG levels were observed in *act1* plants and *nox1* only showed a small increase in SA and SAG levels after glycerol treatment (Figs. 5.8D and E). In addition, exogenous glycerol application also significantly increased Pip levels in WT plants but considerably less in *nox1* plants and not at all in *act1* plants (Fig. 5.8F). I further determined WT, *act1* and *nox1* plants resistance to DC3000 after glycerol treatment. We found that glycerol treatment enhanced disease resistance in WT plants, but not in *act1* or *nox1* plants (Figs. 5.8G and H). Together, these data further support the idea that the *nox1* mutation inhibits 18:1-level decline mediated responses.

5.2.9 The *nox1* plants are not severely impaired in SA and Pip pathways

Earlier reports suggest the *nox1* mutant is compromised in SA biosynthesis and signaling likely due to elevated internal NO levels (Yun et al., 2011; Yun et al., 2016). I showed in previous chapter that NO overproducer *gsnor1* plants are compromised in Pip biosynthesis. It is tempting to know if *nox1* restore *ssi2* phenotypes by suppressing SA and Pip biosynthesis. To test if *nox1* affects SA biosynthesis, I measured SA levels in WT and *nox1* plants after *avrRpt2* inoculation. To our surprise, the induction of free SA and SAG by *avrRpt2* infection in *nox1* were not significantly different from that seen in WT plants (Figs. 5.9A and B). To extend this finding, I also examined the expression of several

genes involved in SA biosynthesis after *avrRpt2* infection, these genes included *SARD1*, *CBP60g* and *SID2*. The expression of *SARD1*, *CBP60g* and *SID2* were not lower in *nox1* than WT plants in response to *avrRpt2* (Fig. 5.9C). The *PR-1* gene is a SA marker, I measured *PR-1* expression in WT and *nox1* plants after *avrRpt2* inoculation. However, I have not got a conclusive result, *PR-1* gene in some experiments showed lower expression in *nox1* plants, but higher expression in *nox1* than WT plants was also observed. These data suggest *nox1* may not significantly affect the SA pathway.

To assess if *nox1* mutation affects Pip levels, I again inoculated WT and *nox1* plants with *avrRpt2* and monitored Pip levels in these plants. Pip biosynthesis was strongly induced by *avrRpt2* infection in both WT and *nox1* plants, and the levels of Pip were slightly less in *nox1* as compared to WT plants (Fig. 5.9D). These results indicate that *nox1* plants may be partially impaired in Pip biosynthesis.

5.2.10 NO levels in the *ssi2 nox1* plants remain high

A mutation in the *NOA1* gene leads to the reduction in NO production and the *noa1* mutation was found to rescue *ssi2* phenotypes by lowering its NO levels (Mandal et al., 2012). This work illuminated the importance of NO in *ssi2*-mediated signaling. The *nox1* mutant was reported to constitutively accumulate NO (He et al., 2004). We asked what role NO plays in the *ssi2 nox1* plant. I measured NO levels in WT, *ssi2*, *nox1*, and *ssi2 nox1* plant by using the NO specific dye DAF-2DA via confocal microscopy analysis. Notably, we confirmed that both *nox1* and *ssi2* contained higher levels of NO than WT plants. Importantly, we noticed that *ssi2 nox1* plants continued to retain higher levels of NO like that seen in *nox1* plants (Figs. 5.10A and B). These data further imply that *nox1* may restore *ssi2* phenotypes by acting downstream of NO.

5.2.11 The relationships between NO overproducers mutant *nox1*, *gsnor1* and autoimmunity mutant *ssi2*, *camta1/2/3*

I have shown earlier that like *nox1*, *gsnor1* plants also accumulate high levels of NO. Several previous studies used *nox1* and *gsnor1* as NO overproducers and attributed their various phenotypes to NO overaccumulation (Yun et al., 2011; Yun et al., 2016).

However, the differences between *nox1* and *gsnor1* have been rarely addressed. Because *nox1* mutation was able to restore *ssi2* activated phenotypes, I asked if the *gsnor1* mutation could do the same. I crossed *ssi2* with *gsnor1* plants and generated *ssi2 gsnor1* homozygous plants. I next measured several important *ssi2* related phenotypes in the *ssi2 gsnor1* plants. Notably, the morphology of *ssi2 gsnor1* plants were bigger than *ssi2* but noticeably smaller than WT and *gsnor1* plants (Fig. 5.11A). In addition, *ssi2 gnsor1* contained significantly less SA and SAG and Pip than *ssi2* but still much higher than WT (Fig. 5.11B and C). The *ssi2 gsnor1* plants also accumulated less cell death and H_2O_2 compared to *ssi2* plants (Fig. 5.11D). Together these data suggest *gsnor1* mutation cannot rescue *ssi2* activated signaling like *nox1* does.

Interestingly, two autoimmune mutants *ssi2* and *camta1/2/3* share many similarities, including stunted size, activated defense signaling and enhanced disease resistance (Fig. 5.11E). To test if *camta1/2/3* triggered autoimmunity depends on 18:1 levels, I determined 18:1 levels in WT, *ssi2* and *camta1/2/3* plants. The *camta1/2/3* plants showed similar levels of 18:1 as compared to WT (Fig. 5.11F). To test if *nox1* can rescue *camta1/2/3* triggered phenotypes, I crossed *nox1* with *camta1/2/3* plant and isolated *nox1 camta1/2/3* homozygous quadruple mutant plants. Interestingly, the n*ox1 camta1/2/3* plants were as small as *camta1/2/3*. In addition, *nox1 camta1/2/3*, much like *camta1/2/3* plants continued to contain elevated levels of SA and SAG as compared to WT plants (Figs. 5.11G and H). Together, these data suggest NOX1 functions differently than GSNOR1 and the *nox1* mutation could not rescue *camta1/2/3* triggered phenotypes.

5.3 Discussion

Over the last three decades, thanks to the isolation and characterization of key immune regulators, we have seen extensive progress being made in the field of plant defense. Plant immunity is tightly controlled under normal conditions, which means an immune response is triggered only upon recognition of pathogens. However, in many cases, the loss-of-function in negative immune regulators and gain-of-function in immune receptors result in the activation of defense responses, which often include constitutive SA accumulation and defense gene expression, and dwarf morphology (van Wersch et al.,

2016). *SSI2* encodes a stearoyl-ACP desaturase. The *ssi2* mutation leads to a drastic decline of 18:1 levels in plants. Exogenous application of glycerol on plant leaves can reduce 18:1 levels and thereby mimicking *ssi2* triggered defense signaling. Moreover, genetic mutations that resulted in a recovery of 18:1 levels in the *ssi2* background can rescue *ssi2* phenotypes. These findings demonstrate that *ssi2*-triggered autoimmunity is associated with 18:1 levels. The 18:1 level appears to regulate NO levels by modulating NOA1 protein stability. However, the downstream signaling of 18:1 in plant defense remains elusive. In this study, we aimed to further explore the underlying mechanism(s) of *ssi2*-activated signaling.

Pip-NHP biosynthesis were significantly upregulated in the *ssi2* mutant. The elevated levels of Pip are dependent on ALD1 because a mutation in *ALD1* nearly blocked Pip biosynthesis in the *ssi2* background. This is further supported by the observation that the expression of both *ALD1* and *FMO1* were markedly increased in *ssi2* plants.

Because *ssi2* plants contain excess Pip and NHP, we reasoned if Pip and NHP contribute to the stunted morphology of *ssi2* plants. Using genetic approach, I generated *ssi2 ald1* and *ssi2 fmo1* mutants. By accessing the morphology of these mutants and WT plants, I show that a mutation in *ALD1* or *FMO1* only slightly increase plant size in the *ssi2* background. Furthermore, I show that a mutation in *ALD1* or *FMO1* does not alter cell death development in *ssi2* plants. Together, these data suggest cell death triggered by *ssi2* mutation is not significantly associated with increased Pip and NHP levels.

Interestingly, a mutation in the *NOX1* gene resulted in the reverse of morphology in *ssi2* plants. We show that *ssi2 nox1* homozygous plants display *nox1* like morphology. Because 18:1 levels were found to be the key force driving *ssi2*-triggered phenotypes, and several previous characterized *ssi2* suppressors rescue *ssi2*-activated phenotypes by altering 18:1 levels (Kachroo et al., 2003a; Kachroo et al., 2004; Xia et al., 2009). I therefore paid special attention to 18:1 levels in *ssi2 nox1* plants. In this study, I show that a mutation in *NOX1* does not alter 18:1 levels in the *ssi2* plants, although we show *nox1* plants contain lower levels of galactolipids MGDG and DGDG than WT plants. Based on these data, we predict *nox1* will help us uncover new insights into *ssi2*-mediated signaling.

As *ssi2 nox1* plants show *nox1* like morphology, we next measured defense related phenotypes in *ssi2 nox1* plants. Our data demonstrate that unlike *ssi*2 plants, which contain high levels of SA/SAG and H_2O_2 and exhibit extensive cell death in leaves, the *ssi2 nox1* plants have WT like SA/SAG levels and H_2O_2, they also display practically no microscopic cell death in their leaves. In addition, we tested the resistance of *ssi2 nox1* plants to compatible and incompatible *P. syringae* strains and I show that *ssi2 nox1* plants completely loss *ssi2*-mediated resistance as they become more susceptible than WT plants upon both DC3000 and *avrRpm1* infections. Based on these observations, we conclude that the *nox1* mutation can largely restore *ssi2*-triggered defense phenotypes.

Previous studies suggested that the chloroplast transporter protein NOX1 is capable of transporting PEP (and inorganic phosphate) across the chloroplast membrane (Knappe et al., 2003; Voll et al., 2003). PEP is also known to serve as a precursor for many metabolites, including aromatic amino acids (Tyr, Trp and Phe, abbreviation TTP) in plants (Maeda and Dudareva, 2012). It was proposed that the reticulate leaf pattern seen in *nox1* plants was caused by TTP deficiency and exogenously supplying *nox1* plants with TTP could recover their reticulate leaf phenotype (Streatfield et al., 1999). We asked if PEP and TTP could convert *ssi2 nox1* back to *ssi2* like plants by complementing *nox1* mutation. Our PEP and TTP feeding experiments conducted on ½ MS plates show that exogenous TTP but not PEP can partially restore the reticulate leaf phenotype in *ssi2 nox1* and *nox1* plants. I further show that TTP treatment reactivate Pip biosynthesis in *ssi2 nox1*, while the nontreated *ssi2 nox1* control plants remain to produce WT like levels of Pip. To determine the role of individual aromatic amino acid in TTP triggered Pip biosynthesis in *ssi2 nox1* plants, I measured Pip levels in *ssi2 nox1* plants grown on ½ MS plates that were supplied with Tyr, Trp, Phe or Tyr+Trp, or Trp+ Phe. The results show that Pip levels in *ssi2 nox1* plants could be increased whenever Phe is included in the treatments. These data suggest that Phe levels play an important role in *ssi2*-triggered phenotypes.

To extend our finding related to Phe. I determined the levels of Phe in WT, *ssi2*, *nox1* and *ssi2 nox1* plants. We show that while *nox1* plants contain significantly less Phe than WT plants, the *ssi2* plants accumulate 2-3 times more Phe than WT plants. Notably, the *nox1* mutation has restored Phe back to WT like levels in *ssi2* background. *ADT* genes

encode key enzymes to produce Phe in plants, I show that the expression of *ADT4* is upregulated in *ssi2* plants by about 5 folds. A previous study reported that Phe levels in *Arabidopsis* plants were highly increased when *ADT4* was overexpressed. These results suggest the elevated Phe levels may contribute to *ssi2* triggered phenotypes. We also show that Phe soil drench could dramatically increase WT plant's resistance to Pst DC3000, despite this effect was less pronounce in *nox1*, *ssi2 nox1* background. These data indicate Phe plays a positive role in plant defense response to DC3000.

Exogenous application of glycerol can lower 18:1 levels thereby mimics *ssi2*-like phenotypes in plants. Although glycerol application was found to lower 18:1 levels in *nox1* plants like it did in WT plants, the *nox1* mutant showed little to no cell death after glycerol treatment. In contrast, glycerol treatment induced extensive cell death in WT plants. Moreover, glycerol treatment can also induce SA accumulation and increase resistance to DC3000 in WT plants, but this phenomenon was also abolished in *nox1* mutant plants. Together, these results indicate exogenous glycerol treatment can lower 18:1 levels in *nox1* plants but the *nox1* mutation can significantly block 18:1 mediated signaling.

In this study, we found that a mutation in the *NOX1* gene could inhibit SA and Pip/NHP biosynthesis in *ssi2* plants. We asked if *nox1* was compromised in SA and Pip biosynthesis. I measured SA and Pip levels in *nox1* plants after avirulent pathogen infection. In contrast to previous reports, I show that *nox1* is not significantly impaired in SA biosynthesis. Meanwhile, *nox1* plants were shown to accumulate just slightly less Pip than WT upon avirulent pathogen infection. In addition, the expression of SA biosynthesis gene *SARD1*, *CBP60g* and *SID2* were also normally induced in *nox1* in response to avirulent pathogen infection. These results suggest *nox1* plants likely are not significantly impaired in SA/Pip biosynthesis.

Previous report revealed that a mutation in *NOA1* gene resulted in NO deficiency and the *noa1* mutation could rescue *ssi2* triggered phenotypes. It was suggested that *ssi2*-triggered signaling was mediated through high levels of NO (Mandal et al., 2012). Notably, both *nox1* and *ssi2* plants accumulate high levels of NO. I show that the *ssi2 nox1* plants continue to accumulate high levels of NO. These results suggest that the NOX1 may act downstream of NO in *ssi2*-triggered defense signaling.

The *nox1* and *gsnor1* mutants have been widely used as NO overproducers and the many phenotypes presented in these two mutants were often attributed to high NO levels in these two plants. However, here in this study, I show evidence that *gsnor1* and *nox1* plants behave very differently. The *gsnor1* plants are significantly compromised in SA and Pip biosynthesis but *nox1* plants appear not to be significantly impaired in SA and Pip biosynthesis. While the *gsnor1* mutation could largely rescue *camta1/2/3* triggered phenotypes, the *nox1* mutation has nearly no effect on *camta1/2/3* triggered phenotypes. Conversely, the *nox1* mutation could largely rescue *ssi2* triggered phenotypes, the *gsnor1* mutation can only partially rescue *ssi2* triggered phenotypes. Lastly, we also measured 18:1 levels in *camta1/2/3* plants, and we conclude that the autoimmunity seen in *camta1/2/3* plants is not caused by a decline in 18:1 level, which is in contrast to *ssi2* mutant.

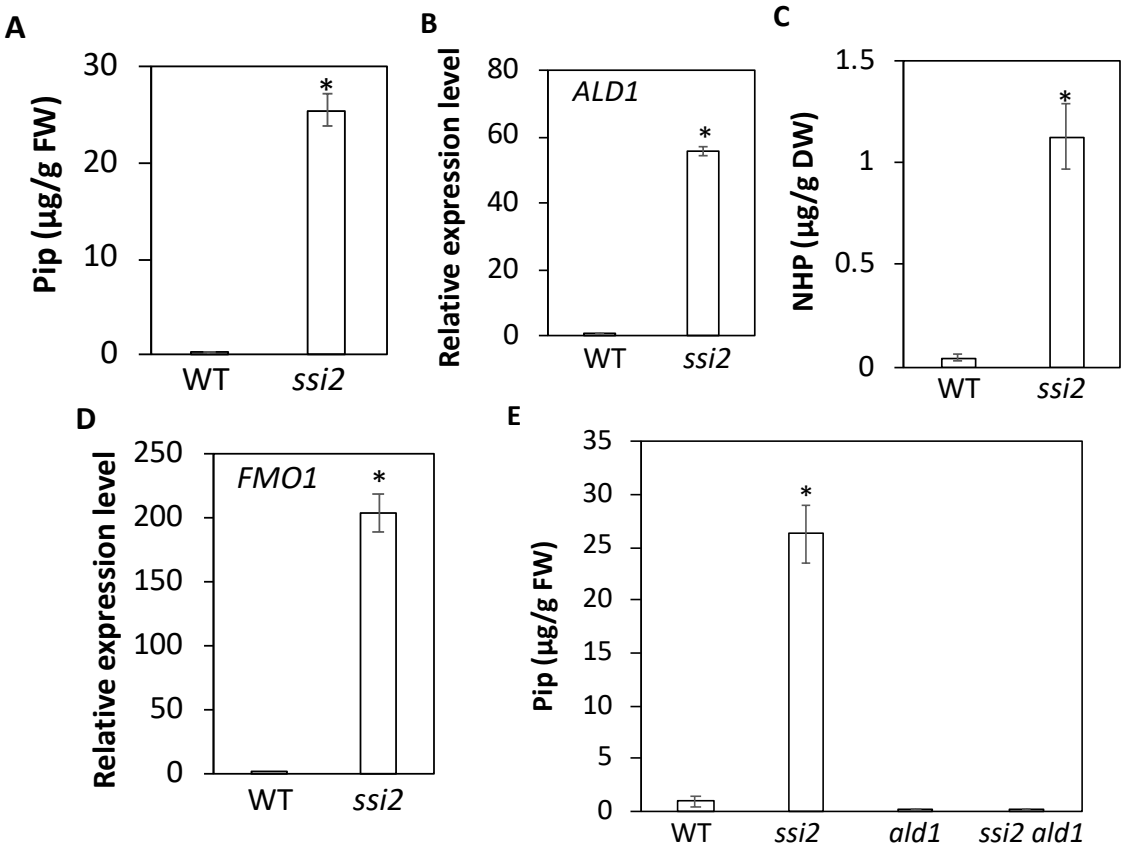

Figure 5.1 The *ssi2* plants constitutively accumulate Pip and Pip derivative NHP and Pip accumulation is dependent on ALD1

(A) Pip and **(C)** NHP levels in WT (Col-0) and *ssi2* plants. **(B)** *ALD1* and **(D)** *FMO1* expression levels in *ssi2* plants. **(E)** Pip levels in indicated genotypes. FW, fresh weight; DW, dry weight. The error bars indicate standard deviation (SD) (n = 4). The "*" denotes significant differences with WT plants (t test, $P < 0.01$). These experiments were repeated at least twice with similar results.

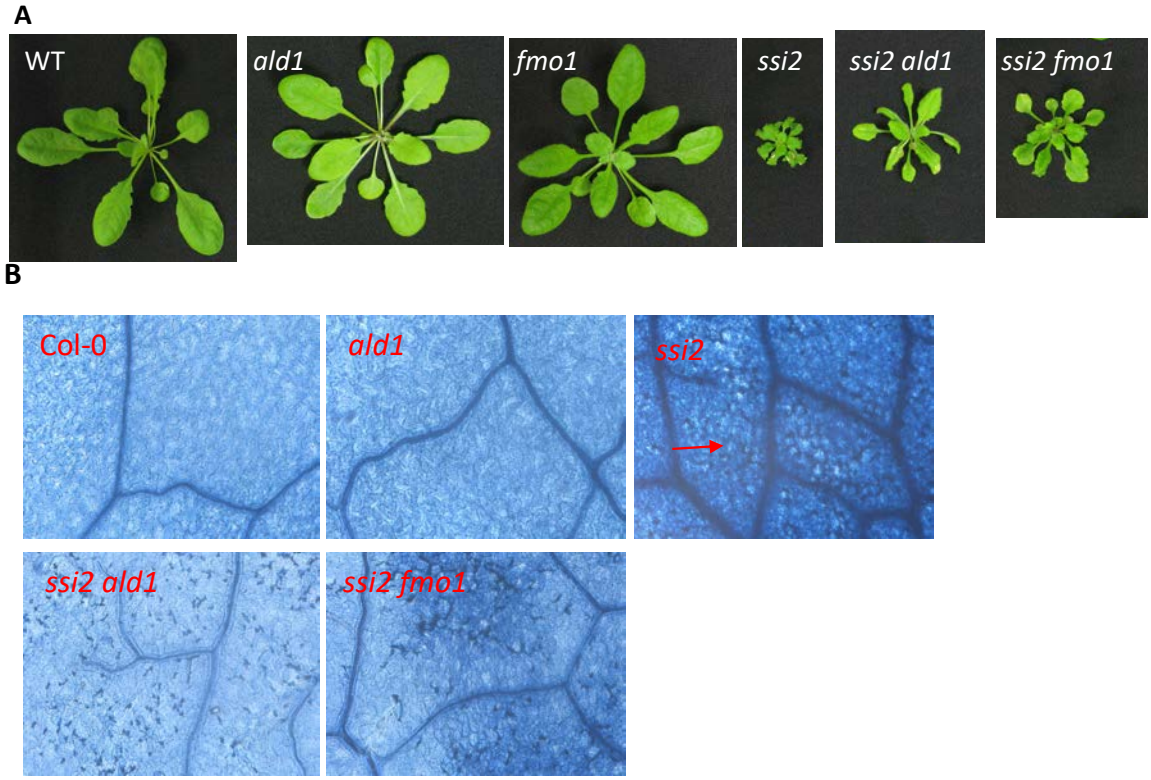

Figure 5.2 A mutation in *ALD1* or *FMO1* slightly increases the morphology of *ssi2* plants but does not significantly alter cell death phenotype in the *ssi2* background
(A) The morphology of indicated genotype of plants. **(B)** Leaf cell death of indicated genotypes of plants stained by trypan blue. At least 3 leaves were observed under microscope, arrow points to dead cells stained by the trypan blue dye.

Figure 5.3 A mutation in *NOX1* rescues *ssi2* morphology

The morphology of 4-week-old Col-0, Nossen, s*si2, nox1* and *ssi2 nox1* plants.

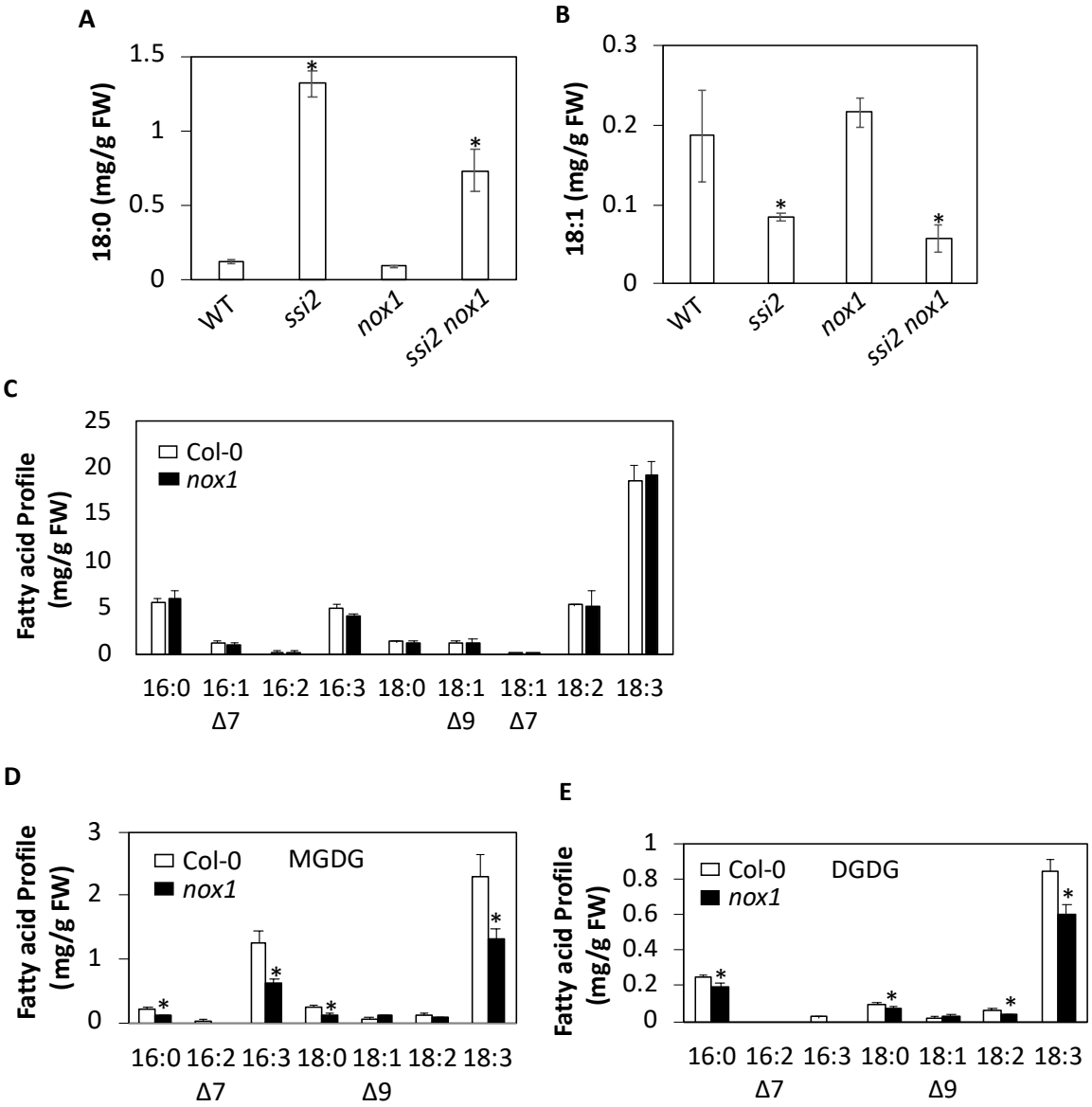

Figure 5.4 The *nox1* mutation does not alter 18:1 levels in *ssi2* plants

(A) The levels of 18: 0 fatty acid in WT (Col-0), *ssi2*, *nox1* and *ssi2 nox1* plants. FW, fresh weight. The error bars indicate SD (n = 4). The "*" denotes a significant difference with WT (t-test, P < 0.01). **(B)** The levels of 18: 1 levels of WT (Col-0), *ssi2*, *nox1* and *ssi2 nox1* plants. FW, fresh weight. The error bars indicate SD (n = 4). The "*" denotes a significant difference with WT (t-test, P < 0.01). **(C)** Total, **(D)** MGDG and **(E)** DGDG fatty acid profiles of Col-0 and *nox1* plants. FW, fresh weight. The error bars indicate SD (n = 4). The "*" denotes a significant difference with WT (t-test, P < 0.01). The experiments were repeated at least twice with similar results.

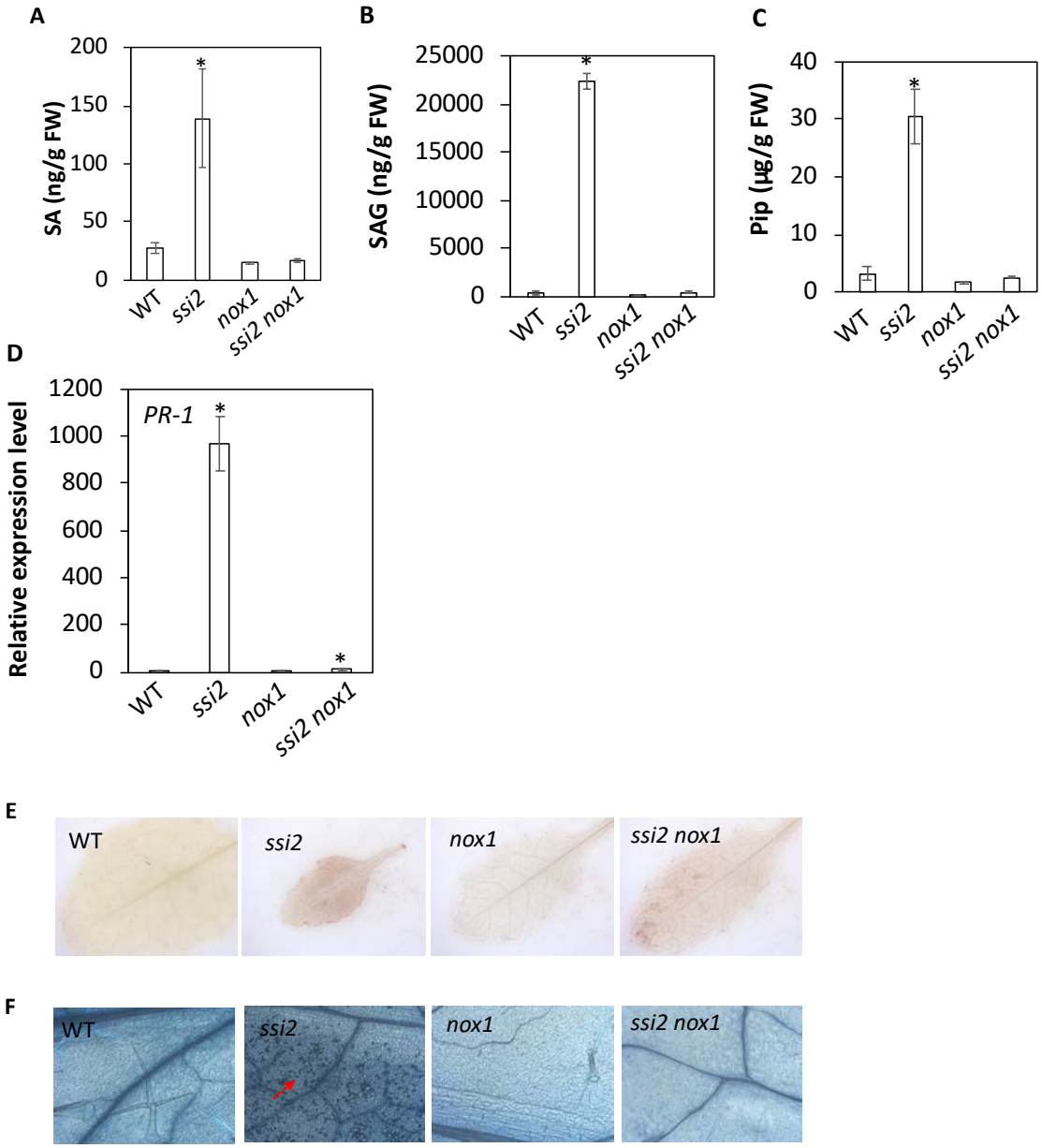

Figure 5.5 The *nox1* mutation alters *ssi2* defense phenotypes

(A) SA, **(B)** SAG and **(C)** Pip levels in WT (Col-0), *ssi2*, *nox1* and *ssi2 nox1* plants. FW, fresh weight. The error bars indicate SD (n = 4). The "*" denotes a significant difference with WT (t-test, $P < 0.01$). **(D)** *PR-1* expression levels in WT (Col-0), *ssi2*, *nox1* and *ssi2 nox1* plants. **(E)** DAB staining to determine H_2O_2 levels in indicated genotypes **(F)** Trypan blue staining to determine cell death in leaves of indicated genotype of plants. Arrow points to dead cells stained by the trypan blue dye. The experiments were repeated at least twice with similar results.

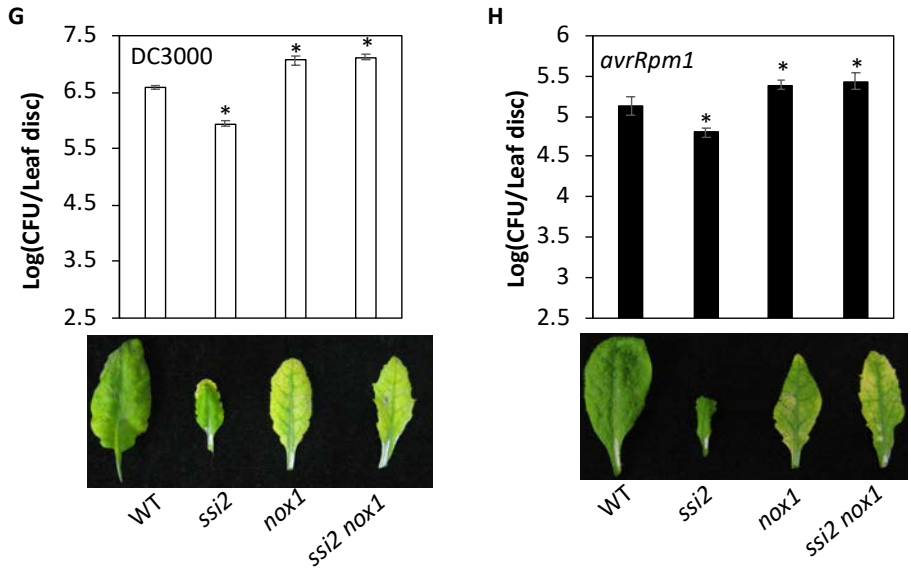

Figure. 5.5 (continued) The *nox1* mutation alters *ssi2* defense phenotypes
(G) Local disease response to compatible DC3000 infection in WT (Col-0), *ssi2*, *nox1* and *ssi2 nox1* plants. The error bars indicate SD (n = 4). The "*" denotes a significant difference with WT (t-test, $P < 0.01$). **(H)** Local disease response to incompatible *avrRpm1* infection in WT (Col-0), *ssi2*, *nox1* and *ssi2 nox1* plants. The error bars indicate SD (n = 4). The "*" denotes a significant difference with WT (t-test, $P < 0.05$). The experiment was repeated at least twice with similar results.

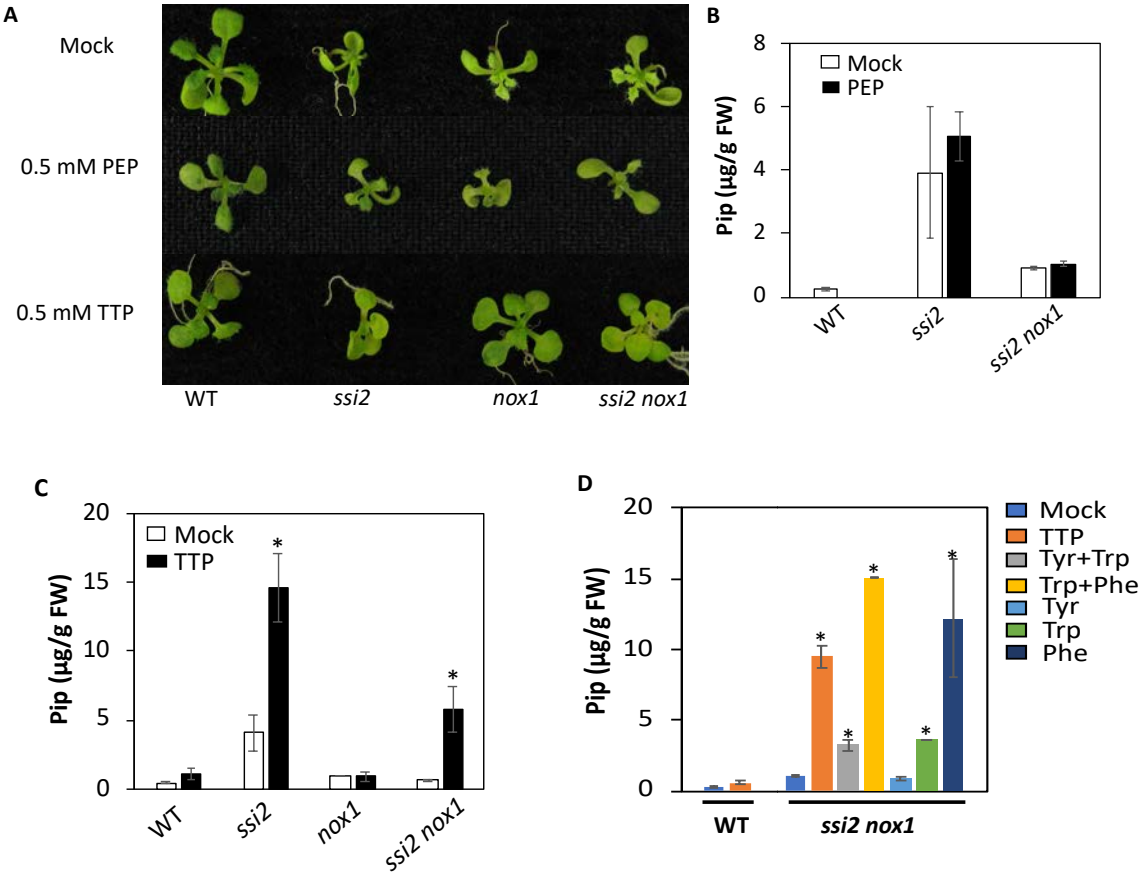

Figure 5.6 Phenylalanine (Phe) reconstitutes *ssi2* like phenotypes in *ssi2 nox1* plants
(A) Morphology of 3-week-old WT (Col-0), *ssi2*, *nox1* and *ssi2 nox1* plants grown on 1/2 MS (Murashige and Skoog medium) plates supplied with Mock (no addition), 0.5 mM PEP (phosphoenolpyruvate) or 0.5 mM TTP (tyrosine, tryptophan and phenylalanine). **(B)** Pip levels in 3-week-old WT (Col-0), *ssi2* and *ssi2 nox1* plants grown on 1/2 MS plates supplied with Mock (no addition) or 0.5 mM PEP. FW, fresh weight. The error bars indicate SD (n = 4). **(C)** Pip levels in 3-week-old WT (Col-0), *ssi2, nox1* and *ssi2 nox1* plants grown on 1/2 MS plates supplied with Mock (no addition) or 0.5 mM TTP. FW, fresh weight. The error bars indicate SD (n = 4). The "*" denotes a significant difference with Mock treatment (t-test, *P < 0.01). **(D)** Pip levels in 3-week-old WT (Col-0), *ssi2 nox1* plants grown on 1/2 MS plates supplied with Mock (no addition) or 0.5 mM of individual aromatic amino acids or a combination of two or three of them. FW, fresh weight. The error bars indicate SD (n = 4). The "*" denotes a significant difference with Mock treatment (t-test, P < 0.01).

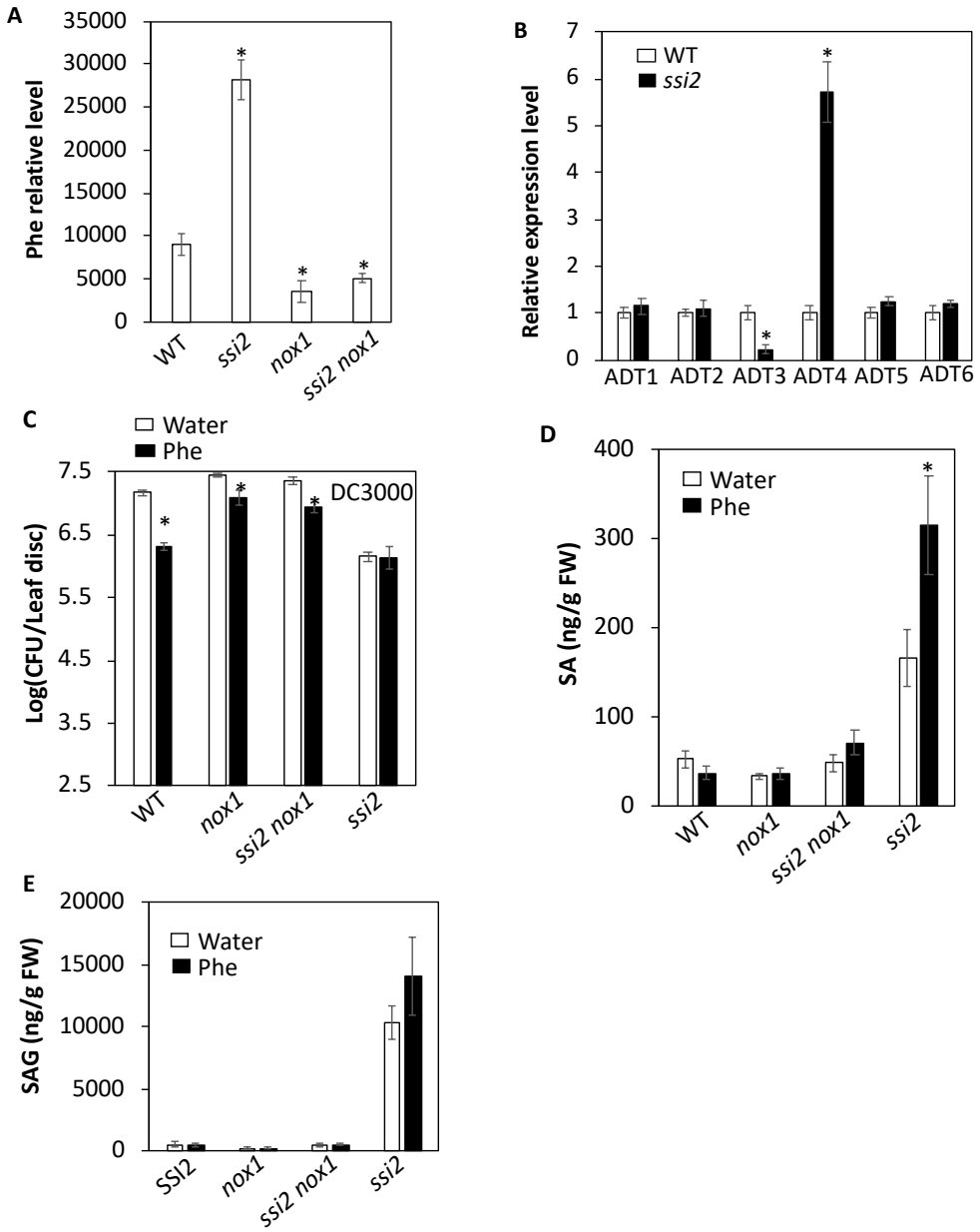

Figure 5.7 Phe levels in *ssi2* and *nox1* plants and Phe plays a role in defense
(A) Relative levels of Phe in WT (Col-0), *ssi2*, *nox1* and *ssi2 nox1* plants. **(B)** *ADT* gene expression levels in WT (Col-0) and *ssi2* plants. Expression level of each gene in WT (Col-0) was set to 1. **(C)** Leaf disease response to DC3000 infection in WT (Col-0), *ssi2*, *nox1* and *ssi2 nox1* after these plants were soil drenched with 20 mM Phe for 1 day. The leaves were sampled at 3 dpi to measure bacterial population. The error bars indicate SD (n = 4). The "*" denotes a significant difference with Mock (water) treatment (t-test, *P <0.01). **(D)** SA and **(E)** SAG levels in leaves of indicated genotype of plants after they were soil drenched with 20 mM Phe for 1 day. FW, fresh weight. The error bars indicate SD (n = 4). The "*" denotes a significant difference with Mock (water) treatment (t-test, *P <0.01).

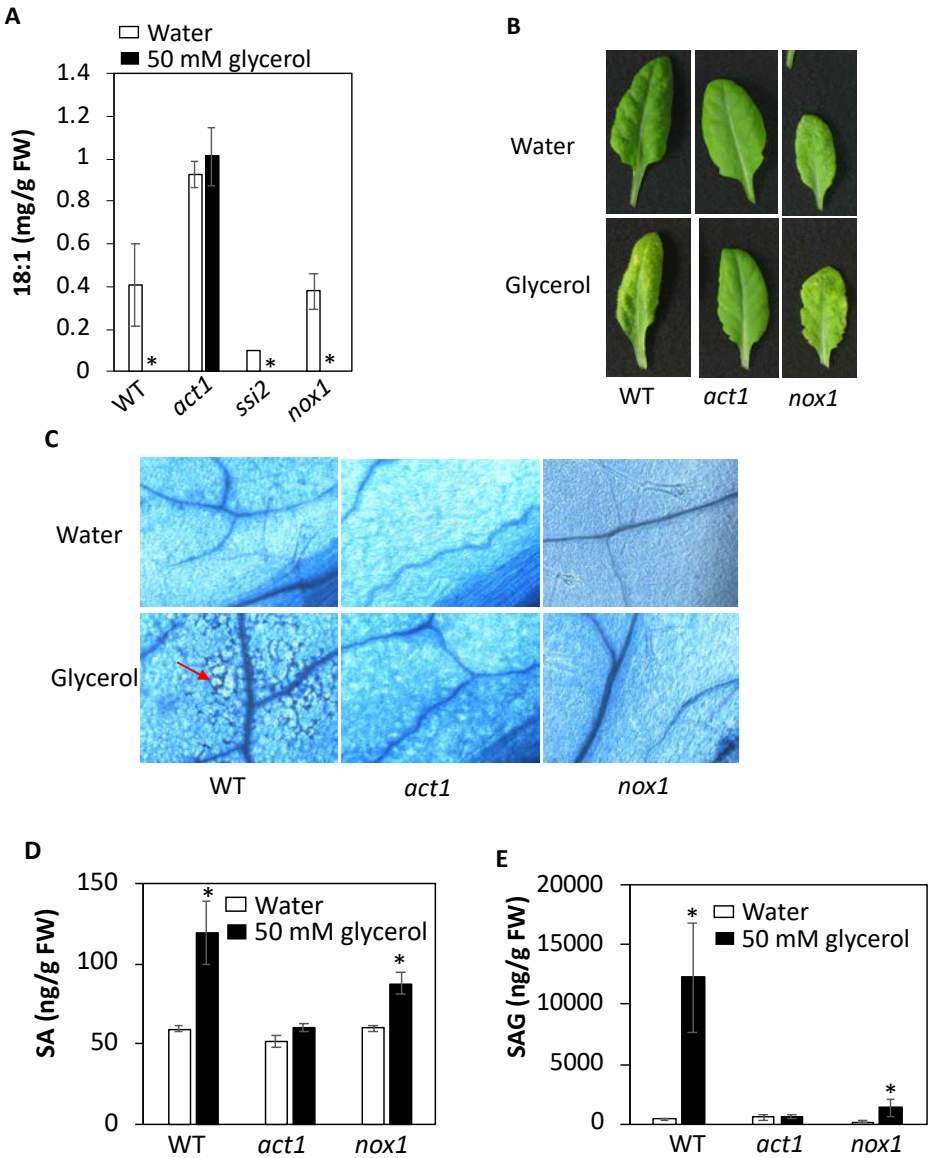

Figure 5.8 The 18:1-triggered defense signaling is inhibited in *nox1* plants

(A) Levels of 18:1 in leaves of WT (Col-0), *act1*, *ssi2* and *nox1* plants after sprayed with Mock (water) or 50 mM for 5 days. Please note that the 18:1 levels in glycerol treated SSI2, *ssi2* and *nox1* plants were very low and near the detection limits. **(B)** Leaf symptoms and **(C)** leaf cell death stained by trypan blue in WT (Col-0), *act1* and *nox1* plants after sprayed with Mock (water) or 50 mM for 5 days. Arrow points to dead cells stained by trypan blue dye. **(D)** SA and **(E)** SAG levels in leaves of WT (Col-0), *act1* and *nox1* plants after sprayed with Mock (water) or 50 mM for 5 days. The error bars indicate SD (n = 4). The "*" denotes a significant difference with water treatment (t-test, P <0.01).

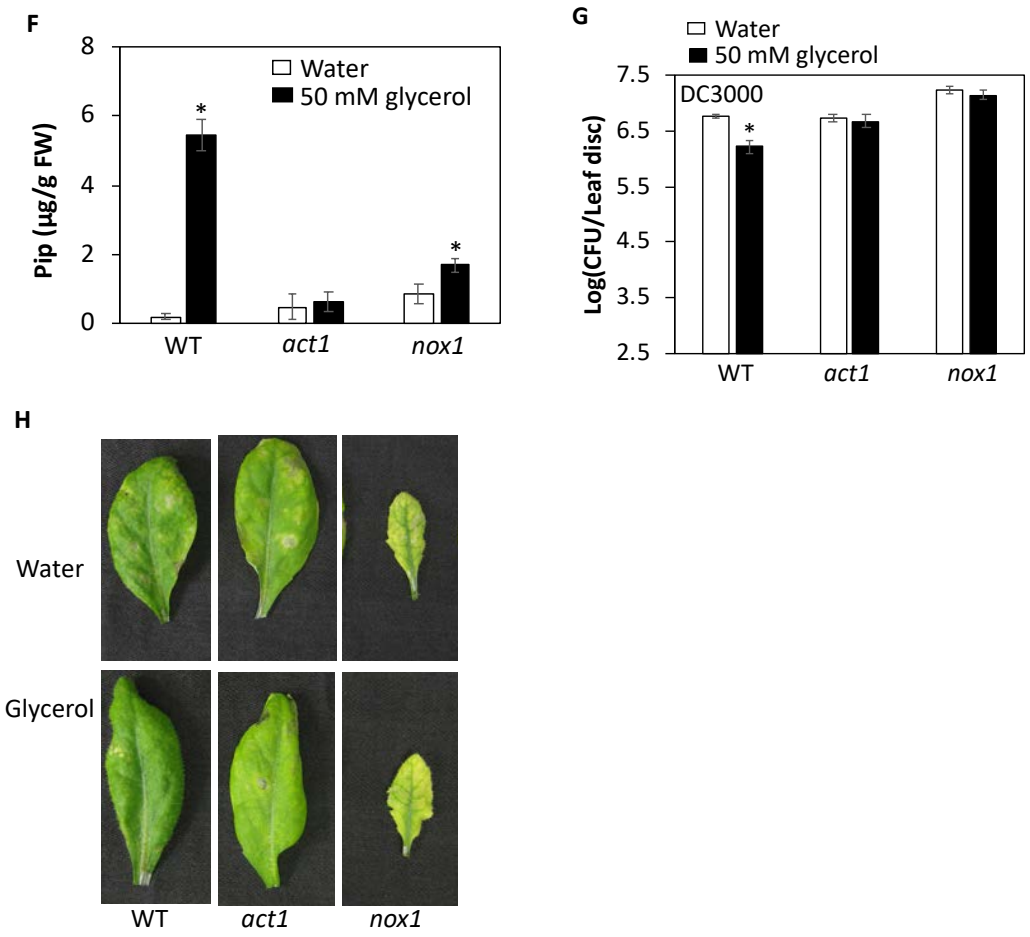

Figure. 5.8 (Continued) 18:1-triggered defense signaling is inhibited in *nox1* plants

(F) Pip levels in leaves of WT (Col-0), *act1* and *nox1* plants after sprayed with Mock (water) or 50 mM for 5 days. FW, fresh weight. The error bars indicate SD (n = 4). The "*" denotes a significant difference with Mock treatment (t-test, $P < 0.05$). **(G)** leaf response to DC3000 infection in WT (Col-0), *act1* and *nox1* plants after these plants had first been sprayed with Mock (water) or 50 mM glycerol for 3 days. DC3000 infected leaves were sampled at 3 dpi to measure bacterial populations. The error bars indicate SD (n = 4). The "*" denotes a significant difference with Mock treatment (t-test, $P < 0.01$). **(H)** Leaf symptoms of WT (Col-0), *act1* and *nox1* plants in response to DC3000 infection (3 dpi) after these plants had first been sprayed with Mock (water) or 50 mM glycerol for 3 days.

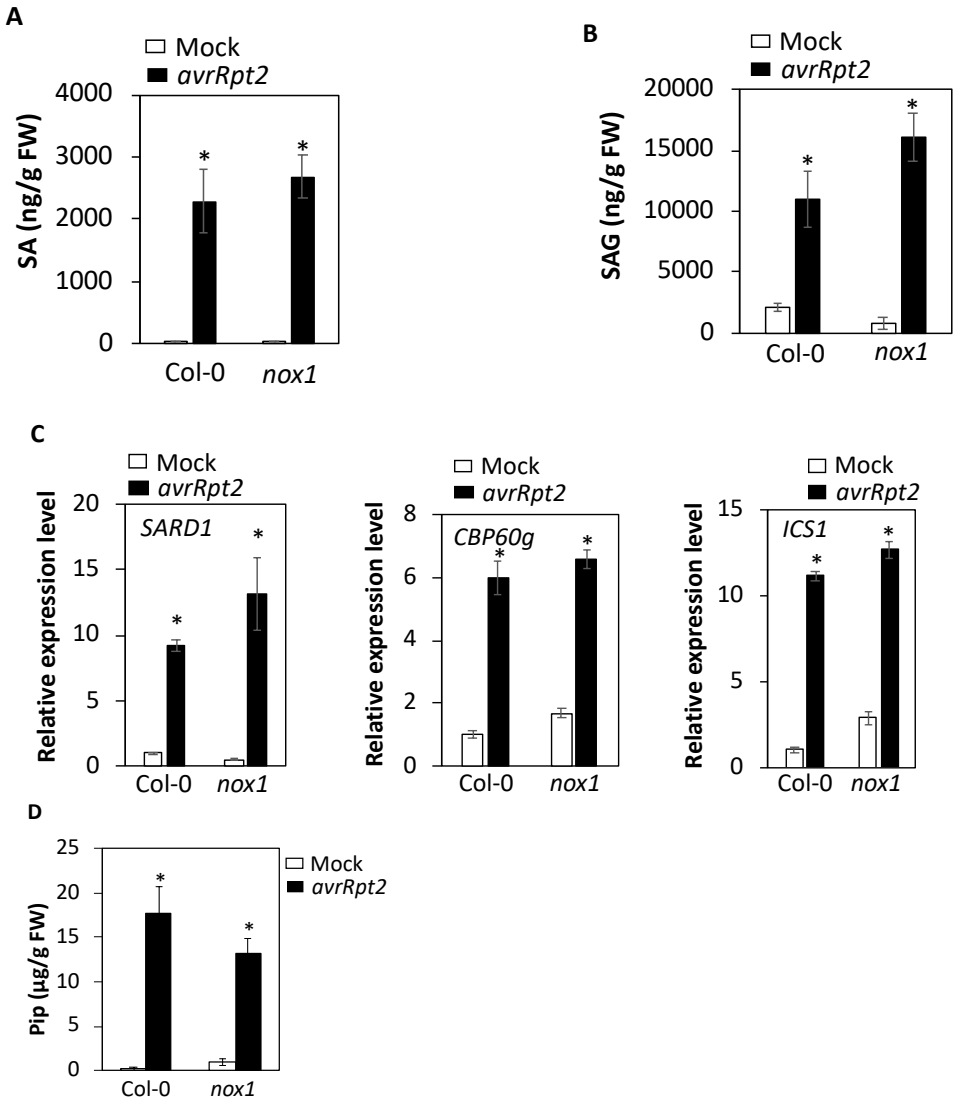

Figure 5.9 The *nox1* plants are not severely impaired in SA and Pip pathways

(A) SA, **(B)** SAG and **(D)** Pip levels in infiltrated leaves of Col-0 and *nox1* plants upon *avrRpt2* infection. Leaves were sampled at 24 hpi. FW, fresh weight. The error bars indicate SD (n = 4). The *"*"* denotes a significant difference with Mock treatment (10 mM $MgCl_2$) (t-test, $P < 0.01$). **(C)** Expression levels of *SARD1*, *CBP60g* and *ICS1* in infiltrated leaves of Col-0 and *nox1* plants upon *avrRpt2* infection. Leaves were sampled at 24 hpi. The error bars indicate SD (n = 4). The *"*"* denotes a significant difference with Mock treatment (10 mM $MgCl_2$) (t-test, $P < 0.01$).

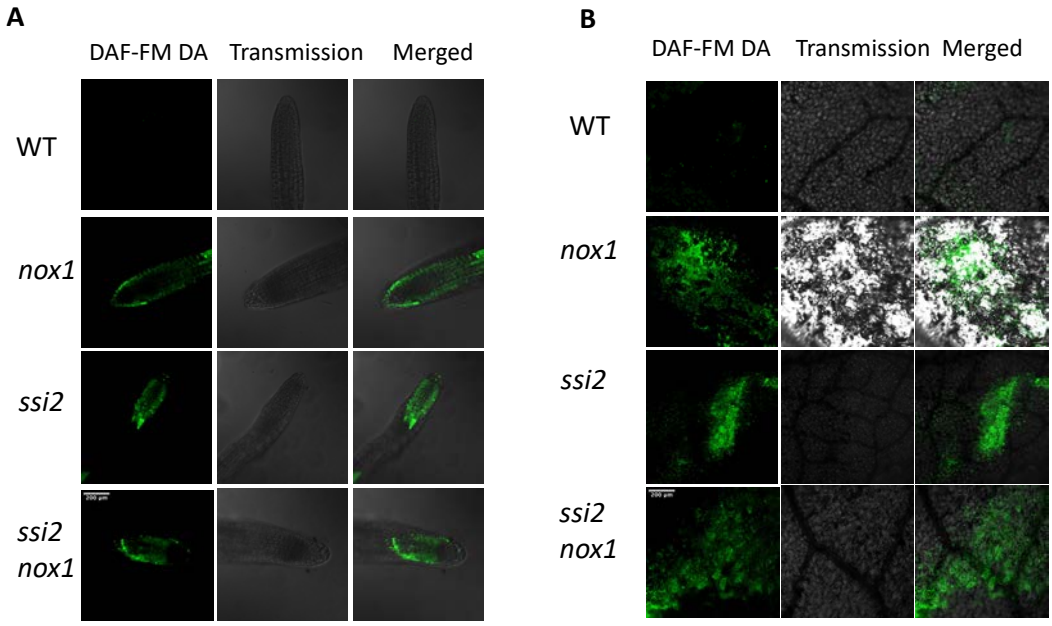

Figure 5.10 The *ssi2 nox1* plants continue to accumulate NO

(A) Root and **(B)** Leaf tissues of WT (Col-0), *nox1*, *ssi2* and *ssi2 nox1* plants were stained with NO specific dye DAF-FM DA (4-amino-5-methylamino-2′,7′-difluorofluorescein diacetate) and overserved under confocal microscope. See Method chapter for more details. The experiment was repeated twice with similar results.

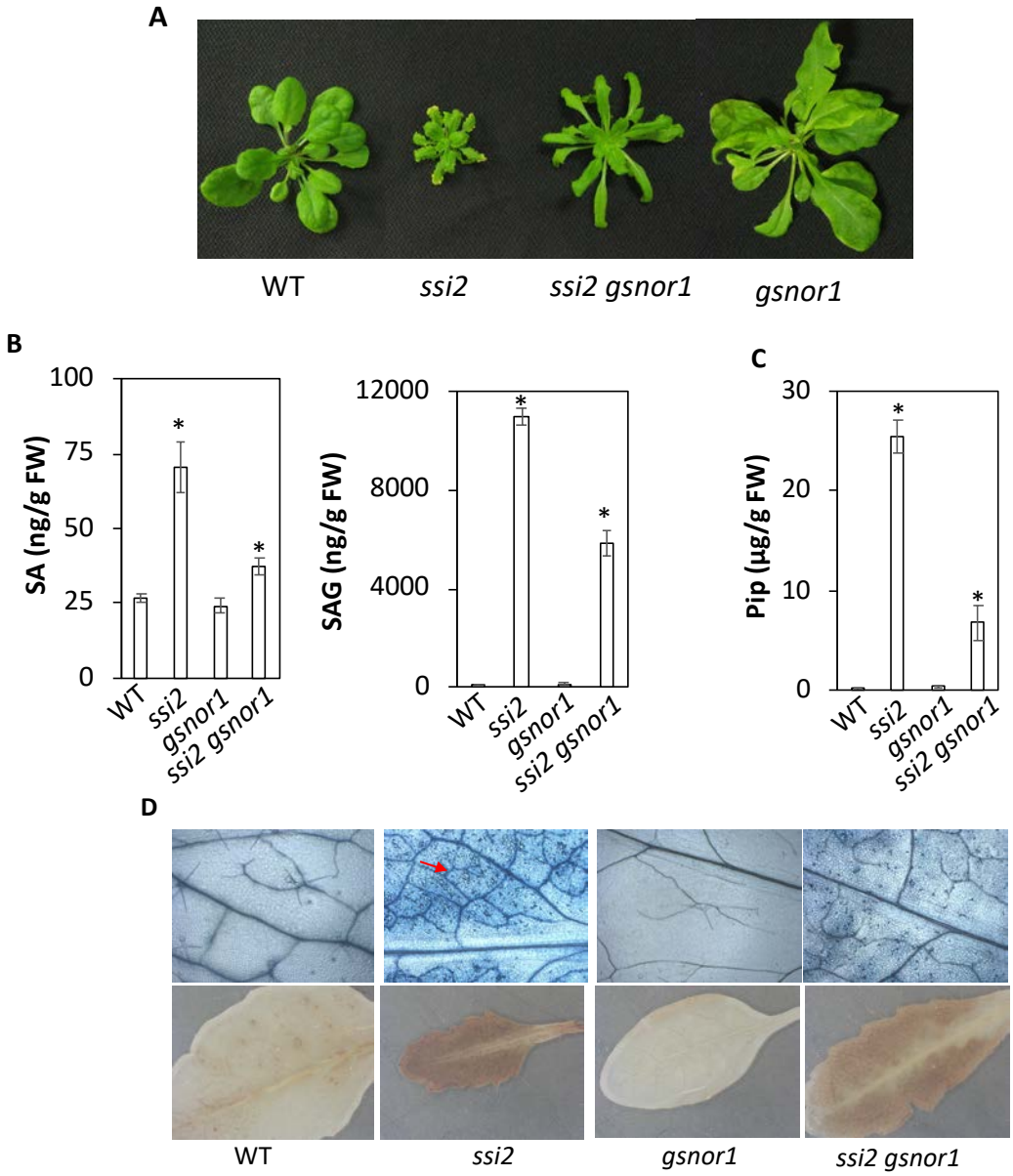

Figure 5.11 The relationship between *nox1* and *gsnor1*, *ssi2* and *camta1/2/3* plants

(A) Morphology of WT (Col-0), *ssi2, gsnor1* and *ssi2 gsnor1* plants. **(B)** SA, SAG and **(C)** Pip levels in leaves of WT (Col-0), *ssi2, gsnor1* and *ssi2 gsnor1* plants. FW, fresh weight. The error bars indicate SD (n = 4). The "*" denotes a significant difference with Mock (10 mM $MgCl_2$) treatment (t-test, P <0.01). **(D)** Cell death measured by trypan blue staining assay (top panel) and H_2O_2 accumulation detected by DAB staining assay (lower panel) in WT (Col-0), *ssi2, gsnor1* and *ssi2 gsnor1* plants. Arrow points to dead cells stained by the trypan blue dye. The experiment was repeated twice with similar results.

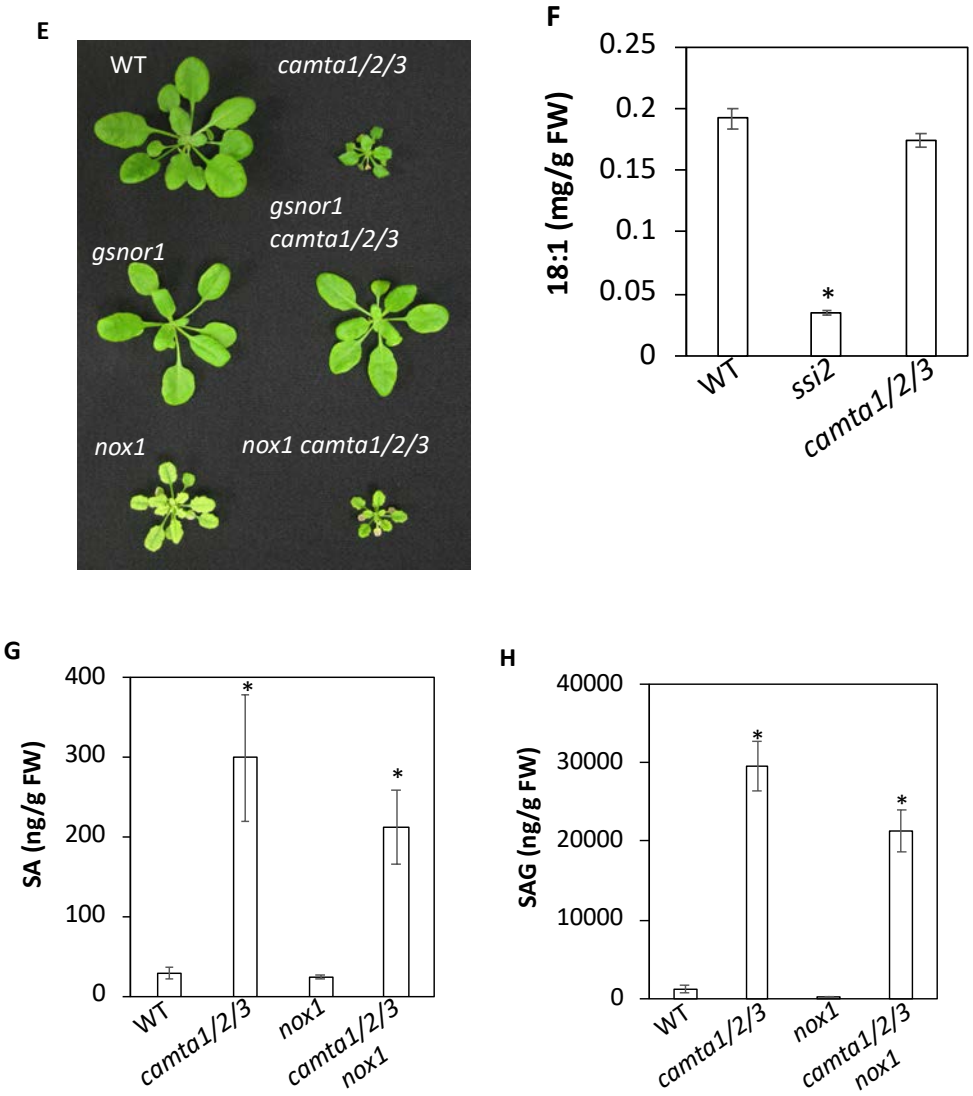

Figure 5.11 (Continued) The relationship between *nox1* and *gsnor1*, *ssi2* and *camat1/2/3* plants

(E) Morphology of 5-week-old WT (Col-0), *camta1/2/3, gsnor1, nox1, camta1/2/3 gsnor1* and *camta1/2/3 nox1* plants. **(F)** The 18:1 levels in leaves of WT (Col-0), *ssi2, camta1/2/3* plants. FW, fresh weight. The error bars indicate SD (n = 4). The "*" denotes a significant difference with WT (t-test, P <0.01). **(G)** SA and **(H)** SAG levels in leaves of WT (Col-0), *camta1/2/3, nox1, camta1/2/3 nox1* plants. FW, fresh weight. The error bars indicate SD (n = 4). The "*" denotes a significant difference with WT (t-test, P <0.01).

SUMMARY

In this dissertation, my work was focused on understanding the role of NO in inter- and intra- cellular defense signaling. In chapter 3, to explore how NO regulates SAR (inter cellular signaling) in plants, I characterized the role of *Arabidopsis* GSNO reductase GSNOR1 in SAR. I show that despite NO could act upstream of AzA/G3P pathway in SAR signaling, the *gsnor1* mutant which accumulates high levels of NO was not impaired in AzA/G3P pathway during SAR because the biosynthesis and transport of AzA/G3P were not altered in gsnor1 as compared to WT plants. I further show that *gsnor1* plants were compromised in SA and Pip biosynthesis and GSNOR1 likely regulates SA and Pip biosynthesis downstream of or in parallel with CAMTA through modulating the transcription of SARD1 and CBP60g. Importantly, my work revealed that high levels of NO in *gsnor1* plants inhibited SA transport and I further demonstrated that SA transport was required for SAR establishment in *gsnor1* plants. In addition, I also found that GSNOR1 mediated NO accumulation was likely independent of NOA1 and NIA2 proteins, which provides new insight on NO biosynthesis regulation in plants.

In addition to SAR, in chapter 5, I presented new findings related to the role of GSNOR1 in local defense response. Previously, it was suggested that high levels of NO in *gnsor1* plants promote cell death development in *Arabidopsis*. Here in my current study, I showed that the cell death development in *gsnor1* plants depends on the types of R-avr interactions. In addition, GSNOR1-regulated cell death is likely not dependent on SA, Pip or ROS and the enhanced disease susceptibility in *gsnor1* plants is not solely caused by the defect in SA biosynthesis. Overall, my results have provided new insights on how GSNOR1 and high levels of NO derived from the *gsnor1* mutation regulate SAR and local defense responses.

Earlier work from our lab showed that NO functions downstream of 18:1 fatty acid to mediate chloroplast-nucleus retrograde defense signaling in *Arabidopsis*. There is a possibility that NO mediated retrograde signaling involves an unknown chloroplast signal. In chapter 4, I show that a loss-of-function mutation in NOX1 significantly attenuated the activated defense signaling in *ssi2* plants. Unlike previously characterized *ssi2* suppressors, the *nox1* mutation does not alter *ssi2* defense phenotypes by normalizing 18:1 level in *ssi2*

plants. Our further investigation suggested that aromatic amino acid phenylalanine likely plays a key role in *ssi2*-activated defense signaling. It is possible that phenylalanine is the retrograde signal that acts downstream of or in parallel with NO in plants. This work reveals novel insights and will help us better understand NO mediated chloroplast-nucleus retrograde signaling.

APPENDIX

LIST OF ABBREVIATIONS

Acronym/abbreviation	Expansion
L/mL/µL	Liter/ milliliter/ microliter
M/mM/µM	Molar/millimolar/ micromolar
g/mg/µg/ng	Gram/ milligram/ microgram/ nanogram
h/min/sec	Hours/minutes/seconds
ACP	Acyl-carrier-protein
ACP	ACYL CARRIER PROTEIN
ACP4	ACYL CARRIER PROTEIN 4
ACT1	ACYLTRANSFERASE 1
ADT	AROGENATE DEHYDRATASE 1
ALD1	AGD2-LIKE DEFENSE RESPONSE PROTEIN1
APX	ASCORBATE PEROXIDASE
Avr	Avirulent
AzA	Azelaic acid
AZI1	AZELAIC ACID INDUCED 1
BAK1	BRASSINOSTEROID INSENSITIVE 1 (BRI1)-ASSOCIATED RECEPTOR KINASE 1
BHT	Butylated hydroxytoluene
BIK1	BOTRYTIS-INDUCED KINASE 1
BRI1	BRASSINOSTEROID INSENSITIVE 1
Ca2+	Calcium
CaCl2	Calcium chroride
CaM	Calmodulin
CAMTA	CALMODULIN BINDING TRANSCRIPTION ACTIVATOR
CBP60g	CALMODULIN-BINDING PROTEIN 60g
CFU	Colony-forming units
DAB	3,3'-diaminobenzidine
DAF-2DA	4,5-diaminofluorescein diacetate
DEPC	Diethyl pyrocarbonate
DETA-NONOate	(Z)-1-[N-(2-aminoethyl)-N-(2-ammonioethyl) amino] diazen-1-ium-1,2-diolate
DGDG	Digalactosyldiacylglycerol
DIR1	DEFECTIVE IN INDUCED RESISTANCE
DMSO	Dimethyl sulfoxide
DNA	Deoxyribonucleic acid

dNTP	Deoxyribo nucleic triphosphate
DPI (dpi)	Days post inoculation
DTT	Dithiothreitol
ECL	Enhanced chemiluminescence
EDS1	ENHANCED DISEASE SUSCEPTIBILITY 1
EDTA	Ethylene diamine tetraacetic acid
EF-Tu	Elongation factor Tu
EGTA	Ethylene glycol tetraacetic acid
FA	Fatty acid
FAD	Flavin adenine dinucleotide
FAD2	FATTY ACID DESATURASE 2
FAM	Fluorescein
FAS	Fatty acid synthase
flg22	Bacterial flagellin 22
FLS2	FLAGELLINE INSENSITIVE 2
G3P	Glycerol-3-phosphate
GC-MS	Gas chromatography–mass spectrometry
GLY1	GLYCEROL-3-PHOSPHATE DEHYDROGENASE 1
GSH	Glutathione
GSNO	S-Nitrosoglutathione
GSNOR	GSNO reductase
GSNOR1	S-NITROSOGLUTATHIONE REDUCTASE 1
H_2O_2	Hydrogen peroxide
H_2SO_4	Sulfuric acid
H_3PO_4	Phosphoric acid
HR	hypersensitive response
ICS	ISOCHORISMATE SYNTHASE
JA	jasmonic acid
K_2HPO_4	Potassium phosphate, dibasic
KAC	ketoacid ε-amino-α-ketocaproic
KCl	Potassium chloride
KH_2PO_4	Potassium phosphate, monobasic
KOH	Potassium hydroxide
LB	Luria-Bertani
lyso-PA	1-acyl-sn-glycerol 3-phosphate
MAPK	Mitogen-activated protein kinase
MES	2-(N-morpholino)ethanesulfonic acid
MeSA	Methyl salicylate
$MgCl_2$	Magnesium chloride

MGDG	Monogalactosyldiacylglycerol
$MgSO_4$	Magnesium sulfate
MS	Murashige and Skoog
MSTFA	N-Methyl-N-(trimethylsilyl) trifluoroacetamide
MTBSTFA	N-Methyl-N-tert-butyldimethylsilyltrifluoroacetamide
Na_2HPO_4	Sodium hydrogen phosphate
NaCl	Sodium chloride
NAD^+	Nicotinamide adenine dinucleotide
NADPH	REDUCED NICOTINAMIDE ADENINE DINUCLEOTIDE PHOSPHATE
NaN_3	Sodium azide
NaOAc	Sodium acetate
NaOH	Sodium hydroxide
NHP	N-hydroxy-pipecolic acid
NO	Nitric oxide
NOA1	NO ASSOCIATED 1
NOE1	NITRIC OXIDE EXCESS 1
NOS	NITRIC OXIDE SYNTHASE
NOX1	NO OVERPRODUCER 1
NPR1	NONEXPRESSER OF PATHOGENESIS-RELATED GENES 1
NR	NITRATE REDUCTASE
^oC	Degrees centigrade
PAD4	PHYTOALEXIN DEFICIENT 4
PAL	PHENYLALANINE AMMONIA LYASE
PAMP	Pathogen-associated molecular patterns
PBS	Phosphate buffered saline
PCR	Polymerase chain reaction
PDLP1	PLASMODESMATA LOCALIZING PROTEIN 1
PDLP5	PLASMODESMATA LOCALIZING PROTEIN 5
PEP	Phosphoenolpyruvate
PEX	Petiole exudate
PFD	Photon flux density
pH	Potential of hydrogen
Phe	Phenylalanine
Pip	Pipecolic acid
PPDK	PLASTID-TARGETED PYRUVATE ORTHOPHOSPHATE DIKINASE
PPT1	PHOSPHOENOLPYRUVATE/PHOSPHATE TRANSLOCATOR 1

PRR	Pattern-recognition receptor
PTI	PAMP triggered immunity
R	Resistant or resistance
RBOHD	RESPIRATORY BURST OXIDASE HOMOLOG D
RLK	Receptor-like kinase
RNA	Ribonucleic acid
RNS	Reactive nitrogen species
ROS	Reactive oxygen species
RPM1	RESISTANCE TO P. SYRINGAE PV MACULICOLA 1
RPS4	RESISTANT TO P. SYRINGAE 4
SA	Salicylic acid
SABP2	SALICYLIC ACID BINDING PROTEIN 2
SAG	Salicylic acid glucoside
SAR	Systemic acquired resistance
SARD1	SYSTEMIC ACQUIRED RESISTANCE DEFICIENT 1
SARD4	SAR-DEFICIENT4
SDS	Sodium dodecyl sulfate
sid2	salicylic acid induction deficient 2
SnRK2.8	SNF1-RELATED PROTEIN KINASE 2.8
SSC	Sodium chloride, sodium citrate
SSI2	SUPPRESSOR OF SA INSENSISTIVE 2
Sulfo-NONOate	Hydroxydiazenesulfonic acid 1-oxide
T3SS	Type III secretion system
TBE	Tris-borate/ EDTA electrophoresis buffer
TCMS	2,2,2-Trifluoro-N-methyl-N-(trimethylsilyl)-acetamide, Chlorotrimethylsilane
TE	TRIS-EDTA
TLC	Thin layer chromatographic
TMV	Tobacco mosaic virus
Tris-HCl	Tris(hydroxymethyl)aminomethane hydrochloride
Trp	Tryptophan
Tyr	Tyrosine
UV	Ultraviolet
WT	Wild-type

REFERENCES

Ahuja, I., Kissen, R., and Bones, A.M. (2012). Phytoalexins in defense against pathogens. Trends Plant Sci *17*, 73-90.

Aoi, Y., Oikawa, A., Sasaki, R., Huang, J., Hayashi, K.I., and Kasahara, H. (2020). Arogenate dehydratases can modulate the levels of phenylacetic acid in Arabidopsis. Biochem Biophys Res Commun *524*, 83-88.

Asai, S., and Shirasu, K. (2015). Plant cells under siege: plant immune system versus pathogen effectors. Curr Opin Plant Biol *28*, 1-8.

Bigeard, J., Colcombet, J., and Hirt, H. (2015). Signaling mechanisms in pattern-triggered immunity (PTI). Mol Plant *8*, 521-539.

Bittel, P., and Robatzek, S. (2007). Microbe-associated molecular patterns (MAMPs) probe plant immunity. Curr Opin Plant Biol *10*, 335-341.

Bouche, N., Scharlat, A., Snedden, W., Bouchez, D., and Fromm, H. (2002). A novel family of calmodulin-binding transcription activators in multicellular organisms. J Biol Chem *277*, 21851-21861.

Cai, J., Jozwiak, A., Holoidovsky, L., Meijler, M.M., Meir, S., Rogachev, I., and Aharoni, A. (2021). Glycosylation of N-hydroxy-pipecolic acid equilibrates between systemic acquired resistance response and plant growth. Mol Plant *14*, 440-455.

Cao, H., Glazebrook, J., Clarke, J.D., Volko, S., and Dong, X. (1997). The Arabidopsis NPR1 gene that controls systemic acquired resistance encodes a novel protein containing ankyrin repeats. Cell *88*, 57-63.

Cecchini, N.M., Jung, H.W., Engle, N.L., Tschaplinski, T.J., and Greenberg, J.T. (2015). ALD1 Regulates Basal Immune Components and Early Inducible Defense Responses in Arabidopsis. Mol Plant Microbe Interact *28*, 455-466.

Chanda, B., Xia, Y., Mandal, M.K., Yu, K.S., Sekine, K.T., Gao, Q.M., Selote, D., Hu, Y.L., Stromberg, A., Navarre, D.*, et al.* (2011). Glycerol-3-phosphate is a critical mobile inducer of systemic immunity in plants. Nat Genet *43*, 421-+.

Chandra-Shekara, A.C., Gupte, M., Navarre, D., Raina, S., Raina, R., Klessig, D., and Kachroo, P. (2006). Light-dependent hypersensitive response and resistance signaling against Turnip Crinkle Virus in Arabidopsis. Plant Journal *45*, 320-334.

Chen, L.C., Wu, R., Feng, J., Feng, T.P., Wang, C., Hu, J.L., Zhan, N., Li, Y.S., Ma, X.H., Ren, B.*, et al.* (2020). Transnitrosylation Mediated by the Non-canonical Catalase ROG1 Regulates Nitric Oxide Signaling in Plants. Developmental Cell *53*, 444-+.

Chen, Q.B., Man, C., Li, D.N., Tan, H.J., Xie, Y., and Huang, J.R. (2016). Arogenate Dehydratase Isoforms Differentially Regulate Anthocyanin Biosynthesis in Arabidopsis thaliana. Molecular Plant *9*, 1609-1619.

Chen, R.Q., Sun, S.L., Wang, C., Li, Y.S., Liang, Y., An, F.Y., Li, C., Dong, H.L., Yang, X.H., Zhang, J.*, et al.* (2009). The Arabidopsis PARAQUAT RESISTANT2 gene encodes an S-nitrosoglutathione reductase that is a key regulator of cell death. Cell Res *19*, 1377-1387.

Chisholm, S.T., Coaker, G., Day, B., and Staskawicz, B.J. (2006). Host-microbe interactions: shaping the evolution of the plant immune response. Cell *124*, 803-814.

Clough, S.J., and Bent, A.F. (1998). Floral dip: a simplified method for Agrobacterium-mediated transformation of Arabidopsis thaliana. Plant J *16*, 735-743.

de Pinto, M.C., Locato, V., Sgobba, A., Romero-Puertas Mdel, C., Gadaleta, C., Delledonne, M., and De Gara, L. (2013). S-nitrosylation of ascorbate peroxidase is part of programmed cell death signaling in tobacco Bright Yellow-2 cells. Plant Physiol *163*, 1766-1775.

Desikan, R., Griffiths, R., Hancock, J., and Neill, S. (2002). A new role for an old enzyme: Nitrate reductase-mediated nitric oxide generation is required for abscisic acid-induced stomatal closure in Arabidopsis thaliana. P Natl Acad Sci USA *99*, 16314-16318.

Doherty, C.J., Van Buskirk, H.A., Myers, S.J., and Thomashow, M.F. (2009). Roles for Arabidopsis CAMTA transcription factors in cold-regulated gene expression and freezing tolerance. Plant Cell *21*, 972-984.

Dou, D., and Zhou, J.M. (2012). Phytopathogen effectors subverting host immunity: different foes, similar battleground. Cell Host Microbe *12*, 484-495.

Durrant, W.E., and Dong, X. (2004). Systemic acquired resistance. Annu Rev Phytopathol *42*, 185-209.

Eitas, T.K., and Dangl, J.L. (2010). NB-LRR proteins: pairs, pieces, perception, partners, and pathways. Curr Opin Plant Biol *13*, 472-477.

Elmore, J.M., Lin, Z.J., and Coaker, G. (2011). Plant NB-LRR signaling: upstreams and downstreams. Curr Opin Plant Biol *14*, 365-371.

Feechan, A., Kwon, E., Yun, B.W., Wang, Y., Pallas, J.A., and Loake, G.J. (2005). A central role for S-nitrosothiols in plant disease resistance. Proc Natl Acad Sci U S A *102*, 8054-8059.

Fu, Z.Q., and Dong, X. (2013). Systemic acquired resistance: turning local infection into global defense. Annu Rev Plant Biol *64*, 839-863.

Fu, Z.Q., Yan, S.P., Saleh, A., Wang, W., Ruble, J., Oka, N., Mohan, R., Spoel, S.H., Tada, Y., Zheng, N.*, et al.* (2012). NPR3 and NPR4 are receptors for the immune signal salicylic acid in plants. Nature *486*, 228-+.

Gaffney, T., Friedrich, L., Vernooij, B., Negrotto, D., Nye, G., Uknes, S., Ward, E., Kessmann, H., and Ryals, J. (1993). Requirement of Salicylic-Acid for the Induction of Systemic Acquired-Resistance. Science *261*, 754-756.

Gao, Q.M., Kachroo, A., and Kachroo, P. (2014a). Chemical inducers of systemic immunity in plants. J Exp Bot *65*, 1849-1855.

Gao, Q.M., Yu, K., Xia, Y., Shine, M.B., Wang, C., Navarre, D., Kachroo, A., and Kachroo, P. (2014b). Mono- and digalactosyldiacylglycerol lipids function nonredundantly to regulate systemic acquired resistance in plants. Cell Rep *9*, 1681-1691.

Grunwald, N.J. (2005). The social impact of fungal diseases: From the Irish potato famine to sudden oak death. Phytopathology *95*, S129-S129.

Guo, F.Q., Okamoto, M., and Crawford, N.M. (2003). Identification of a plant nitric oxide synthase gene involved in hormonal signaling. Science *302*, 100-103.

Hartmann, M., and Zeier, J. (2019). N-hydroxypipecolic acid and salicylic acid: a metabolic duo for systemic acquired resistance. Current Opinion in Plant Biology *50*, 44-57.

Hartmann, M., Zeier, T., Bernsdorff, F., Reichel-Deland, V., Kim, D., Hohmann, M., Scholten, N., Schuck, S., Brautigam, A., Holzel, T.*, et al.* (2018). Flavin Monooxygenase-Generated N-Hydroxypipecolic Acid Is a Critical Element of Plant Systemic Immunity. Cell *173*, 456-+.

He, Y.K., Tang, R.H., Hao, Y., Stevens, R.D., Cook, C.W., Am, S.M., Jing, L.F., Yang, Z.G., Chen, L.G., Guo, F.Q.*, et al.* (2004). Nitric oxide represses the Arabidopsis floral transition. Science *305*, 1968-1971.

Holmes, E.C., Chen, Y.C., Mudgett, M.B., and Sattely, E.S. (2021). Arabidopsis UGT76B1 glycosylates N-hydroxy-pipecolic acid and inactivates systemic acquired resistance in tomato. Plant Cell *33*, 750-765.

Jung, H.W., Tschaplinski, T.J., Wang, L., Glazebrook, J., and Greenberg, J.T. (2009). Priming in Systemic Plant Immunity. Science *324*, 89-91.

Kachroo, A., and Kachroo, P. (2020). Mobile signals in systemic acquired resistance. Curr Opin Plant Biol *58*, 41-47.

Kachroo, A., Lapchyk, L., Fukushige, H., Hildebrand, D., Klessig, D., and Kachroo, P. (2003a). Plastidial fatty acid signaling modulates salicylic acid- and jasmonic acid-mediated defense pathways in the Arabidopsis ssi2 mutant. Plant Cell *15*, 2952-2965.

Kachroo, A., Venugopal, S.C., Lapchyk, L., Falcone, D., Hildebrand, D., and Kachroo, P. (2004). Oleic acid levels regulated by glycerolipid metabolism modulate defense gene expression in Arabidopsis. Proc Natl Acad Sci U S A *101*, 5152-5157.

Kachroo, P., Kachroo, A., Lapchyk, L., Hildebrand, D., and Klessig, D.F. (2003b). Restoration of defective cross talk in ssi2 mutants: Role of salicylic acid, jasmonic acid, and fatty acids in SSI2-mediated signaling. Mol Plant Microbe In *16*, 1022-1029.

Kachroo, P., Shanklin, J., Shah, J., Whittle, E.J., and Klessig, D.F. (2001). A fatty acid desaturase modulates the activation of defense signaling pathways in plants. Proc Natl Acad Sci U S A *98*, 9448-9453.

Kachroo, P., Venugopal, S.C., Navarre, D.A., Lapchyk, L., and Kachroo, A. (2005). Role of salicylic acid and fatty acid desaturation pathways in ssi2-mediated signaling. Plant Physiol *139*, 1717-1735.

Kadota, Y., Shirasu, K., and Zipfel, C. (2015). Regulation of the NADPH Oxidase RBOHD During Plant Immunity. Plant and Cell Physiology *56*, 1472-1480.

Kim, Y., Gilmour, S.J., Chao, L., Park, S., and Thomashow, M.F. (2020). Arabidopsis CAMTA Transcription Factors Regulate Pipecolic Acid Biosynthesis and Priming of Immunity Genes. Mol Plant *13*, 157-168.

Kim, Y., Park, S., Gilmour, S.J., and Thomashow, M.F. (2013). Roles of CAMTA transcription factors and salicylic acid in configuring the low-temperature transcriptome and freezing tolerance of Arabidopsis. Plant J *75*, 364-376.

Kinkema, M., Fan, W., and Dong, X. (2000). Nuclear localization of NPR1 is required for activation of PR gene expression. Plant Cell *12*, 2339-2350.

Knappe, S., Lottgert, T., Schneider, A., Voll, L., Flugge, U.I., and Fischer, K. (2003). Characterization of two functional phosphoenolpyruvate/phosphate translocator (PPT) genes in Arabidopsis-AtPPT1 may be involved in the provision of signals for correct mesophyll development. Plant Journal *36*, 411-420.

Kunst, L., Browse, J., and Somerville, C. (1988). Altered Regulation of Lipid Biosynthesis in a Mutant of Arabidopsis Deficient in Chloroplast Glycerol-3-Phosphate Acyltransferase Activity. P Natl Acad Sci USA *85*, 4143-4147.

Lee, H.J., Park, Y.J., Seo, P.J., Kim, J.H., Sim, H.J., Kim, S.G., and Park, C.M. (2015). Systemic Immunity Requires SnRK2.8-Mediated Nuclear Import of NPR1 in Arabidopsis. Plant Cell *27*, 3425-3438.

Leitner, M., Vandelle, E., Gaupels, F., Bellin, D., and Delledonne, M. (2009). NO signals in the haze: nitric oxide signalling in plant defence. Curr Opin Plant Biol *12*, 451-458.

Lenk, M., Wenig, M., Bauer, K., Hug, F., Knappe, C., Lange, B., Timsy, Haussler, F., Mengel, F., Dey, S.*, et al.* (2019). Pipecolic Acid Is Induced in Barley upon Infection and Triggers

Immune Responses Associated with Elevated Nitric Oxide Accumulation. Mol Plant Microbe In *32*, 1303-1313.

Li, H.M., Culligan, K., Dixon, R.A., and Chory, J. (1995). Cue1 - a Mesophyll Cell-Specific Positive Regulator of Light-Controlled Gene-Expression in Arabidopsis. Plant Cell *7*, 1599-1610.

Li, J., Brader, G., Kariola, T., and Palva, E.T. (2006). WRKY70 modulates the selection of signaling pathways in plant defense. Plant Journal *46*, 477-491.

Lim, G.H., Kachroo, A., and Kachroo, P. (2016). Role of plasmodesmata and plasmodesmata localizing proteins in systemic immunity. Plant Signaling & Behavior *11*.

Lim, G.H., Liu, H.Z., Yu, K.S., Liu, R.Y., Shine, M.B., Fernandez, J., Burch-Smith, T., Mobley, J.K., McLetchie, N., Kachroo, A.*, et al.* (2020). The plant cuticle regulates apoplastic transport of salicylic acid during systemic acquired resistance. Science Advances *6*.

Lim, G.H., Singhal, R., Kachroo, A., and Kachroo, P. (2017). Fatty Acid- and Lipid-Mediated Signaling in Plant Defense. Annual Review of Phytopathology, Vol 55 *55*, 505-536.

Lin, A., Wang, Y., Tang, J., Xue, P., Li, C., Liu, L., Hu, B., Yang, F., Loake, G.J., and Chu, C. (2012). Nitric oxide and protein S-nitrosylation are integral to hydrogen peroxide-induced leaf cell death in rice. Plant Physiol *158*, 451-464.

Maeda, H., and Dudareva, N. (2012). The Shikimate Pathway and Aromatic Amino Acid Biosynthesis in Plants. Annual Review of Plant Biology, Vol 63 *63*, 73-105.

Mandal, M.K., Chandra-Shekara, A.C., Jeong, R.D., Yu, K.S., Zhu, S.F., Chanda, B., Navarre, D., Kachroo, A., and Kachroo, P. (2012). Oleic Acid-Dependent Modulation of NITRIC OXIDE ASSOCIATED1 Protein Levels Regulates Nitric Oxide-Mediated Defense Signaling in Arabidopsis. Plant Cell *24*, 1654-1674.

Martin, K., Kopperud, K., Chakrabarty, R., Banerjee, R., Brooks, R., and Goodin, M.M. (2009). Transient expression in Nicotiana benthamiana fluorescent marker lines provides enhanced definition of protein localization, movement and interactions in planta. Plant Journal *59*, 150-162.

Melotto, M., Underwood, W., and He, S.Y. (2008). Role of stomata in plant innate immunity and foliar bacterial diseases. Annu Rev Phytopathol *46*, 101-122.

Mishina, T.E., and Zeier, J. (2007). Pathogen-associated molecular pattern recognition rather than development of tissue necrosis contributes to bacterial induction of systemic acquired resistance in Arabidopsis. Plant J *50*, 500-513.

Nandi, A., Moeder, W., Kachroo, P., Klessig, D.F., and Shah, J. (2005). Arabidopsis ssi2-conferred susceptibility to Botrytis cinerea is dependent on EDS5 and PAD4. Mol Plant Microbe In *18*, 363-370.

Navarova, H., Bernsdorff, F., Doring, A.C., and Zeier, J. (2012). Pipecolic Acid, an Endogenous Mediator of Defense Amplification and Priming, Is a Critical Regulator of Inducible Plant Immunity. Plant Cell *24*, 5123-5141.

Nicaise, V., Roux, M., and Zipfel, C. (2009). Recent advances in PAMP-triggered immunity against bacteria: pattern recognition receptors watch over and raise the alarm. Plant Physiol *150*, 1638-1647.

Olah, D., Feigl, G., Molnar, A., Ordog, A., and Kolbert, Z. (2020). Strigolactones Interact With Nitric Oxide in Regulating Root System Architecture ofArabidopsis thaliana. Frontiers in Plant Science *11*.

Park, S.W., Kaimoyo, E., Kumar, D., Mosher, S., and Klessig, D.F. (2007). Methyl salicylate is a critical mobile signal for plant systemic acquired resistance. Science *318*, 113-116.

Peng, Y., Yang, J., Li, X., and Zhang, Y. (2021). Salicylic Acid: Biosynthesis and Signaling. Annu Rev Plant Biol *72*, 761-791.

Pitzschke, A., Datta, S., and Persak, H. (2014). Salt stress in Arabidopsis: lipid transfer protein AZI1 and its control by mitogen-activated protein kinase MPK3. Mol Plant *7*, 722-738.

Rast, J.P., Smith, L.C., Loza-Coll, M., Hibino, T., and Litman, G.W. (2006). Review - Genomic insights into the immune system of the sea urchin. Science *314*, 952-956.

Riedlmeier, M., Ghirardo, A., Wenig, M., Knappe, C., Koch, K., Georgii, E., Dey, S., Parker, J.E., Schnitzler, J.P., and Vlot, A.C. (2017). Monoterpenes Support Systemic Acquired Resistance within and between Plants. Plant Cell *29*, 1440-1459.

Rigling, D., and Prospero, S. (2018). Cryphonectria parasitica, the causal agent of chestnut blight: invasion history, population biology and disease control. Molecular Plant Pathology *19*, 7-20.

Rivas-San Vicente, M., and Plasencia, J. (2011). Salicylic acid beyond defence: its role in plant growth and development. J Exp Bot *62*, 3321-3338.

Robbins, W.J. (1944). The importance of plants. Science *100*, 440-443.

Robert-Seilaniantz, A., Grant, M., and Jones, J.D. (2011). Hormone crosstalk in plant disease and defense: more than just jasmonate-salicylate antagonism. Annu Rev Phytopathol *49*, 317-343.

Sanchez-Martin, J., and Keller, B. (2019). Contribution of recent technological advances to future resistance breeding. Theor Appl Genet *132*, 713-732.

Shah, J., Kachroo, P., Nandi, A., and Klessig, D.F. (2001). A recessive mutation in the Arabidopsis SSI2 gene confers SA- and NPR1-independent expression of PR genes and resistance against bacterial and oomycete pathogens. Plant Journal *25*, 563-574.

Shine, M.B., Xiao, X., Kachroo, P., and Kachroo, A. (2019). Signaling mechanisms underlying systemic acquired resistance to microbial pathogens. Plant Sci *279*, 81-86.

Shine, M.B., Yang, J.W., El-Habbak, M., Nagyabhyru, P., Fu, D.Q., Navarre, D., Ghabrial, S., Kachroo, P., and Kachroo, A. (2016). Cooperative functioning between phenylalanine ammonia lyase and isochorismate synthase activities contributes to salicylic acid biosynthesis in soybean. New Phytologist *212*, 627-636.

Strange, R.N., and Scott, P.R. (2005). Plant disease: a threat to global food security. Annu Rev Phytopathol *43*, 83-116.

Streatfield, S.J., Weber, A., Kinsman, E.A., Hausler, R.E., Li, J.M., Post-Beittenmiller, D., Kaiser, W.M., Pyke, K.A., Flugge, U.I., and Chory, J. (1999). The phosphoenolpyruvate/phosphate translocator is required for phenolic metabolism, palisade cell development, and plastid-dependent nuclear gene expression. Plant Cell *11*, 1609-1621.

Sun, T., Busta, L., Zhang, Q., Ding, P., Jetter, R., and Zhang, Y. (2018). TGACG-BINDING FACTOR 1 (TGA1) and TGA4 regulate salicylic acid and pipecolic acid biosynthesis by modulating the expression of SYSTEMIC ACQUIRED RESISTANCE DEFICIENT 1 (SARD1) and CALMODULIN-BINDING PROTEIN 60g (CBP60g). New Phytol *217*, 344-354.

Sun, T., Zhang, Y., Li, Y., Zhang, Q., Ding, Y., and Zhang, Y. (2015). ChIP-seq reveals broad roles of SARD1 and CBP60g in regulating plant immunity. Nat Commun *6*, 10159.

Sun, T.J., Huang, J.H., Xu, Y., Verma, V., Jing, B.B., Sun, Y.L., Orduna, A.R., Tian, H.N., Huang, X.C., Xia, S.T., *et al.* (2020). Redundant CAMTA Transcription Factors Negatively Regulate the Biosynthesis of Salicylic Acid and N-Hydroxypipecolic Acid by Modulating the Expression of SARD1 and CBP60g. Molecular Plant *13*, 144-156.

Tada, Y., Spoel, S.H., Pajerowska-Mukhtar, K., Mou, Z.L., Song, J.Q., Wang, C., Zuo, J.R., and Dong, X.N. (2008). Plant immunity requires conformational charges of NPR1 via S-nitrosylation and thioredoxins. Science *321*, 952-956.

Torres, M.A., and Dangl, J.L. (2005). Functions of the respiratory burst oxidase in biotic interactions, abiotic stress and development. Current Opinion in Plant Biology *8*, 397-403.

Tsuda, K., and Katagiri, F. (2010). Comparing signaling mechanisms engaged in pattern-triggered and effector-triggered immunity. Curr Opin Plant Biol *13*, 459-465.

van Wersch, R., Li, X., and Zhang, Y. (2016). Mighty Dwarfs: Arabidopsis Autoimmune Mutants and Their Usages in Genetic Dissection of Plant Immunity. Front Plant Sci *7*, 1717.

Vernooij, B., Friedrich, L., Morse, A., Reist, R., Kolditzjawhar, R., Ward, E., Uknes, S., Kessmann, H., and Ryals, J. (1994). Salicylic-Acid Is Not the Translocated Signal Responsible for Inducing Systemic Acquired-Resistance but Is Required in Signal Transduction. Plant Cell *6*, 959-965.

Villiers, F., and Kwak, J.M. (2013). Rapid apoplastic pH measurement in Arabidopsis leaves using a fluorescent dye. Plant Signal Behav *8*, e22587.

Voll, L., Hausler, R.E., Hecker, R., Weber, A., Weissenbock, G., Fiene, G., Waffenschmidt, S., and Flugge, U.I. (2003). The phenotype of the Arabidopsis cue1 mutant is not simply caused by a general restriction of the shikimate pathway. Plant J *36*, 301-317.

Wang, C., El-Shetehy, M., Shine, M.B., Yu, K., Navarre, D., Wendehenne, D., Kachroo, A., and Kachroo, P. (2014). Free radicals mediate systemic acquired resistance. Cell Rep *7*, 348-355.

Wang, C., Huang, X., Li, Q., Zhang, Y., Li, J.L., and Mou, Z. (2019). Extracellular pyridine nucleotides trigger plant systemic immunity through a lectin receptor kinase/BAK1 complex. Nat Commun *10*, 4810.

Wang, C., Liu, R., Lim, G.H., de Lorenzo, L., Yu, K., Zhang, K., Hunt, A.G., Kachroo, A., and Kachroo, P. (2018). Pipecolic acid confers systemic immunity by regulating free radicals. Sci Adv *4*, eaar4509.

Wang, W., Withers, J., Li, H., Zwack, P.J., Rusnac, D.V., Shi, H., Liu, L., Yan, S., Hinds, T.R., Guttman, M.*, et al.* (2020). Structural basis of salicylic acid perception by Arabidopsis NPR proteins. Nature *586*, 311-316.

Wang, Y., and Chu, C. (2020). S-Nitrosylation Control of ROS and RNS Homeostasis in Plants: The Switching Function of Catalase. Mol Plant *13*, 946-948.

Wendehenne, D., Gao, Q.M., Kachroo, A., and Kachroo, P. (2014). Free radical-mediated systemic immunity in plants. Curr Opin Plant Biol *20*, 127-134.

Wilson, I.D., Neill, S.J., and Hancock, J.T. (2008). Nitric oxide synthesis and signalling in plants. Plant Cell Environ *31*, 622-631.

Xia, Y., Gao, Q.M., Yu, K.S., Lapchyk, L., Navarre, D., Hildebrand, D., Kachroo, A., and Kachroo, P. (2009). An Intact Cuticle in Distal Tissues Is Essential for the Induction of Systemic Acquired Resistance in Plants. Cell Host & Microbe *5*, 151-165.

Yu, K., Liu, H., and Kachroo, P. (2020). Pipecolic Acid Quantification Using Gas Chromatography-coupled Mass Spectrometry. Bio Protoc *10*, e3841.

Yu, K., Soares, J.M., Mandal, M.K., Wang, C., Chanda, B., Gifford, A.N., Fowler, J.S., Navarre, D., Kachroo, A., and Kachroo, P. (2013). A feedback regulatory loop between G3P and lipid transfer proteins DIR1 and AZI1 mediates azelaic-acid-induced systemic immunity. Cell Rep *3*, 1266-1278.

Yuan, M., Ngou, B.P.M., Ding, P., and Xin, X.F. (2021). PTI-ETI crosstalk: an integrative view of plant immunity. Curr Opin Plant Biol *62*, 102030.

Yun, B.W., Feechan, A., Yin, M., Saidi, N.B., Le Bihan, T., Yu, M., Moore, J.W., Kang, J.G., Kwon, E., Spoel, S.H.*, et al.* (2011). S-nitrosylation of NADPH oxidase regulates cell death in plant immunity. Nature *478*, 264-268.

Yun, B.W., Skelly, M.J., Yin, M.H., Yu, M.D., Mun, B.G., Lee, S.U., Hussain, A., Spoel, S.H., and Loake, G.J. (2016). Nitric oxide and S-nitrosoglutathione function additively during plant immunity. New Phytologist *211*, 516-526.

Zhang, Y., and Li, X. (2019). Salicylic acid: biosynthesis, perception, and contributions to plant immunity. Curr Opin Plant Biol *50*, 29-36.

Zhou, M., Lu, Y., Bethke, G., Harrison, B.T., Hatsugai, N., Katagiri, F., and Glazebrook, J. (2018). WRKY70 prevents axenic activation of plant immunity by direct repression of SARD1. New Phytologist *217*, 700-712.

Zipfel, C. (2009). Early molecular events in PAMP-triggered immunity. Curr Opin Plant Biol *12*, 414-420.

Zipfel, C., and Robatzek, S. (2010). Pathogen-associated molecular pattern-triggered immunity: veni, vidi...? Plant Physiol *154*, 551-554.

Ziv, C., Zhao, Z., Gao, Y.G., and Xia, Y. (2018). Multifunctional Roles of Plant Cuticle During Plant-Pathogen Interactions. Front Plant Sci *9*, 1088.

VITA

FAN XIA

EDUCATION

M.S. Biochemistry and Molecular Biology, Huazhong Agricultural University

2013-2016 Wuhan, China

B.S. Plant Protection, Huazhong Agricultural University

2009-2013 Wuhan, China

PROFESSIONAL EXPERIENCE

Graduate Research Assistant, University of Kentucky, 2016-2022

Graduate Research Assistant, Huazhong Agricultural University, 2013-2016

HONORS

Richards Graduate Student Research Activity Award, University of Kentucky, 2021

China National Scholarship for Graduate Students, Ministry of Education of China, 2015

PUBLICATIONS

- Liu Duan, Wenfei Xiao, **Fan Xia**, Hongbo Liu, Jinghua Xiao, Xianghua Li, Shiping Wang*. Two Different Transcripts of a LAMMER Kinase Gene Play Opposite Roles in Disease Resistance. *Plant Physiol.* 2016, 172(3):1959-1972
- Keming Hu, Jianbo Cao, Jie Zhang, **Fan Xia**, Yingen Ke, Haitao Zhang, Hongbo Liu, Ying Cui, Yinglong Cao, Xinli Sun, Jinghua Xiao, Xianghua Li, Qinglu Zhang, Shiping Wang*. Improvement of multiple agronomic traits by a disease resistance gene via cell wall reinforcement. *Nature Plants,* 2017, 3:17009
- M. B. Shine, Kai Zhang, Huazhen Liu, Gah-hyun Lim, **Fan Xia**, Keshun Yu, Arthur G. Hunt, Aardra Kachroo*, Pradeep Kachroo*. Phased small RNA-mediated systemic signaling in plants. *Science Advance*, 2022, In press